Investigating the function of transmembrane channel-like (TMC) proteins in sensory transduction using the nematode *Caenorhabditis elegans.*

Rhianna Clare Knable

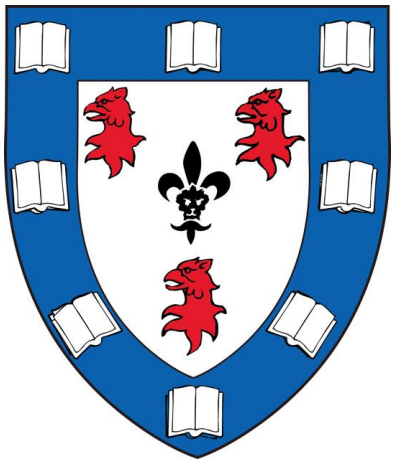

MRC Laboratory of Molecular Biology
Homerton College, University of Cambridge

This dissertation is submitted for the degree of Doctor of Philosophy, *Month* 2017

Preface

This dissertation is the result of my own work and includes nothing that is the outcome of work done in collaboration except as specified in the text. It is not being submitted for any other degree or qualification at the University of Cambridge or any other University. It does not exceed the 60,000-word limit for the Biological Sciences Degree Committee.

Summary

Sensory transduction is fundamental to our ability to sense stimuli from the surrounding environment and to affect the ensuing behavioural response. Although our understanding of the signaling pathways behind some senses has progressed rapidly, those mediated by ionotropic receptors directly gated by stimuli such as hearing, touch and pain are still not well understood.

Recent studies have implicated the transmembrane channel-like (TMC) family of proteins in a number of hearing-related disorders, suggesting they may be a key part of this mechanotransduction machinery. By studying these proteins we may therefore be able to uncover important insights into how mechanosensory channels function. In particular, I have focused on the Subfamily A members TMC1-3, which are more restrictively expressed than the rest of the TMC protein family and have been implicated in a number of sensory functions. I have found that the Tmc3 protein, previously unstudied in mice, is able to generate ectopic touch responses when expressed in *Caenorhabditis elegans*, supporting the notion that it may function as a part of the mechanotransduction complex.

In the second part of my study, I identified an extracellular domain of the TMC proteins that is able to determine their different sensory specificities. Chimeric proteins exchanging this short loop have altered response profiles, suggesting a modular nature to the channel's ability to sense and respond to stimuli. I also collected further data supporting a six transmembrane-spanning domain model of the TMC proteins' membrane topology.

Finally, I conducted immunohistochemistry in mouse DRG slices, identifying a subset of sensory neurons that express Tmc1 and Tmc3. I examined TMC knockout mice for touch defects using the Von Frey apparatus, but these animals were indistinguishable from wild type. However, the immunohistochemistry also identified a possible role for Tmc3 in thermosensation, which I investigated again using heterologous expression in *C. elegans*. The calcium imaging from these animals suggest a possible role for Tmc3 in thermosensation, a sensory activity previously unlinked to the TMC family.

Table of Contents

List of Tables and Figures

Abbreviations

CDH23: Cadherin 23

CFP: Cyan fluorescent protein

DIC: Differential interference contrast

DRG: Dorsal root ganglia

ER: Endoplasmic reticulum

FRET: Fluorescence/Förster resonance energy transfer

GFP: Green fluorescent protein

GPCR: G-protein coupled receptor

HA: Hemagglutinin

HT: High threshold

IHC: Inner hair cell

LT: Low threshold

NGM: Nematode growth medium

OHC: Outer hair cell

PCDH15: protocadherin 15

PFA: Paraformaldehyde

RA: Rapidly adapting

RFP: Red fluorescent protein

SA: Slowly adapting

SEM: Standard error of the mean

TM: Transmembrane

TMC: Transmembrane channel-like

WTSI: Wellcome Trust Sanger Institute

YFP: Yellow fluorescent protein

Chapter 1: Introduction

1.1 Sensory transduction

In all organisms, the ability to sense aversive environmental stimuli is critical to survival. Mechanosensation is one of our most ancient senses, and has been honed to develop a specialized sensitivity to proprioception, physical touch, osmotic pressure and sound waves. Among the five key senses defined by Aristotle - hearing, sight, smell, touch and taste - touch (and by extension, hearing) remains the least defined at the molecular level. Our senses of smell, taste and sight are largely governed by G-protein coupled receptors (GPCRs), whereby specific ligands bind to receptors, stimulating a second messenger cascade that leads to channel opening and membrane depolarization (Mombaerts 1999). For example, odorant detection occurs by binding of odor molecules to specific GPCRs, in turn elevating levels of cyclic AMP and causing cation permeable channels to open which depolarize the cell and propagate an action potential (Buck & Axel 1991). A similar mechanism occurs in taste receptor cells to detect sweet, bitter and umami taste (Firestein 2000). Finally, vision arises by the capture of photons causing activation of a GPCR and the ensuing downstream signaling cascade which ends with hyperpolarization of the cell, reduction in glutamate release, and thus depolarization of separate 'On' bipolar cells that allow transmission of information about absorbed light (Ebrey & Koutalos 2001; Pugh 1999).

In comparison to these models, mechanosensory cells are thought to be directly gated by force, as the response times involved are too rapid for second-messenger systems

(Corey & Hudspeth 1983; Kang et al. 2010; O'Hagan et al. 2005). Such cells are able to respond to changes in pressure, stretch, flow and acceleration, and must be able to detect sound waves. Consequently, mechanosensation is crucially important in a number of tissues and biological contexts (Jaalouk & Lammerding 2009). It plays some role in adapting muscle tension (Lammerding et al. 2004; Haga et al. 2007), bone remodeling and cartilage adaptation (Burger & Klein-Nulend 1999), regulating blood pressure (Lammerding et al. 2004; Ng et al. 2004), and in modeling kidney morphogenesis based on urine flow (Serluca et al. 2002). However, the two aspects of mechanosensation that are least understood (and of most interest to us) are in hearing, and in mechanosensitive and nociceptive touch.

Touch sensation relies on sensory afferents that project from the central nervous system, via the dorsal root ganglion (DRG) and into the outer layers of mammalian skin, often ending in specialized organelles (**Fig 1.1**). These sensory afferents can be divided into a number of categories based on their function and properties. Most animals have specialized polymodal afferents for detecting noxious stimuli called nociceptors, which are usually exposed nerve endings. These nociceptors are only activated once a stimulus reaches the noxious range (Basbaum et al. 2009). In comparison, mechanoreceptors have specialized nerve endings in the skin which help to discern milder stimuli (Basbaum et al. 2009; Hao et al. 2014). Hair follicles are important for sensing light touch, while the Pacinian corpuscle detects vibration and small displacements of the skin to a very sensitive level (Delmas et al. 2011). Meissner's corpuscle detects ridges and other changes in texture on smooth surfaces, including information about skin motion and slip as objects are handled (Hao et al. 2014). Merkel cell–neurite complexes are gentle touch receptors that map the

contours of objects, helping to discern surface curvature and detecting indentation depth on the skin (Sanjeev S. Ranade et al. 2014; Woo et al. 2014).

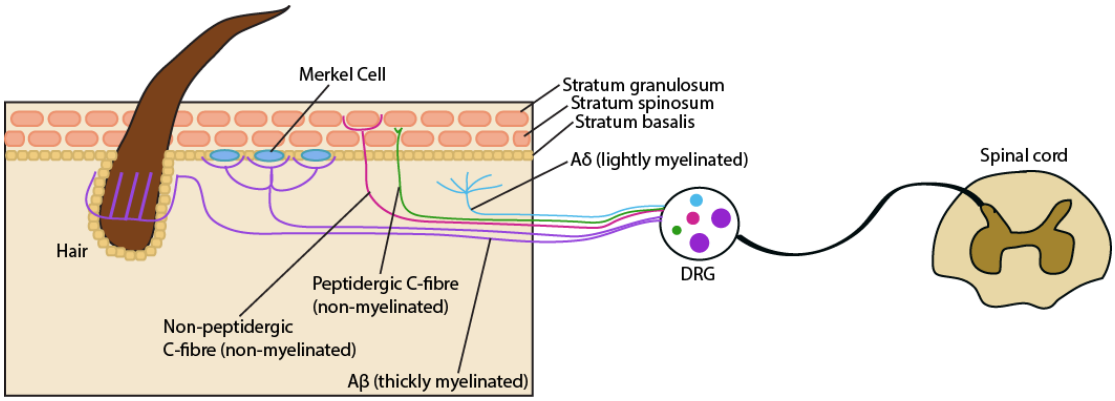

Fig 1.1: Somatosensory neurons in the mammalian skin. Specialized organelles such as Merkel cells project fibres into the spinal cord via the DRG. Aβ fibres are believed to be touch receptors, while Aδ and C-fibres act as thermoreceptors and nociceptors. Aδ fibres terminate in the dermis, while C-fibres terminate in the epidermis. Image reproduced from Lumpkin & Caterina (2007).

Several advances have recently shown that Merkel cells themselves are mechanosensitive, expressing the Piezo2 channel (Maksimovic et al. 2014; Ikeda et al. 2014; Woo et al. 2014). Piezo2 has since been shown to be the primary channel for proprioception in mammals (Woo et al. 2015), and DRG cultures in Piezo2 mutant mice lack rapidly adapting, mechanically activated currents (Ranade et al. 2014). This exciting discovery has significantly expanded our understanding of proprioceptive touch. However, it has also highlighted the range of components involved in the mechanosensitive machinery, as Piezo2 does not rescue defects in any other forms of touch.

Sensory afferents can be further subdivided into populations based on their myelination and conduction velocity. Heavily myelinated Aβ afferents that mainly sense non-noxious mechanical stimuli have the largest axon diameter and fastest conduction velocity. Lightly myelinated Aδ afferents are smaller and have slower conduction, as do the unmyelinated C-fibres. Finally, the fibres can be characterized based on their mechanical threshold (the force needed to evoke a response). It is expected that nociceptive neurons will have a higher threshold for activation than low threshold mechanoreceptors, and that they may also be activated by chemical or thermal stimuli. Aβ afferents mostly have low thresholds, whereas the C- and Aδ fibres have much higher thresholds and are known to project into the central nervous system (Smith & Lewin 2009; Lumpkin et al. 2010). Nociceptive C-fibres are mostly slowly-adapting, whereas populations proposed to respond to gentle or pleasant touch are predominantly more rapidly-adapting (Bessou & Perl 1969; Smith & Lewin 2009). Because of these high activation thresholds and slow inactivation kinetics, the majority of nociceptive neurons are identified as unmyelinated C-fibres, although a subset of Aδ fibres are also involved (Smith & Lewin 2009). In comparison, Aβ and the remaining Aδ fibres are identified as the mechanoreceptors which have their specially formed nerve endings described above (Lumpkin & Caterina 2007; Delmas et al. 2011) (**Table 1.1**).

	Sensory ending	Perception	Characteristics
Aβ fibre Large, thickly myelinated soma	Pacinian corpuscle	Vibration	LT, RA
	Meissner corpuscle	Skin motion, texture	LT, RA
	Merkel cell-neurite complex	Touch sensors, contours	LT, SA
Aδ fibre Medium-sized, thinly myelinated soma	D-hairs	Skin brush	LT, RA
	Open	Nociceptive	HT, SA
C fibre Small, unmyelinated soma	Open	Nociceptive	HT, SA
	Open	Pleasant, social touch	LT, SA

Table 1.1: Breakdown of the organelles found in mammalian skin and their projections. Each of the fibres have specialized properties that align with their functional roles. LT: low threshold, HT: high threshold, RA: rapidly adapting, SA: slowly adapting.

After prolonged stimulation nociceptors can become sensitized, a protective mechanism that leads to stimuli being treated as noxious at lower levels or causes the nociceptive response to be of a greater magnitude. Misregulation of this process can lead to touch hypersensitivity and chronic pain (Gilron et al. 2006; Lumpkin et al. 2010), including clinical conditions such as mechanical allodynia (perceiving normally innocuous stimuli as painful) or hyperalgesia (eliciting pain of a greater intensity than normal) (Basbaum et al. 2009; Le Pichon & Chesler 2014). In extreme cases individuals may even lack any sense of pain at all, a debilitating condition that means they do not take protective actions against potentially life threatening injuries such as broken bones, burns and internal wounds (Basbaum et al. 2009).

Besides noxious and mechanosensitive touch, another sensory modality we are particularly interested in is hearing. Like touch sensation on the skin, hearing relies on specialized tissues to sense mechanical stimuli. Sound waves are funneled through the ear until they reach the inner ear, where the cochlear is responsible for auditory transduction (**Fig 1.2**). Within the cochlear is the Organ of Corti, which comprises a row of inner hair cells (IHCs) and three rows of outer hair cells (OHCs) (Brown et al. 2008; Schwander et al. 2010). Hair cells are highly specialized for mechanosensation, featuring actin-filled stereocilia at their apical surface that are arranged in a staircase formation. Adjacent stereocilia are connected by tip links between the top of lower cilia and the side of their taller neighbour (Hudspeth 1989; Schwander et al. 2010). When sound waves reach the inner ear, they cause deflections of the stereocilia and the opening of the key hair cell mechanotransducer channel, allowing cation influx from the potassium-rich endolymph the cells are bathed in (Brown et al. 2008). A plethora of associated proteins and auxiliary subunits necessary for this channel function have been identified, but the pore forming subunit remains elusive.

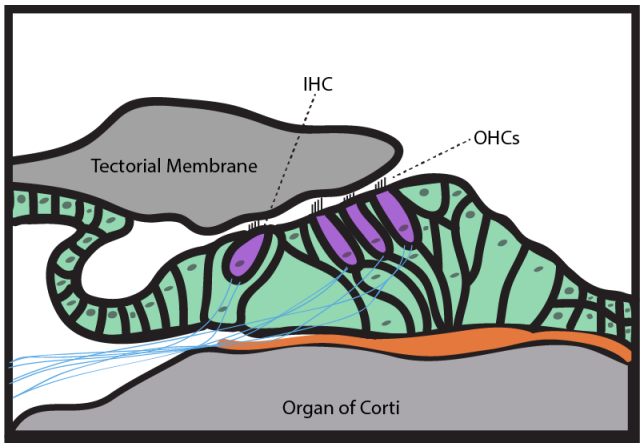

Fig 1.2: Anatomy of the mammalian inner ear. The Organ of Corti contains three rows of outer hair cells (OHCs), which amplify sound signals, and a single row of inner hair cells (IHCs), which carry this information to the nervous system.

Hearing loss is still a major concern in human populations, currently rating as the most common sensory disorder in newborns (Hilgert et al. 2009). Heritable hearing loss can be broadly characterized into two groups – that caused by structural defects in the ear, or hearing loss related to more specific genetic defects in the transduction channel or inner ear machinery. Clinically, patients therefore present as either 'syndromic' – with physical defects in the ear and often other medical problems, or as 'nonsyndromic' – with specific difficulties hearing unrelated to another medical condition (Smith et al. 1999). Nonsyndromic deafness accounts for the majority (around 70%) of hereditary hearing loss (Nance 2003), and epidemiological studies in this area have unmasked a number of candidate genes that are crucially required for hearing - narrowing these down to the components of the mechanotransduction channel is now the key challenge facing researchers.

1.2 Mechanisms of mechanosensation

Fundamentally, mechanical stimuli are detected by tension on a transmembrane channel causing conformational changes and increasing its open probability, with the resulting influx of ions effectively amplifying the signal. In all systems, forces must be rapidly and sensitively transmitted to the transduction channel, such that small changes in sound, pressure or gravitational force are detectable (Gillespie & Walker 2001). Accordingly, three main models of mechanosensory channel function have emerged. Based on studies from the *Escherichia coli* channels MscL and MscS (Kung 2005), the 'membrane force' model proposes that only changes in these membrane forces surrounding the channel are required for gating. While this is certainly the case in bacteria, it is now generally accepted that in eukaryotes the mechanoreceptor must

rely on detecting deflection of an external force sensor in relation to an internal anchor (Gillespie & Walker 2001), and that membrane forces alone are not sufficient to open the channel. The 'dual tethering' (or 'gating spring') model proposes that mechanosensory channels are attached to both extracellular and intracellular tethers, as is hypothesized to be the case in vertebrate hair cell transduction (Pickles & Corey 1992). Finally, a 'single tether' model would suggest that manipulation via one tether point repositions the channel on the membrane, changing the forces that gate it. In this model, it is the effect of the tether on membrane forces that is important for channel gating (**Fig 1.3**).

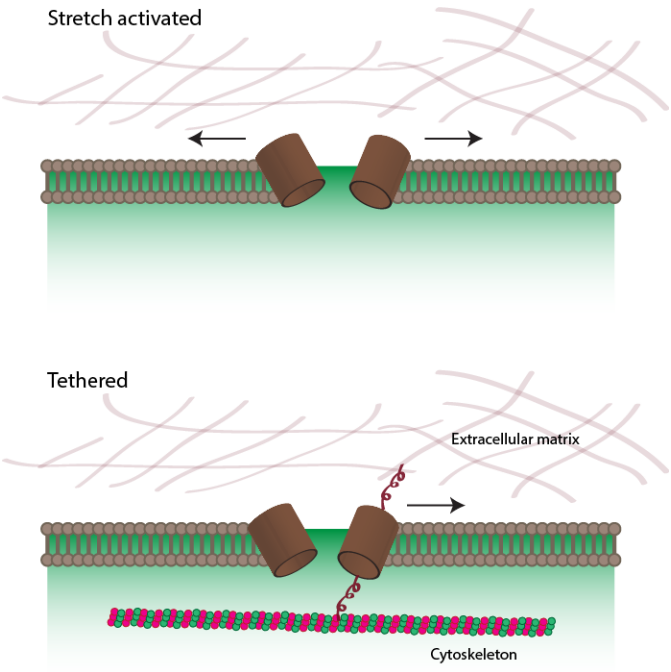

Fig 1.3: Proposed models for gating of mechanotransduction channels. A) Stretch-activated channels respond to changes in the lipid bilayer (depicted by arrows). **B)** Tethers linking the channel to cytoskeletal proteins are proposed to open the channel by conveying changes in tension, either directly to the channel or by changing the membrane tension around it.

Because both of these models involve tethering proteins, it has been difficult to reconstitute mechanotransduction channels in a heterologous system in a way that would replicate this gating mechanism. This may explain part of the difficulty in identifying *bona-fide* mechanotransduction channels. Indeed, while many candidates have been proposed to function as a mechanotransducers, only three classes of channels have so far been confirmed – DEG/ENaCs, TRPN and Piezos (Delmas & Coste 2013). In response to these difficulties, various studies have proposed four main criteria for a mechanosensory receptor (Arnadóttir & Chalfie 2010; Christensen & Corey 2007):

1. The candidate must be expressed in the right place and at the right time during development for mechanosensation.
2. The candidate must be directly required for mechanotransduction, rather than for the development of the organ or downstream signaling.
3. The candidate should remain mechanically sensitive when expressed in heterologous systems (with the caveat that if cofactors are required this may not be possible).
4. Finally, the candidate must be a pore-forming subunit of the channel, such that alteration of the ion selectivity of the channel affects the mechanical response.

Although various channels have been identified that fit some of these criteria, very little is known about touch receptors in the skin, and a true mechanosensory receptor in the mammalian ear is yet to be identified. Advantageously, conservation of the underlying mechanisms of mechanosensation means that it is feasible to use simpler models such as *Caenorhabditis elegans* to address these questions. In fact, it was in *C. elegans* that both the TRPN and DEG/ENaC channels were first studied and

confirmed to be mechanosensitive (O'Hagan et al. 2005; Kang et al. 2010; Delmas & Coste 2013).

1.3 An introduction to *C. elegans* and its genetics

Since Sydney Brenner's introduction of *C. elegans* as a model organism in the 1960s, it has proven to be an invaluable model for scientific research in the fields of neurobiology, cell biology, development and genetics. The small size of the nematode worm, its ease of cultivation and self-fertilization, short lifespan and well-defined genetics mean it can be used to approach questions fundamental to biology. *C. elegans* has a number of classical behavioural responses to touch stimuli, allowing molecular models to be paired with the animal's behavioural responses. Additionally, the transparent nature of the worm has meant that as *in vivo* imaging techniques and fluorescent imaging advanced it has become a crucial tool in studying neuron morphology and function. With the advent of electrophysiology techniques in *C. elegans* (O'Hagan et al. 2005; Goodman et al. 2012), it is now a viable model in which to study ionotropic channel form and function.

C. elegans grow to be approximately one millimeter long, passing through four larval stages (L1-L4) in three days before living as adults for a number of months. The worm has two sexes; hermaphrodites and males, with hermaphrodites passing through a defined series of cell divisions to result in the invariant lineage of 959 somatic cells, 302 of which are neurons (Riddle DL, Blumenthal T, Meyer BJ 1997; Sulston & Horvitz 1977; Sulston et al. 1983). These neurons are structurally similar between individuals and invariantly positioned, allowing for consistent analysis between

animals. In *C. elegans*, the mechanosensory circuit is primarily defined by the six touch receptor cells AVM, PVM, ALM (bilateral) and PLM (bilateral), but other neurons such as the multidendritic nociceptor PVD and polymodal sensory neurons found in the nerve ring such as the IL2s and ASH also have sensory functions. There are also a number of other neurons in the head of the animal that are important for sensing chemicals, pheromones and temperature (**Fig 1.4**).

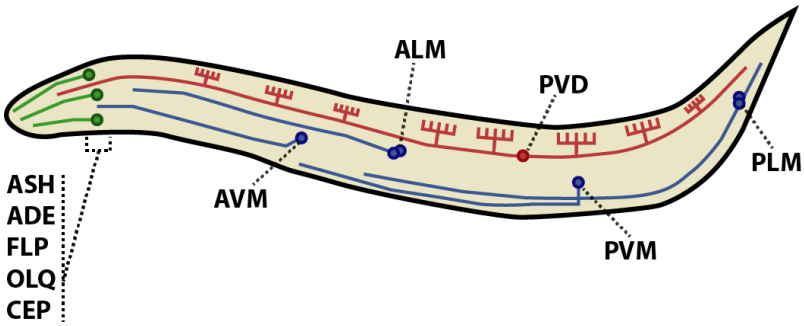

Fig 1.4: Mechanosensory neurons in *C. elegans*. The main mechanosensory neurons in *C. elegans* include the harsh-touch neurons (PVD, in red), ciliated head neurons (in green), and the gentle body touch neurons (in blue). Most neurons are bilateral but only one side is shown for simplicity.

The simple genetics of *C. elegans* make it especially attractive for basic biological research, with forward genetic screens proving successful in identifying novel genes involved in a number of processes. In particular, Martin Chalfie led the charge in categorizing a plethora of genes involved in touch receptor function and development (Chalfie & Sulston 1981). The best characterized mechanosensory proteins in *C. elegans* are the DEG/ENaC channels, particularly the MEC-4 complex for gentle touch sensation (Chalfie 2009; O'Hagan et al. 2005; Goodman et al. 2002). The complex is formed of the MEC-4 and MEC-10 proteins, which serve as pore-forming subunits, accessory proteins MEC-6 and MEC-2, which affect the lipid environment

around the channel, and a specialized extracellular matrix composed of MEC-5, MEC-1 and MEC-9. Mutations in MEC-4 or MEC-10 were found to leave the structure of touch receptor neurons intact but rendered them insensitive to mechanical stimuli (Bazopoulou & Tavernarakis 2007). They were further shown to interact by co-immunoprecipitation (Goodman et al. 2002), co-expression (Huang & Chalfie 1994), and through genetic interactions (Gu et al. 1996). Verification that the MEC-4/MEC-10 complex is mechanically gated came from patch clamp recordings that showed external forces result in mechanosensory currents carried by Na^+, and that mutation of select residues affects ion selectivity of the channel (O'Hagan et al. 2005). Subsequently, MEC-6 (Chelur et al. 2002) and MEC-2 were shown to coimmunoprecipitate with the rest of the channel complex (Goodman et al. 2002), and MEC-2 was found to be needed for activation of the channel (Zhang et al. 2004). Finally, a number of periphery anchoring proteins necessary for the channel's function were identified: the β tubulin MEC-7 and α tubulin MEC-12 intracellularly (Gu et al. 1996), and the extracellular matrix proteins MEC-1, MEC-5 and MEC-9 (Chalfie & Sulston 1981; Emtage et al. 2004) (**Fig 1.5**). Together, these components make up one of the best-defined mechanosensory units in the animal kingdom, reflecting the power of studying these complex units in a simple organism.

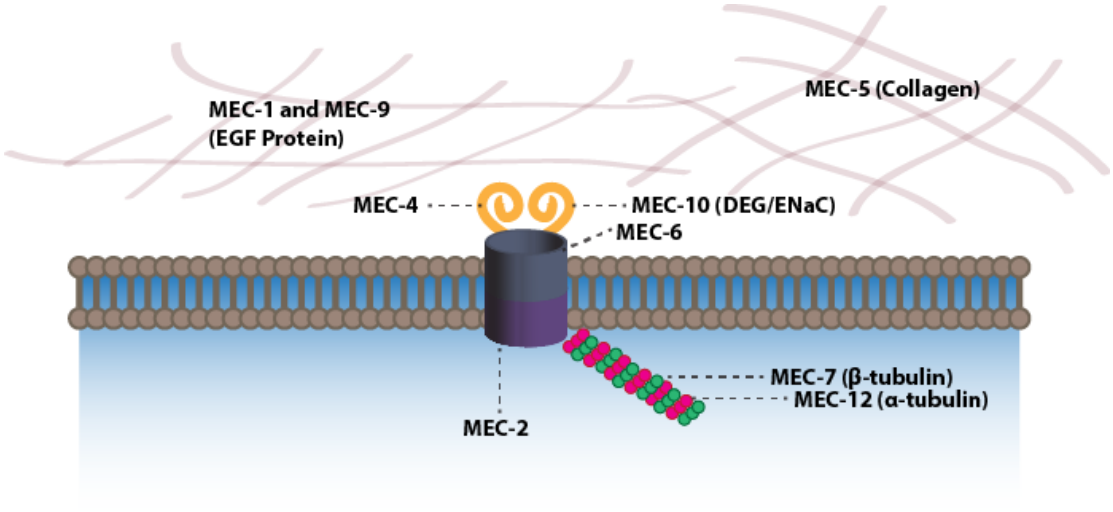

Fig 1.5: The gentle touch machinery of *C. elegans*. The channel complex itself is composed of the subunits MEC-4 and MEC-10, which are anchored to the membrane by MEC-2 and MEC-6. Extracellular linkages are achieved with MEC-1, MEC-9 and the collagen MEC-5, while the channel is attached intracellularly to the specialized microtubules MEC-7 and MEC-12

In addition to the gentle touch machinery, another well-characterized complex in *C. elegans* is the nose touch circuit in ASH. ASH is a polymodal nociceptor in the head of the worm that responds to touch, osmotic pressure and certain odorants (Bazopoulou & Tavernarakis 2007). This nose touch response is absent in animals with a mutation in *osm-9*, the homolog of the TRPV4 channel (Colbert et al. 1997). OSM-9 localizes to the sensory cilia at the end of these neurons and is dependent on the TRPV proteins OCR-2 and OCR-9 for correct localization (Tobin et al. 2002). It is a six-transmembrane domain protein with a number of N-terminal Ankyrin motifs (Bazopoulou & Tavernarakis 2007), a structural feature that confers elasticity and acts as a critical tether mechanism in another mechanosensitive TRPN homolog; the drosophila NOMPC channel (W. Zhang et al. 2015).

These are just a few examples of the mechanosensory circuits found in *C. elegans*, though the organism also has behavioural responses to harsh and gentle touch, nose touch, osmotic sensation, contact with food, and stimuli evoked during male-mating (Riddle DL, Blumenthal T, Meyer BJ 1997) (**Table 1.2**). Touch stimuli will evoke reversal or accelerative behavioural responses away from the stimuli, with different sets of neurons responsible for detecting gentle or harsh touch (Chalfie & Sulston 1981). Sensory neurons in the worm's head are able to respond to multiple noxious stimuli including mechanical touch, pain, hot or cold temperatures, and osmolarity. They are similar in certain capacities to the multidendritic nociceptors found in humans – making *C. elegans* sensory neurons an ideal model for these studies.

Mechanosensitive Behaviour	Neurons Involved
Gentle body touch	ALM, AVM, PLM, PVM
Harsh body touch	PVD, PVC
Head-on collision	ASH, FLP, OLQ
Head withdrawal	OLQ, IL1
Proprioception	Ventral motor neurons, DVA
Tap withdrawal	ALM, PVM, PLM, AVD
Basal Slowing	CEP, ADE, PDE

Table 1.2: Mechanosensitive behaviours of *C. elegans*. Body and head touch responses detect stimuli on the animal's cuticle, while proprioceptors sense muscle contractions and relaxations. Basal slowing occurs in response to changes in the culture substrate the animal is on, and the tap response is a withdrawal in reaction to vibrations in the substrate.

1.4 Structure of mechanosensory channels and the vertebrate hair cell mechanotransducer

Ion channels are often made up of several subunits, usually homologous structures that arrange to leave a central pore. As described previously, work in *C. elegans* has identified a number of protein subunits required to form a mechanosensitive channel in the primary mechanosensory neurons (O'Hagan et al. 2005). Progress in higher organisms has been much slower and met a number of hurdles. One question that still eludes researchers is the identity of the vertebrate hair cell mechanotransduction channel – although many plausible molecules have been put forward, none have been definitively confirmed.

Ion channels are gatekeepers of cells, ensuring that the resting membrane potential of approx. -70mV is preserved. Additionally, channel opening and the subsequent flow of ions is the mechanism of electrical signaling in nerves. Channels that are potassium- (outward flowing) or anion-selective will hyperpolarize (make more negative) cells, whereas calcium-, sodium- or non-selective cation channels will depolarize (make more positive) cells. Calcium may also double as a second messenger. In general, ion channels can be opened in a number of ways, including changes in membrane voltage or tension, and by ligand gating or other chemical signals. For many years it has been assumed that mechanosensory channels must be directly gated by force due to their rapid reactions to stimuli (Corey & Hudspeth 1983).

In humans, the hair bundle is the mechanosensitive organelle responsible for our ability to hear. It is composed of actin-based stereocilia arranged in rows of increasing height, with extracellular linkages called tip-links thought to be responsible for conveying forces to mechanically gated channels (Gillespie & Walker 2001). Movement of these cilia therefore transmits information relating to sound, movement, and body position (Hudspeth & Jacobs 1979; Vollrath et al. 2007). In an effort to determine the identity of the channel, its transduction and adaptation properties have been extensively characterized, unfortunately finding nothing to meaningfully distinguish it from a pool of candidates (Gillespie & Walker 2001). The vertebrate hair cell mechanotransducer is known to be a non-selective cation channel with a large conductance (about 100pS) and substantial permeability to Ca^{2+} (Corey & Hudspeth 1979a; Crawford et al. 1991; Ricci & Fettiplace 1998). It is blocked by amiloride (Rüsch et al. 1994), Ca^{2+}-channel antagonists (Baumann & Roth 1986; Jørgensen & Kroese 1995), and aminoglycoside antibiotics (Kroese et al. 1989).

Although the identity of the channel is elusive, a number of essential accessory proteins have been identified. Within stereocilia, the channel is believed to be secured to actin filaments by myosin 1c, which may be involved in hair cell adaptation (Holt et al. 2002; Stauffer et al. 2005). Adaptation is an important process which helps reject constant, low level stimuli so that biologically relevant stimulus changes can be distinguished (Vollrath et al. 2007). This could be achieved by readjustment of tension in some aspect of the complex through an active process, although it is still not well understood (Gillespie & Walker 2001).

Additionally, cilia are connected to each other by the tip link complex, which is formed of protocadherin 15 (PCDH15) at the lower end and cadherin 23 (CDH23) at the upper end (Kazmierczak et al. 2007; Pan & Holt 2015). Another protein known to interact with the tip link complex that is likely an accessory subunit to the channel is TMHS (Xiong et al. 2012). Alternative splicing of any of these components can also affect their function and interactions with each other. For example, Zhao et al. (2014) suggest that alternative splicing of PCDH15 is responsible for changing the manner in which it interacts with TMIE, another accessory protein which may in turn be responsible for variations in the responsiveness of the hair cell mechanotransducer channel along the tonotopic axis of the cochlear.

More recently, PCDH15 has also been shown to interact with the transmembrane channel-like (TMC) proteins TMC1 and TMC2 (Maeda et al. 2014), components which are required for hair cell mechanotransduction (Kawashima et al. 2011), and which are linked to a number of forms of deafness in humans (Kurima et al. 2002; Vreugde et al. 2002). Additionally, TMHS has been shown to be required for proper localization of TMC1 to the tips of stereocilia, and may stabilize its reaction with PCDH15 (Beurg, Xiong, et al. 2014). As a result, TMC proteins are one of the more promising candidates for the hair cell mechanotransduction channel to have been put forward.

1.5 The transmembrane channel-like family of proteins

TMC proteins are characterized by the so-called TMC domain (CWETXVGQEly(K/R)LtvXD), which is broadly conserved between species

(Keresztes et al. 2003). There are two TMC genes in *C. elegans*, and eight vertebrate members that are categorized into three subfamilies. Members of subfamily A, consisting of TMC1, TMC2 and TMC3, are more restrictively expressed and have been mostly implicated as having roles in sensory transduction (Keresztes et al. 2003). The subfamily A members are the longest of the TMC genes, ranging from 757 to 1130 amino acids in length in mice, with most of this increased length compared to the other subfamilies coming from a longer loop in the region around the conserved TMC domain (Keresztes et al. 2003). Furthermore, there is 36-56% overall sequence identity within subfamily A, and conservation of position for more than 73% of introns in the genes' core region (Keresztes et al. 2003).

Subfamily B consists of TMC5 and TMC6, while TMC4, TMC7 and TMC8, the shortest TMC proteins, make up subfamily C. Both subfamily B and C members are much more widely expressed than subfamily A, with mRNA detected in most major organs in mice (Kurima et al. 2003; Keresztes et al. 2003). TMC6 and TMC8 have been implicated in epidermodysplasia verruciformis, a condition which increases susceptibility to HPV virus infections and their associated skin cancers (Ramoz et al. 2002; Kurima et al. 2003). The functions of most of the other TMC proteins are unknown, but because of their much broader expression, they are not of interest to this thesis. Interestingly, Keresztes et al. (2003) suggest that the two *C. elegans* subfamily A-like proteins may be representative of a primordial TMC protein sequence that existed prior to the expansion of the protein family (**Fig 1.6**).

Fig 1.6: Phylogeny of the TMC genes in humans, mice and *C. elegans*. TMC proteins cluster into three subfamilies: A, comprising TMCs 1-3; B, comprising TMCs 5-6; and C, comprising TMCs 4, 7 and 8. The *C. elegans* family members are distinct but most closely related to subfamily A. Image reproduced from Keresztes et al. (2003).

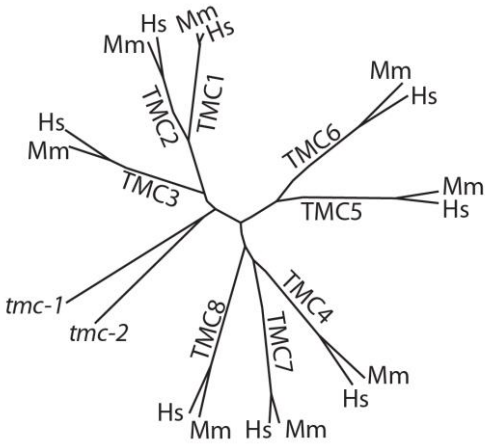

In humans, mutations in *TMC1* have been linked to two nonsyndromic deafness loci - DFNA36, which covers a dominant mutation in *TMC1* and is linked to progressive hearing loss, and DFNB7/B11, comprising a recessive mutation of *TMC1* that is linked to profound congenital deafness (Kurima et al. 2002; Vreugde et al. 2002). These mutations are recapitulated in the mouse models Beethoven (*Bth*) and deafness (*dn*), respectively. In addition to the crucial role of TMC1, its homolog, TMC2, also plays an important redundant role at early developmental time points. In *Tmc1* mutant animals, TMC2 expression can still compensate for its function in mice aged up to postnatal day eight, before the switch from TMC2 to TMC1 expression is complete. Thus, although not the main mediator of hearing, TMC2 expression is sufficient to maintain mechanotransduction currents in young animals for a short period of time in the place of TMC1 (Kawashima et al. 2011).

There is an increasing body of evidence that TMC1 may be the long sought-after mechanotransduction channel responsible for transmitting mechanical stimuli in hair cell cilia, but this has not yet been definitively confirmed. Thus far, it has only been

shown that TMC1 is necessary for mechanotransduction and that it is expressed in vestibular and cochlear hair cells at the appropriate times (Kawashima et al. 2011), and at the site of mechanotransduction (Kurima et al. 2015). Any attempts to express TMC1 and TMC2 in heterologous systems have been unsuccessful, with the expressed proteins not being trafficked to the membrane where they could be tested for channel properties (Kawashima et al. 2011). Additionally, although many *Tmc1* mutations that cause deafness seem to cluster around a few key amino acids that may be necessary for its wild type function, it has not been possible to assert whether this is the channel pore region. Using the *Bth* mutant in IHCs, Pan et al. (2013) showed that TMC1 and TMC2 are at the very least components of the hair cell mechanotransduction channel, and that they contribute to its permeation properties. Corns et al. (2016) have replicated this finding in OHCs, where the same mutation (*Bth*) was shown to reduce calcium permeability and conductance of the mechanotransduction channel.

Although TMC1 and TMC2 are clearly involved in sensory transduction, the final subfamily A member, TMC3, has not been well studied. The only significant publication surrounding this gene is the identification of a new nonsyndromic deafness locus (DFNB48), which maps to a region of chromosome 15 that contains *TMC3*, making it a candidate gene (Ahmad et al. 2005). However, further studies indicate that *CIB2* is the causative gene at the DFNB48 locus. *CIB2* encodes a calcium binding protein that is localized to mechanosensory stereocilia of the inner ear hair cells in mice, and is responsible for helping to maintain calcium homeostasis (Riazuddin et al. 2012). Interestingly, CIB2 interacts with TMC1 and can enhance

mechanosensory responses when co-expressed with this protein in heterologous systems (unpublished work, Yiquan Tang).

In *C. elegans*, the two TMC genes have been shown to have more diverse functions. *tmc-1* plays a role in sensing aversive stimuli such as high levels of salt, and is believed to be the sodium specific receptor (Chatzigeorgiou et al. 2013). In comparison, *tmc-2* is implicated in mechanotransduction in some neurons (unpublished work, Marios Chatzigeorgiou), with initial work indicating that TMC-2 may be responsible for harsh touch responses in the PVD neuron. TMC-2 expression is enriched in PVD (Smith et al. 2010), a nociceptive neuron that has been shown to sense harsh touch and cold (Way & Chalfie 1989; Chatzigeorgiou et al. 2010). These results demonstrate that although *C. elegans tmc-1* and *tmc-2* are distantly related to vertebrate subfamily A members, they still maintain a conserved function in sensory transduction.

1.6 Conclusion and project aims

TMC proteins have recently emerged as promising candidates that could function as part of the vertebrate hair cell mechanotransduction channel. There is strong evidence that TMC1 and TMC2 have a core role in hearing, but the closely related protein TMC3 remains relatively uninvestigated. Like the other subfamily A members, TMC3 is more restrictively expressed than TMCs 4 to 8, but the function of TMC3 is still unknown, with very few studies focusing on this last subfamily A member. The high level of sequence similarity within TMC subfamily A (Keresztes et al. 2003) is suggestive of the fact that there could be some preservation of the genes' function.

Although TMC3 is not expressed in *C. elegans*, previous work from our laboratory has shown that murine TMC proteins can be functionally expressed in worm neurons (unpublished work, Marios Chatzigeorgiou). As such, the primary aim of my project is to determine what function, if any, TMC3 plays in sensory transduction, through heterologous expression of murine TMC3 in *C. elegans*. Alongside this goal, I will be further characterizing the function of the other murine TMC proteins both *in vivo* and *in vitro*, particularly focusing on elucidating the structure and functional characteristics of the proteins. While most work on the TMC proteins thus far has been focused on their role in hearing, I will also be investigating whether they have a more general mechanosensitive function elsewhere in the body. These results may give vital clues as to whether mechanosensory proteins are intrinsically touch sensitive, or if such a function is context-dependent.

Chapter 2: Identifying a novel function for TMC3 using *C. elegans*

2.1 Introduction

For many years, TMC proteins have been suggested as leading candidates to form part of the hair cell mechanotransduction machinery, or to have a more general function in mechanosensation (Holt et al. 2014; Fettiplace 2016). Numerous studies have confirmed that TMC1 and TMC2 are crucial for mechanotransduction in the inner ear of mice and are strongly linked to deafness in humans, but their exact function remains elusive. Mutations in *Tmc1* result in the loss of mechanosensory currents and alteration of the conductance and Ca^{2+} selectivity of the hair cell channel, meaning that if it is not the pore forming subunit then it must be very intimately related to the mechanotransduction channel. While the role of these proteins will be addressed (particularly in later chapters), the primary aim of this project is to determine if the final member of this subfamily, TMC3, plays a similar role in sensory transduction.

Human and mouse TMC1 and 2 share around 60% sequence homology, while both human and mouse TMC3 have more than 40% sequence similarity over the length of the transcript (**Table 2.1**). Previous studies have also shown that these proteins are more restrictively expressed than the rest of the TMC family (Keresztes et al. 2003). In mammals TMC1 and TMC2 are expressed in the cochlear (Kawashima et al. 2011), and hair cells also express TMC3, TMC4 and TMC7 (Corey & Holt 2016). Research in chickens has also identified Tmc1, Tmc2, Tmc3 and Tmc6 in the basilar

papilla, the sensory organ homologous to the Organ of Corti of the mammalian cochlear (Mutai et al. 2005). Taken together, this shared expression and evolutionary similarity has led us to hypothesise that TMC3 may also have a function in sensory transduction like the rest of the members of TMC subfamily A.

	hTMC3						
mTmc3	81.55	**mTmc3**					
hTMC1	41.34	40.96	**hTMC1**				
mTmc1	40.97	40.87	96.55	**mTmc1**			
hTMC2	43.04	42.28	57.92	57.24	**hTMC2**		
mTmc2	42.19	40.81	58.00	57.58	83.33	**mTmc2**	
tmc-1	35.97	34.68	33.15	32.82	33.46	33.42	***tmc-1***
tmc-2	32.54	32.70	32.13	31.21	31.69	31.68	42.08

Table 2.1: Percent Identity Matrix for TMC gene family members, showing sequence homology (%). Created with Clustal2.1, see also **Fig 1.6** in Chapter One.

In contrast to *Tmc1-/-* and *Tmc2-/-*, OHC mechanotransduction currents in *Tmc3 -/-* mice are normal, and knocking out *Tmc3* in combination with *Tmc1*, *Tmc2*, or both, does not further disrupt mechanotransduction in the ear (Beurg, Kim, et al. 2014). Regardless, with increasing evidence of the TMC genes functioning in other capacities besides hearing (Chatzigeorgiou et al. 2013; L. Zhang et al. 2015), this does not rule TMC3 out as a potential sensory protein functioning elsewhere in the body. Because the identity of the hair cell mechanotransducer is still unknown, we cannot say if it functions solely in the ear for hearing, or if it is expressed throughout the body, with its function dependent on the specialized microenvironment around it. Even within the ear, the channel's sensitivity is finely tuned along the tonotopic gradient (Ricci et al. 2003), suggesting at least some dependence on location for function. The operating frequency of the hair cell channel is significantly higher than

other mechanosensory channels (up to 100kHz compared to 100Hz) (Effertz et al. 2015) – but could this difference be due to their unique environments and cofactors – or are completely different channel proteins at work? Because of this huge variety in the function of mechanosensory proteins, we believe a more general role for the TMCs in mechanosensation outside of the ear cannot be excluded, and expect to find components of the hair mechanotransduction apparatus in other sensory systems throughout the body.

Another confounding factor is the so-called 'anomalous' mechanotransduction currents which have been observed in vertebrate hair cells. Also called 'reverse-polarity' currents, they are observed when the tip links between stereociliary bundles are disrupted, interrupting the channel's normal response to deflections of the hair bundles towards their tallest edge. Instead, a mechanical current can be evoked by deflection of the hair bundles near their base in the opposite (negative) direction (Marcotti et al. 2014). This current persists in *Tmc1/Tmc2* double mutants, and can be elicited early in development, before the onset of normal mechanosensory currents. Clearly, TMC proteins are not as important in this context and other factors must be required for these reverse polarity currents (Beurg et al. 2016).

Although the reverse polarity current has some similarities to that from the main mechanotransduction channel, it lacks the rectification seen in normal currents and is not blocked by the same pharmaceutical agents (Marcotti et al. 2014). After much debate, recent work has excluded the PIEZO1 channel (Corns & Marcotti 2016) and instead identified PIEZO2 as the source of these anomalous currents (Wu et al. 2016). This exemplifies how even within one structural unit like the hair cell, many different

mechanosensory molecules can be at work, acting distinctly from each other. Significantly, we have observed that mechanosensory molecules can be repurposed in different functions throughout the body – PIEZO2 has now been shown to be involved in rapidly adapting touch sensation in Merkel cells (Sanjeev S. Ranade et al. 2014), in proprioception (Woo et al. 2015; Florez-Paz et al. 2016), and in mechanically-activated gastrointestinal secretion in the small bowel (Wang et al. 2016). On this basis, there is significant merit both in confirming whether TMC proteins are the mechanosensory unit in hair cells, but also in investigating whether they function in other forms of mechanosensation, such as touch, proprioception or nociception.

One of the key requirements for identifying a channel protein is that it must be reconstituted and function when expressed in heterologous systems (Arnadóttir & Chalfie 2010). While there have been many failed attempts at expressing the TMCs in mammalian cell culture (Kawashima et al. 2011), we have shown that human and mice TMC genes can be functionally expressed in worm neurons such as the ASKs and IL2s (Chatzigeorgiou et al. 2013). Fluorescently tagged TMC proteins can be observed trafficking to the specialized ciliary endings of these neurons, indicating that the difficulties encountered with detainment in the endoplasmic reticulum (ER) in higher organisms are absent in *C. elegans*. As a result, we have been utilising *C. elegans* as a heterologous system in which to dissect the function of the TMCs. Using *C. elegans* allows us to narrow down the search for these genes' function with calcium imaging, before returning to mouse experiments to confirm their effect.

The model neuron being used is the bilateral pair of ASKs, found in the head of the worm (**Fig 2.1**). ASK neurons are ciliated and open to the outside environment, allowing direct detection of chemicals and odourants (Altun et al. 2014). The presence of these cilia is another benefit of using worm neurons as an expression system, since a number of vertebrate sensory processes also rely on primary cilia. For example, specialized cilia can be found in the rod and cone cells of the visual system, in olfactory neurons and in the vertebrate hair cell apparatus (Bae & Barr 2008). Despite these exposed cilia in *C. elegans*, we have shown the ASKs are unresponsive to mechanical touch stimuli and most chemicals (including salt), allowing them to be used as an inert system to ectopically express our proteins of interest in. Other studies have shown that the ASKs are normally responsive to a more limited range of stimuli such as pheromones, quinine or lysine (Bargmann & Horvitz 1991; Hilliard et al. 2004; Macosko et al. 2009).

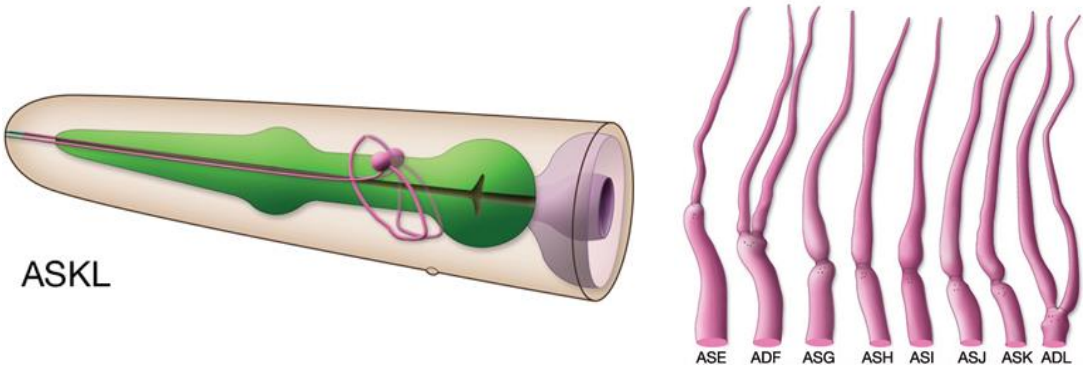

Fig 2.1: Location of the ASK neurons and example of their ciliated endings. Images taken from WormAtlas (Altun et al. 2014).

In line with the main aim of my project, to characterise TMC3, I generated lines that heterologously express both murine and human TMC3 in *C. elegans* in order to determine its function. We can then stimulate animals that ectopically express TMC3

with a range of aversive stimuli in the aim of identifying its agonists and characterizing the function of this largely ignored subfamily member.

2.2 Results

2.2.1 Uncovering a novel mechanosensory function of TMC3

The ASK neurons are not believed to respond to salt or touch stimuli, but in order to confirm this I defined the native response of the ASKs using the cameleon protein YC3.60 expressed under the ASK-specific *sra-9* promoter. Cameleon allows us to visualize the influx of calcium when a neuron is activated, and has previously been utilized to show that ASH, another ciliated sensory neuron, shows a robust response to a 10s flow of 500mM NaCl (Chatzigeorgiou et al. 2013). Wild type animals with the cameleon protein (strain AQ3093) did not respond to the 500mM NaCl salt solution, confirming that ASK is not a sodium sensor. The recordings did show a slight downward trend in the fluorescence ratio, which we have found to be characteristic of recordings from the ASK neurons. I went on to test mechanosensation, using a nose press paradigm that lasts for 10s. Once again, the ASK neurons remained unresponsive, confirming they will act as an inert neuron in which to examine TMC3 function (**Fig 2.2**).

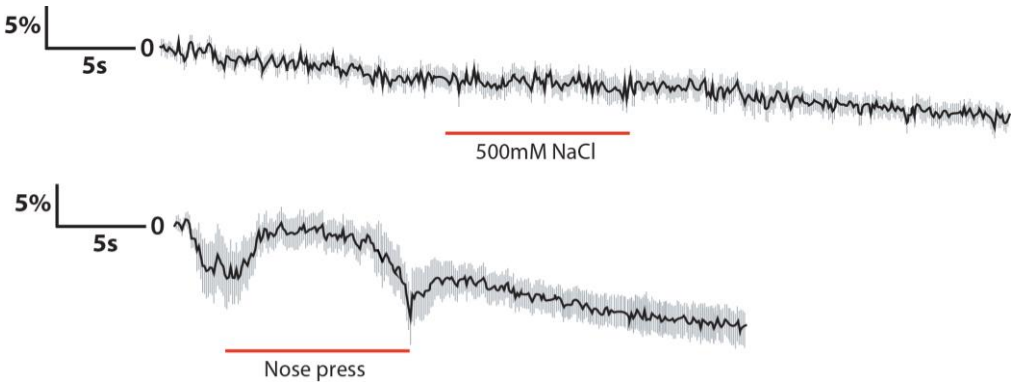

Fig 2.2: Calcium responses to 500mM NaCl and touch stimuli in the ASK neurons of wild type animals. Traces show the average change in fluorescence ratio of YFP to CFP (R/R_0), with the red line indicating stimulus application. Grey shading shows the SEM of the mean response. n >19 individual recordings.

Using a *Tmc3* construct that has been codon-optimized for expression in *C. elegans*, I engineered an expression cassette for the ASK neurons and injected this plasmid into the ASK::YC3.60 line to generate the TMC3 imaging line AQ3353. These animals were then probed with the same salt solution used on wild type animals, but remained unresponsive even with TMC3 expression (**Fig 2.3**). This suggests that expressing TMC3 alone is not sufficient to provide salt sensitivity, unlike its homolog in *C. elegans*, TMC-1 (Chatzigeorgiou et al. 2013).

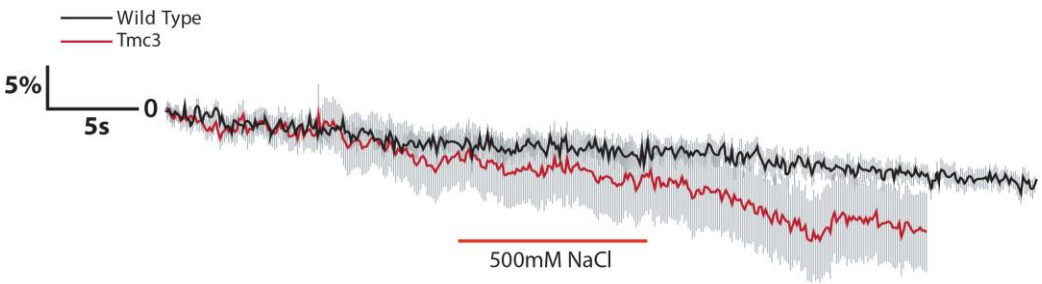

Fig 2.3: Salt responses in ASK neurons ectopically expressing TMC3 are not significantly different from the endogenous baseline. Traces show the average change

in fluorescence ratio of YFP to CFP (R/R_0), with the red line indicating stimulus application. Grey shading shows the SEM of the mean response. n >13.

Subsequently, the TMC3 expressing animals were tested for mechanosensory responses using the nose press paradigm. Unlike the wild type, animals ectopically expressing TMC3 showed a significant mechanosensory response when poked for 10s (**Fig 2.4**). These results indicate that TMC3 expression is sufficient to constitute a mechanosensor, either alone or by utilizing accessory proteins that are native to the worm.

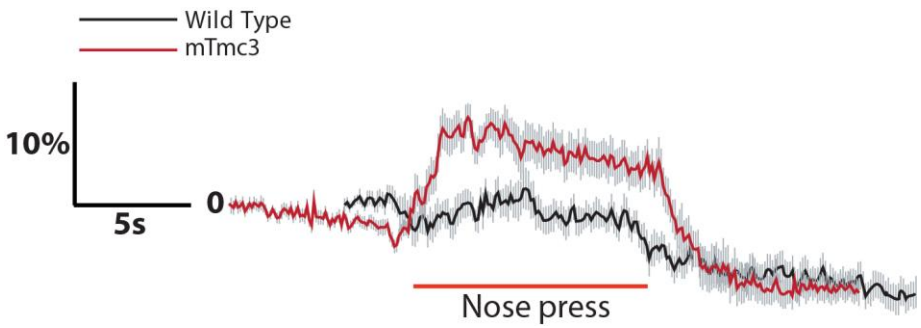

Fig 2.4: Ectopic expression of TMC3 in the ASK neurons confers a mechanosensory response to *C. elegans*. Traces show the average change in fluorescence ratio of YFP to CFP (R/R_0), with the red line indicating stimulus application. Grey shading shows the SEM of the mean response. n > 20.

2.2.2 Human TMC3 also functions in mechanosensation

In addition to the murine *Tmc3*, I also engineered a *C. elegans* expression cassette for human *TMC3*, expressing it in the ASK neurons along with the YC3.60 cameleon indicator (line AQ3690). As with the murine protein, ectopic expression of human TMC3 resulted in a mechanosensory response that was not seen in wild type animals,

again suggesting that TMC3 expression alone is sufficient for mechanosensation (**Fig 2.5**).

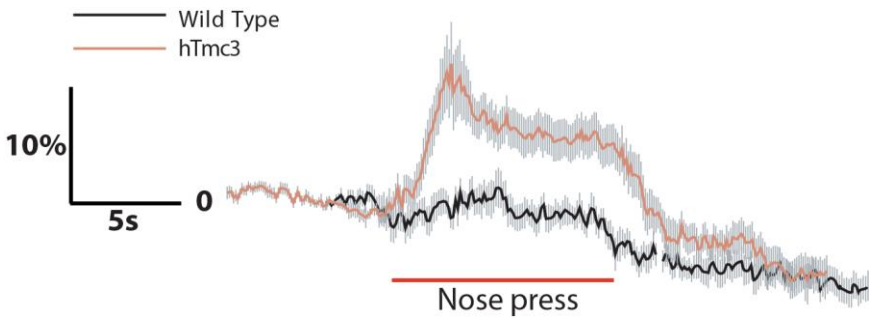

Fig 2.5: Ectopic expression of human TMC3 in ASK neurons generates a mechanosensory response in *C. elegans* ASK neurons. Traces show the average change in fluorescence ratio of YFP to CFP (R/R_0), with the red line indicating stimulus application. Grey shading shows the SEM of the mean response. n > 20.

2.2.3 The CIB2 homologue CALM-1 is required for mechanosensory responses in *C. elegans*

Although the heterologous expression experiments would suggest that both mouse and human TMC3 are sufficient to generate mechanosensory responses in *C. elegans*, it is possible that they are making use of endogenous proteins in the worm that help to form the mechanosensor. Indeed, most known mechanosensory channels are formed of multiple components (Schafer 2014; Chen et al. 2015), and past attempts to ectopically express TMC proteins in cell culture systems have failed due to the presumed lack of supporting subunits (Labay et al. 2010; Kawashima et al. 2011). Since *C. elegans* does express its own native forms of the TMC proteins (TMC-1 and

TMC-2), though not in the ASK neurons, it is possible that its nervous system is already primed with the supporting proteins necessary to ensure TMC function.

Other work in our laboratory has identified the calcium binding protein CIB2 and its *C. elegans* orthologue CALM-1 as potential interactors with the TMC proteins (unpublished work, Yiquan Tang). We therefore considered it possible that CALM-1, which is widely expressed in *C. elegans* neurons, may be able to interact with the ectopically expressed TMCs and facilitate their function. To test this hypothesis, I looked at the Tmc3 imaging strain with an additional background of either *calm-1 (tm1353)* mutation or CALM-1 overexpression. Overexpression of CALM-1 did not appear to have a significant effect on the mechanosensory response in TMC3 expressing animals, but *calm-1* mutation completely abolished this activity (**Fig 2.6**).

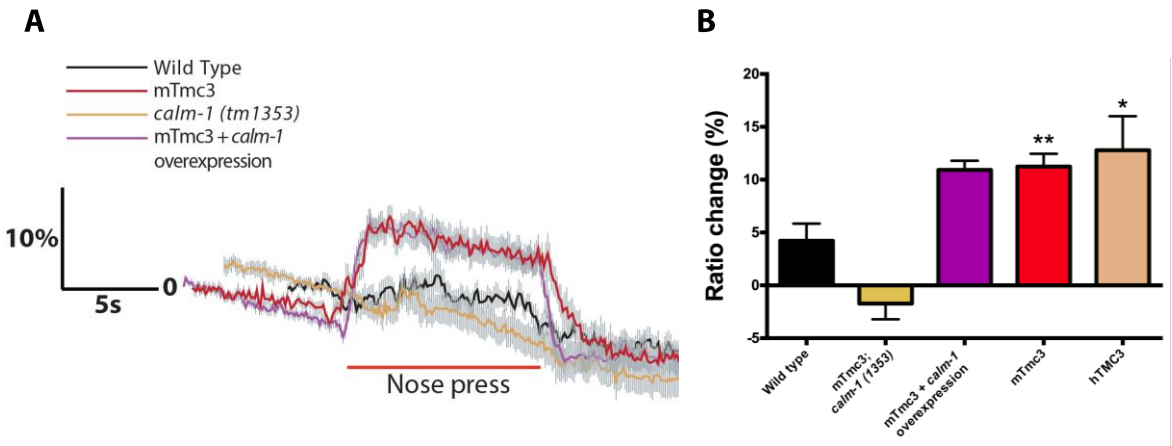

Fig 2.6: Mutation of the *C. elegans* gene *calm-1* abolishes the ectopic mechanosensory response conferred by TMC3 expression in the ASK neurons. However, CALM-1 overexpression does not appear to significantly increase the mechanosensory response. **A)** Traces show the average change in fluorescence ratio of YFP to CFP (R/R_0), with the red line indicating stimulus application. Grey shading shows the SEM of the mean response. **B)** Columns show peak R/R_0 with SEM error

bars. Statistical significance calculated with t-test compared to wild type (* P<0.05, ** P<0.01). n > 20.

TO ADD: hTMC3 with calm-1 mutation, CIB2 and CIB3 overexpression with Tmc3.

2.3 Discussion and conclusions

In these experiments, I have revealed a novel function for the previously unstudied TMC protein, TMC3. TMC1 and TMC2 have been closely linked to normal mechanosensory function in hair cells, leading to deafness in humans and mice that carry mutations. However, *Tmc3* knockout mice had not been found to have any defects in mechanotransduction currents in cochlear hair cells (Beurg, Kim, et al. 2014), or in an auditory brainstem response (Brown & Moore 2012). Despite this, we hypothesized that its similarity to *Tmc1* and *Tmc2* and common descent meant it was possible that *Tmc3* may still have some function in another form of sensory transduction.

I have demonstrated that both mouse and human TMC3 are capable of generating an ectopic response to mechanosensory stimuli when heterologously expressed in *C. elegans* neurons, suggesting they may be a key component of the mechanotransduction machinery in mammals. This was an unexpected result, as previous attempts to heterologously express TMC proteins have failed due to protein mislocalisation and lack of function, presumably due to the absence of crucial accessory proteins and other channel subunits. However, further clues as to how these proteins function in *C. elegans* began to emerge when we studied the calcium binding protein CIB2, which has a homologue in worms designated CALM-1.

CIB2 mutations have been identified as the causative factor behind non-syndromic deafness form DFNB48 (Riazuddin et al. 2012), a loci which was first hypothesized to include TMC3 as a protein of interest (Ahmad et al. 2005). More recently, unpublished work from our own laboratory (Yiquan Tang) has shown that CIB2 is able to physically interact with TMC1, and may therefore be a component of the vertebrate hair cell mechanotransducer. Based on this discovery, we thought that the endogenous form of the protein in *C. elegans*, CALM-1, may be acting to allow the ectopically expressed TMCs to function correctly. This appears to be the case, as I have shown that expressing TMC3 in *C. elegans* that also have a mutation in *calm-1 (tm1353)* completely abolishes the ectopic mechanosensory response. Taken together, these results suggest that TMC3 is a crucial component of a mechanosensory complex, and that its presence is necessary to generate a response to touch stimuli. However, by looking at mutations of *calm-1*, it is clear that other components are needed to maintain this response, meaning TMC3 alone is not sufficient to form the mechanosensor.

In most mammalian systems, mechanotransduction is thought to rely on a series of tethers that help to keep the mechanotransduction channel at the correct tension and that transmit force onto it – so it is particularly interesting that a usually touch-insensitive *C. elegans* neuron can adopt such a complex response with the addition of a single component (TMC3 expression). In the touch receptor complex found in the primary mechanosensory neurons of *C. elegans*, the channel is anchored to specialized microtubules by a series of proteins (the MEC complex outlined in Chapter One). Is TMC3 able to co-opt similar proteins to tether itself, or is it an intrinsically touch-sensitive channel that can be pushed open by stimuli? We hope

that using *C. elegans* to examine the structure of the TMC proteins will help us to unravel these mysteries. For example, amongst the *C. elegans* and murine TMCs, there are mechanosensors (*tmc-2*, *Tmc1* and *Tmc3*), chemosensors (*tmc-1*), and *Tmc2*, which seems to function as both – so how are such similar proteins able to adopt such distinct functions? Are these proteins fundamentally different, or do their functions diverge based on the location of expression and interacting partners? Going forward, we will need to study the structure and function of the TMC proteins in more detail, in order to determine exactly how they function in sensory transduction. In particular, knowledge of the membrane topology of the TMCs and of which domains are important for their ability to interact with accessory units may enable us to unravel other components of the mechanosensor.

2.4 Materials and methods

2.4.1 Maintenance of *C. elegans* and basic techniques

All *C. elegans* strains were maintained at room temperature (approximately 22°C) on nematode growth medium (NGM) agar plates seeded with OP50 *Escherichia coli* bacteria for animals to feed on (Brenner 1974). Unless stated otherwise, animals were analyzed and scored at the young adult stage.

Transgenic animals can be generated by injecting plasmids into the worm gonad, resulting in an extrachromosomal array that stably transmits this cassette on to progeny (Mello et al. 1991). Microinjections were performed using standard methods (Mello et al., 1991) with an inverted Zeiss AxioObserver microscope equipped with

differential interference contrast (DIC), a Narishige needle holder, and an Eppendorf FematoJet Pump. Promoters and coinjection markers were injected at the following concentrations: P*sra-9* (80ng/ul), *unc-122::rfp* or *unc-122::gfp* (50ng/ul), *elt-2::rfp* (30ng/ul).

For CALM-1 overexpression, strain AQ3670, containing the ljEx919 CALM-1 expression cassette, was crossed into the AQ3353 TMC3 imaging line to generate strain AQ3730. For *calm-1 (tm1353)* mutants, males (strain AQ3524) were crossed with AQ3353 to generate strain AQ3705. Genotyping of *calm-1 (tm1353)* mutant progeny was conducted using the primers GAACGAGATTCTTCGTAGCAA GATGACT, AACTTATTCGCTGAATTTTTGAATTTTTGGC, and AACTT CCTCGTGATCCTGAAGGCG on genomic DNA templates obtained from whole animal lysates (Wicks et al. 2001).

2.4.2 Molecular biology and *Tmc3* cloning

Molecular biology was performed using standard techniques (Sambrook et al. 1989). To investigate TMC3, I began by obtaining synthesized (Life Technologies), *C. elegans* codon optimized transcripts based on both the murine and human TMC3 (Redemann et al. 2011). Standard Gateway cloning approaches (Life Technologies) were used to create a P*sra-9::Tmc3::unc-54* and P*sra-9::TMC3::unc-54* expression cassette for the ASK neurons, which was then injected into the gonads of hermaphrodite worms carrying the extra-chromosomal imaging array P*sra-9::YC3.60* (strain AQ3093), to specifically examine calcium responses in the ASK neurons.

2.4.3 *In vivo* calcium imaging

Although electrophysiology is a more informative tool for measuring neuronal activity, the small size of *C. elegans* make this a difficult (but not impossible) technique. Instead, genetically encoded calcium sensors such as Cameleon have become a popular method to record neural responses in *C. elegans*. These sensors can be specifically expressed in the target neurons, and use fluorescence resonance energy transfer (FRET) to detect calcium influxes in response to sensory stimuli. Cameleon is formed of the fluorophores YFP and CFP, normally separated by a calmodulin-binding domain (Nagai et al. 2004). Upon calcium influx, the fluorophores are brought together and the change in fluorescence intensity gives a measure of the intracellular calcium response. I have used this sensor as a read-out of channel opening after stimulation of immobilized worms.

Recordings are performed on a Zeiss Axioskop 2 upright compound microscope with a 63x Zeiss Achroplan water-immersion objective, equipped with a Dual View beam splitter and a Uniblitz Shutter. Adult worms are immobilized on 2% agar pads with Dermabond 2-Octyl Cyanoacrylate glue before a perfusion pencil delivers a 10s flow of osmotically balanced CTX buffer, followed by a 10s flow of the chemical of interest, and then continues imaging for another 10s. Imaging for mechanosensory responses in ASK involves delivering a 8µm poke stimulus to the nose of the immobilized animal with a blunted glass needle (~10µm tip) from a motorized stage (Polytec/PI M-111.1DG microtranslation stage with C-862 Mercury II controller). Images are recorded at 100ms exposure using an iXon EM camera (Andor Technology) and captured with IQ1.9 software (Andor Technology). Analysis of

both recordings was conducted in a custom written MatLab program (Mathlabs) that focuses on a region of interest around the cell body and compares fluorescence intensity from each channel to deliver a ratio change of fluorescence.

Chapter 3: Determining the structure and molecular function of TMC proteins

3.1 Introduction

Ion channels are necessary both to control the flow of ions across the cell membrane, and in order to integrate and respond to external signals. This response is characterized by the channel transitioning between an open (active) and closed (inactive) state (Minor 2010). In general, ion channels are composed of a few main subunits: the transmembrane domains, which have a helical structure and are more hydrophobic; the selectivity filter, which only allows particular ions to pass based on chemical and energetic activity; and the sensor domain, which often contains charged residues that begin the process of the channel's physical response to changes around the membrane (Purves et al. 2001). Taken together, these subunits help to regulate the key functional elements of ion channels: ion conductance, pore gating, and regulation.

Although very little is known about the structure and function of mechanically activated ion-channels, recent work has determined the gating mechanism of the human TRAAK K^+ channel, which belongs to a family of proteins that are involved in mechanical and temperature nociception in mice (Noel et al. 2009). Brohawn et al. (2014) show that the channel responds to changes in membrane tension by rotating a transmembrane helix in order to seal an intramembrane opening and prevent the lipid block of the pore-cavity, in turn allowing ion entry. Similar mechanisms have been confirmed in bacterial channels, with the mechanosensitive MscL relying on

rearrangements in the transmembrane regions in response to membrane tension in order to allow ion entry (Perozo et al. 2002).

In the case of hearing-related proteins found in cochlear hair cells, mechanical sensitivity is believed to be conferred by a more complex system of tethers between the channel and membrane components. Some of the proteins identified thus far that are believed to be involved in force sensation and transmission include MYO1C, MYO7A, MYO5A, HARMONIN, WHIRLIN, SANS, PCDH15, CDH23, THMS, TMIE, CIB2, TMC1 and TMC2 (Fettiplace 2016). With such a broad range of proteins required in some form, it has been difficult to break down each component's exact function, or to reconstitute the mechanotransducer in a heterologous system for closer investigation.

While it had previously been believed that direct gating of mechanosensitive channels by membrane forces was only seen in prokaryotic channels, Liu & Montell (2015) have recently proposed that many eukaryotic proteins may also be intrinsically touch sensitive and able to respond to changes in membrane curvature. This is an increasingly popular hypothesis, suggesting that forces within the lipid bilayer can do work on the channel and stabilize it into the open or closed state (Sukharev & Sachs 2012). While the hearing apparatus needs to be highly complex in order to tune the channel and discriminate a range of frequencies (Zhao & Muller 2015), other sensory modalities do not need this level of complexity – and so may do away with the network of tethers and auxiliary proteins. In both *C. elegans* and mice, MEC-2 is an accessory unit that can modulate the function of mechanosensory channels, but its importance differs between organisms. *C. elegans* MEC-2 is a tether between the

channel and the microtubule cytoskeleton which is critically required (Huang et al. 1995), while its homologue, STOML3, has been shown to modulate membrane stiffening and facilitate opening of the Piezo channels (Qi et al. 2015). Thus, in mammals its function is indirect – rather than physically linking to the channel, it instead tunes membrane stiffness in order to facilitate force transfer onto the channel. As previously mentioned, we also know that the TRAAK and TREK1 channels transmit force from the lipid membrane, rather than from attached tethers (Brohawn, Su, et al. 2014). These observations raise the possibility that TMC3 could also be able to directly sense and transmit force, as heterologous expression of the protein alone was able to generate mechanosensory responses in *C. elegans*.

Returning to the hair cell channel, Farris et al. (2004) have conducted a comprehensive analysis of the mechanotransducer of the inner ear based on ionic permeability, finding that the pore is likely to be surrounded by a hydrophobic vestibule that funnels ions down towards a negatively charged external mouth (**Fig 3.1**). One issue the authors highlight is that changes in channel conductance along the length of the cochlear may reflect different assemblies of channel subunits (Schwander et al. 2010), and that this could therefore result in different pore makeups. Nevertheless, this is the most comprehensive structural model of the channel produced to date. Other well characterized properties of the mechanotransducer include that it is a non-selective cation channel with a large conductance (from 100pS to 300pS along the cochlear) (Corey & Hudspeth 1979b; Crawford et al. 1991), and that the channel is blocked by a number of Ca^{2+}-channel antagonists and certain antibiotics (Baumann & Roth 1986; Kroese et al. 1989). Unfortunately, none of these

properties is unique enough to identify the channel protein without supporting research.

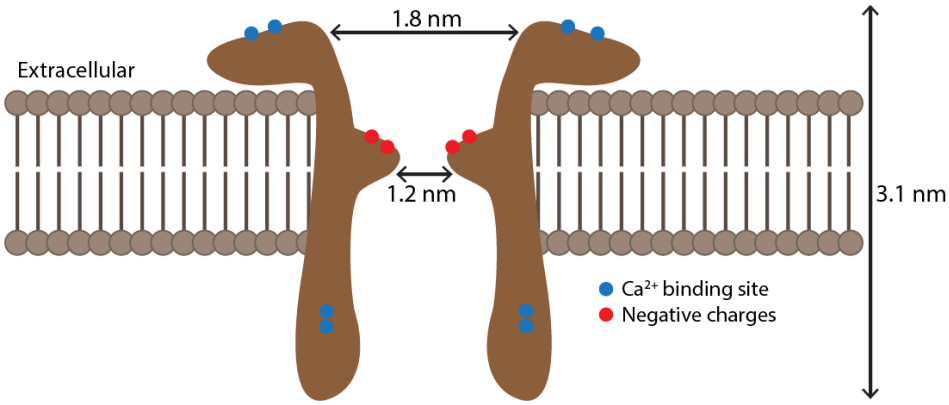

Fig 3.1: Representative diagram of the hair cell mechanotransducer pore from Farris et al. (2004). The authors propose a hydrophobic vestibule funnelling into a negatively charged channel mouth.

Because of the many difficulties encountered when investigating the hair cell mechanotransducer, the channel subunits are still unknown. Although the TMC proteins have emerged as leading candidates for this role, their structure has also not been definitely resolved. As such there is still much debate over their topology, with various studies estimating anywhere from six to ten transmembrane-spanning domains (Kurima et al. 2003) (**Fig 3.2**). Epitope tagging experiments in mammalian cells have established the position of most membrane-crossing regions, but there are still a few undetermined regions that could possibly pass the membrane. Additionally, because of the problems in trafficking of heterologously expressed TMCs, this topology was observed in ER-retained proteins and may not reflect the structure of the native functional protein. As such, one aim I have is to confirm the structure of the

TMC proteins by repeating these epitope-tagging experiments in the neurons of live animals, where we will be able to confirm that the protein retains its function.

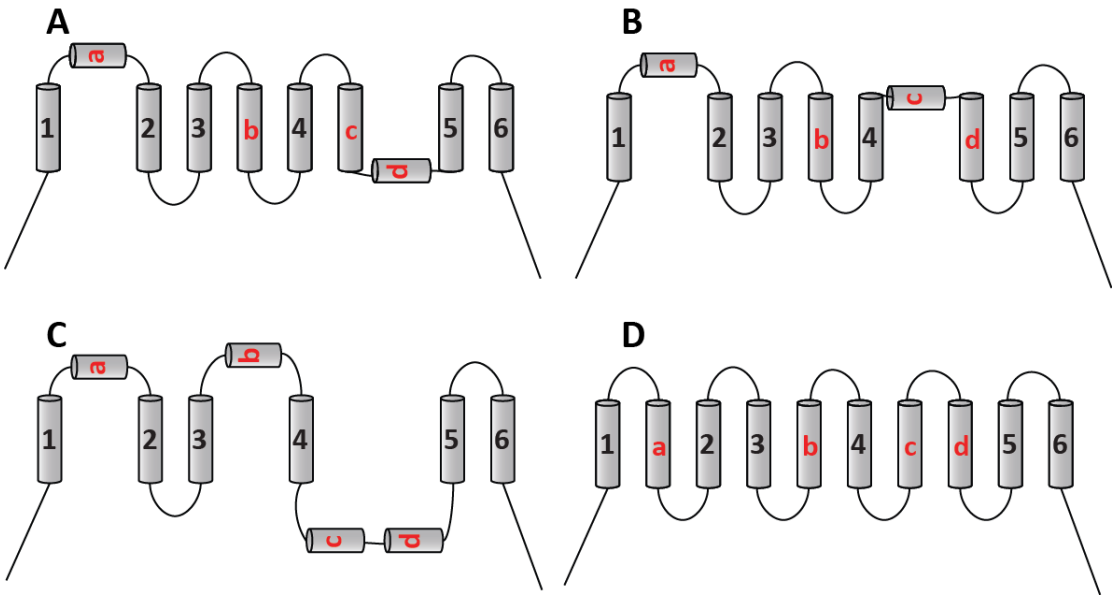

Fig 3.2: Alternative models of TMC protein membrane topology. **A)** Heller model (Keresztes et al. 2003). **B)** Sun Wook model (unpublished, personal communication). **C)** Griffith model (Labay et al. 2010). **D)** Holt model (unpublished, personal communication). Intracellular side is to the bottom, extracellular is to the top. Hydrophobic regions not confirmed to be membrane-passing are shown in red, while agreed-upon TM domains are numbered in black.

Secondly, it is interesting that the different TMC proteins seem to have different sensory specificity – while both mouse TMC1 and TMC2 are involved in hearing, preliminary research suggests TMC2 may also be involved in salt sensation (unpublished results, Marios Chatzigeourgiou). Conversely, in *C. elegans*, TMC-1 has been shown to function as a salt sensor (Chatzigeorgiou et al. 2013), while TMC-2 has been implicated in a number of mechanosensory roles (unpublished work, Marios

Chatzigeorgiou). Despite these differences, the proteins still share a high degree of sequence similarity. Whether these differences in sensory modality are due to the TMC proteins functioning as adaptable auxiliary subunits or is because they are truly distinct channels with differences in specificity is an interesting question that remains unanswered.

An obvious parallel to the TMCs is the TRP family of channels. Not only are members of the TRP family implicated in everything from vision, smell, taste, touch and thermosensation, but individual members have also been shown to activate in response to a range of different stimuli. For example, TRPV1 is activated by capsaicin, mustard oil and wasabi, heat and acidic pH (Caterina et al. 1997; Zygmunt et al. 1999; Everaerts et al. 2011). Like TMC proteins, this has left researchers questioning whether these stimuli may be acting through a common mechanism. Together with the increasing support for a membrane-tension model of force transmission (Liu & Montell 2015), it is possible that the TMCs are intrinsically force sensitive proteins, which can be modulated in certain contexts (e.g. the inner ear) to enhance this capability – but they may also have unique domains that account for the responses to salt and other stimuli seen in some subfamily members.

As such, another approach I have taken is to examine chimeras formed between the TMC1, TMC2 and TMC3 proteins, to try to find regions important for sensory specificity. Together with the epitope-tagging study, these experiments should give us a greater understanding of the membrane topology of the TMCs, which may provide clues as to whether they could function as part of the mechanotransduction machinery either in the inner ear or in peripheral tissues.

3.2 Results

3.2.1 TMC proteins appear to have six membrane-crossing domains

It has already been established that antibodies raised against particular epitopes can indicate whether a particular portion of a membrane protein is extracellularly exposed (Labay et al. 2010). However, previous use of this technique with the TMC proteins was carried out in ER-retained proteins in mammalian cell lines, raising some questions over whether the true topology of the protein was captured. Additionally, a previous attempt to define the topology of TMC1 did not sufficiently distinguish some putative hydrophobic domains, leaving it unclear whether they are membrane passing or not (Labay et al. 2010). In *C. elegans*, fluorescently conjugated antibodies can be injected into worms, allowing visualization of these epitope tags in live animals. I therefore repeated and expanded on the earlier topological study of the TMC proteins by examining hemagglutinin (HA) epitopes in both TMC1 and TMC3, including around the remaining putative hydrophobic regions (**Fig 3.3**).

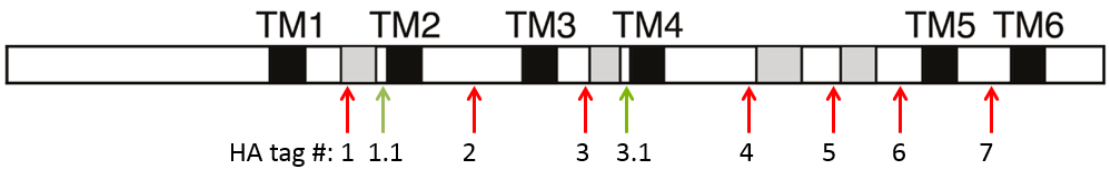

Fig 3.3: Location of HA tags along the TMC protein transcript. 'Confirmed' transmembrane-spanning domains are shown as black boxes while other predicted hydrophobic regions are shaded in grey. Novel tags that were not previously examined by Labay et al. (2010) are shown in green.

To confirm that antibody injection does not result in non-specific staining, wild type N2 worms were injected with Alexa488 conjugated anti-HA antibody, and examined for fluorescence four-to-five hours later. N2 animals only showed fluorescence in the coelomocytes (scavenger cells that take up waste material), confirming that neurons are not promiscuously labelled by the antibody (**Fig 3.4**).

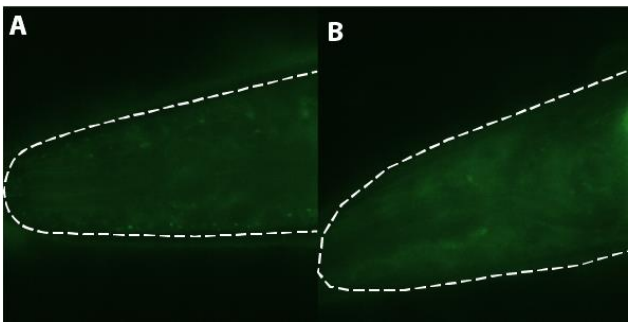

Fig 3.4: HA-antibody staining in negative controls. Exemplar images from N2 animals confirms that there is no background staining in head neurons (**A** & **B**).

Finally, to confirm that our HA-tagged constructs are still functional in *C. elegans* neurons, a strain with an extracellular tag (AQ3766) was used in calcium imaging of the nose press response, showing no significant difference from an untagged TMC3 expressing strain (**Fig 3.5**).

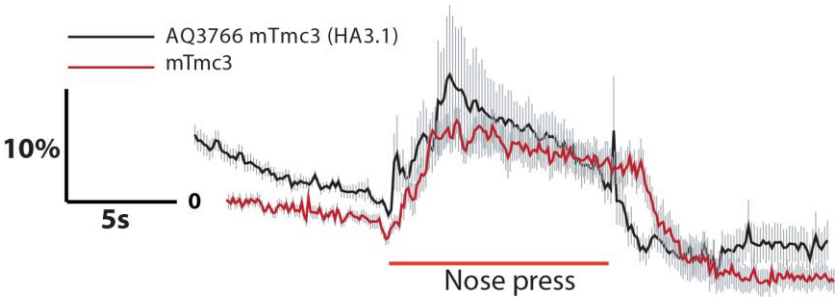

Fig 3.5: Calcium imaging of HA-tagged TMC3 confirms it retains functionality. HA3.1 tagged TMC3 is not significantly different in its response to nose press compared to untagged TMC3. Traces show the average change in fluorescence ratio of YFP to CFP (R/R_0), with the red line indicating stimulus application. Grey shading shows the SEM of the mean response. n > 15 traces.

In both TMC1 and TMC3, the results seem to mirror those previously published: tags one and three (between TM domains one and two, and three and four respectively) are accessible on the exterior of the cell, while tags two and four (between TM domains two and three, and four and five respectively) are not, suggesting intracellular localization (**Fig 3.6**). Interestingly, the two novel tags I have examined, around the putative hydrophobic regions in the first and third loops, are also accessible to the antibody staining (**Fig 3.7**). This would suggest that the most likely topology is that suggested by the Griffith laboratory (Labay et al. 2010).

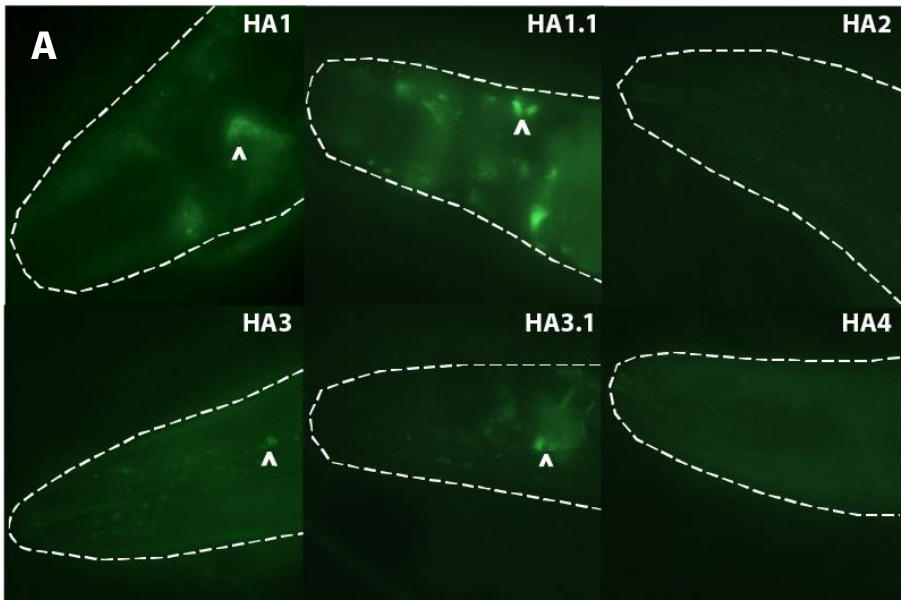

Fig 3.6: Immunofluorescence of HA tags. Visualization of the indicated epitope tags in TMC1 (**A,** above) and TMC3 (**B**, next page) using fluorescently-conjected anti-HA antibodies. Arrowheads denote neuronal cell bodies; anterior of the worm is to the left.

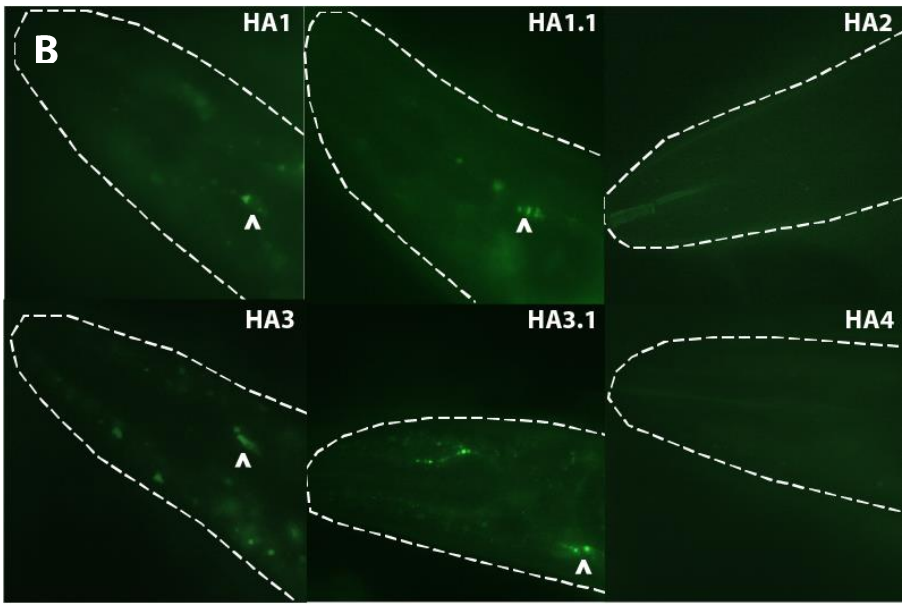

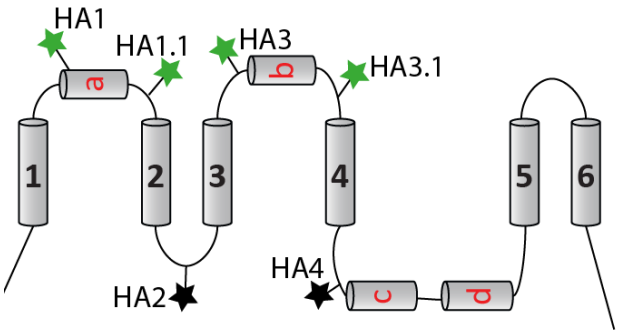

Fig 3.7: Diagram of resolved TMC protein membrane topology. Our results suggest that the 'a' and 'b' hydrophobic regions must be extracellular, while the 'c' and 'd' regions around the TMC motif are intracellular, confirming Labay et al.'s (2010) predictions.

To confirm whether the staining we observed was specific to the ASK neurons, these strains were crossed with a line expressing a mCherry marker under the P*sra-9* promoter. However, confocal microscopy showed some unexpected results, indicating that the cells being labelled by the antibody may not in fact be ASK (**Fig 3.8**). In a few cases, we are able to see overlap of the mCherry and anti-HA GFP markers, but in other animals only the mCherry or GFP alone is visible. Where the markers do

overlap, the structure of the cell body indicates that damage may have occurred, as they do not resemble the wild type shape. Nevertheless, there is still no staining observed in the wild type N2 strain, indicating that the fluorescence must be in some way specific to expression of the HA epitope within the worm. It is not immediately clear if this is an instance of mislocalisation/export of the TMC proteins, or if perhaps the promoter used in these constructs is non-specific.

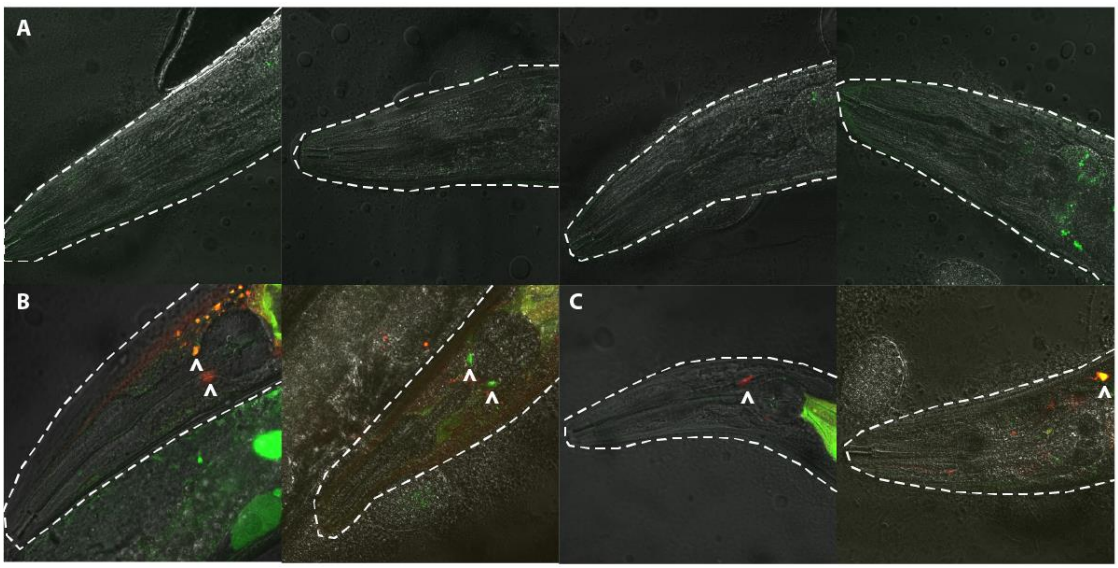

Fig 3.8: Localization of an ASK cell-type marker and anti-HA antibodies. A) N2 animals injected with the GFP-conjugated anti-HA antibody and imaged six hours later, showing no cell body fluorescence. **B)** Worms containing HA1 tagged TMC1 and an RFP marker in the ASK neurons imaged after injection of the GFP-conjugated anti-HA antibody. **C)** Worms containing HA1.1 tagged TMC1 and an RFP marker in the ASK neurons imaged after injection of the GFP-conjugated anti-HA antibody. Anterior is to the left, cell bodies are marked with arrowheads.

3.2.2 The region between TM domains 3 & 4 is important for TMC function

Engineering chimeric proteins is an established method for determining regions important for channel structure and function. Recently, Coste et al. (2015) used this technique to identify key domains in the PIEZO1 protein, a mechanosensory channel important for vascular development (Li et al. 2014; Ranade et al. 2014). Zhao et al. (2016) went one step further, identifying separate pore and mechanosensitive modules in PIEZO1. Chimeras have also revealed clues about structurally important residues in bacterial transporters (Cosgriff et al. 2000). Based on the success of these studies, we set out to uncover which regions of the TMC proteins are important for their sensory function. I hypothesized that there were two possible loops in the TMC proteins which may be important for their activity – the extracellular loop between TM passing domains three and four (denoted TM3/4), and the intracellular loop between TM passing domains four and five (denoted TM4/5). These regions are of interest because a number of important mutations, including *Bth*, are located in the TM3/4 loop, and the conserved TMC domain is in the TM4/5 loop.

Because TMC2 has a salt response in *C. elegans* neurons and TMC1 and TMC3 have mechanosensory responses, I constructed chimeras that swap these loops from TMC2 with those in TMC1/3, and vice-versa. Remarkably, when the TM3/4 loop from TMC2 was expressed in TMC1 or TMC3, these proteins lost their usual mechanosensory response and instead activated in response to salt stimuli (**Fig 3.9**). Conversely, animals expressing TMC2 with the TM3/4 loop from TMC1 or TMC3 now responded to mechanosensory stimuli, losing their salt sensitivity (**Fig 3.10**).

Fig 3.9: Calcium imaging of TM3/4 chimeras in response to 500mM NaCl.

Exchanging the TM3/4 loop from TMC2 animals confers TMC1 and TMC3 animals with a salt response, while inserting the loop from TMC1 or TMC3 into TMC2 abolishes its native salt response. Traces show the average change in fluorescence ratio of YFP to CFP (R/R_0), with the blue line indicating stimulus application. Grey shading shows the SEM of the mean response. Columns show peak R/R_0 with SEM error bars. Statistical significance (chimeras compared to unmodified protein) calculated by ordinary one-way ANOVA with multiple comparisons (Sidak's test) (* P<0.05, ** P<0.01, **** P<0.0001). n > 11.

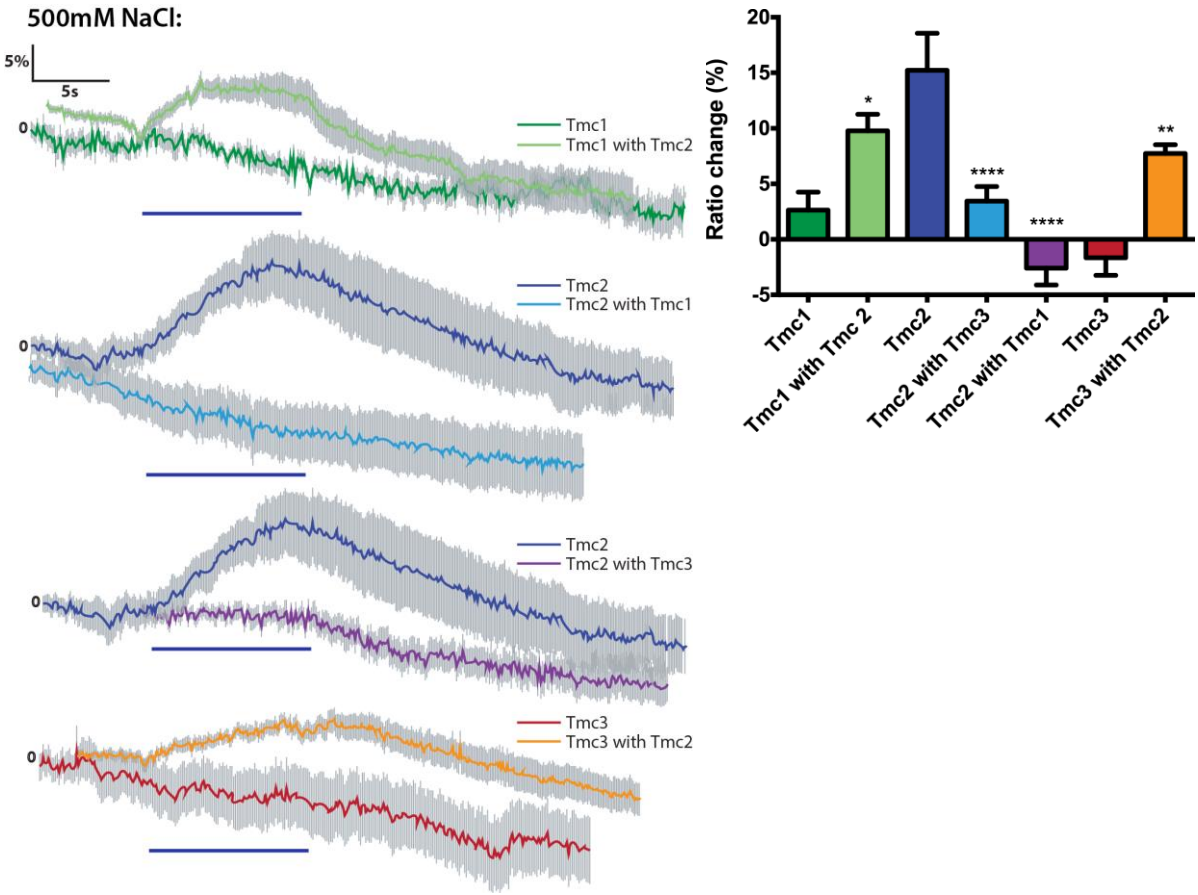

Fig 3.10: Calcium imaging of TM3/4 chimeras in response to mechanical stimuli. Exchanging the TM3/4 loop from TMC1 or TMC3 animals confers TMC2 animals with a mechanosensory response, while inserting the loop from TMC2 into TMC1 or TMC3 abolishes their native mechanosensory responses. Traces show the average change in fluorescence ratio of YFP to CFP (R/R_0), with the blue line indicating stimulus application. Grey shading shows the SEM of the mean response. Columns show peak R/R_0 with SEM error bars. Statistical significance (chimeras compared to unmodified protein) calculated by ordinary one-way ANOVA with multiple comparisons (Sidak's test) (** P<0.01, **** P<0.0001). n > 14.

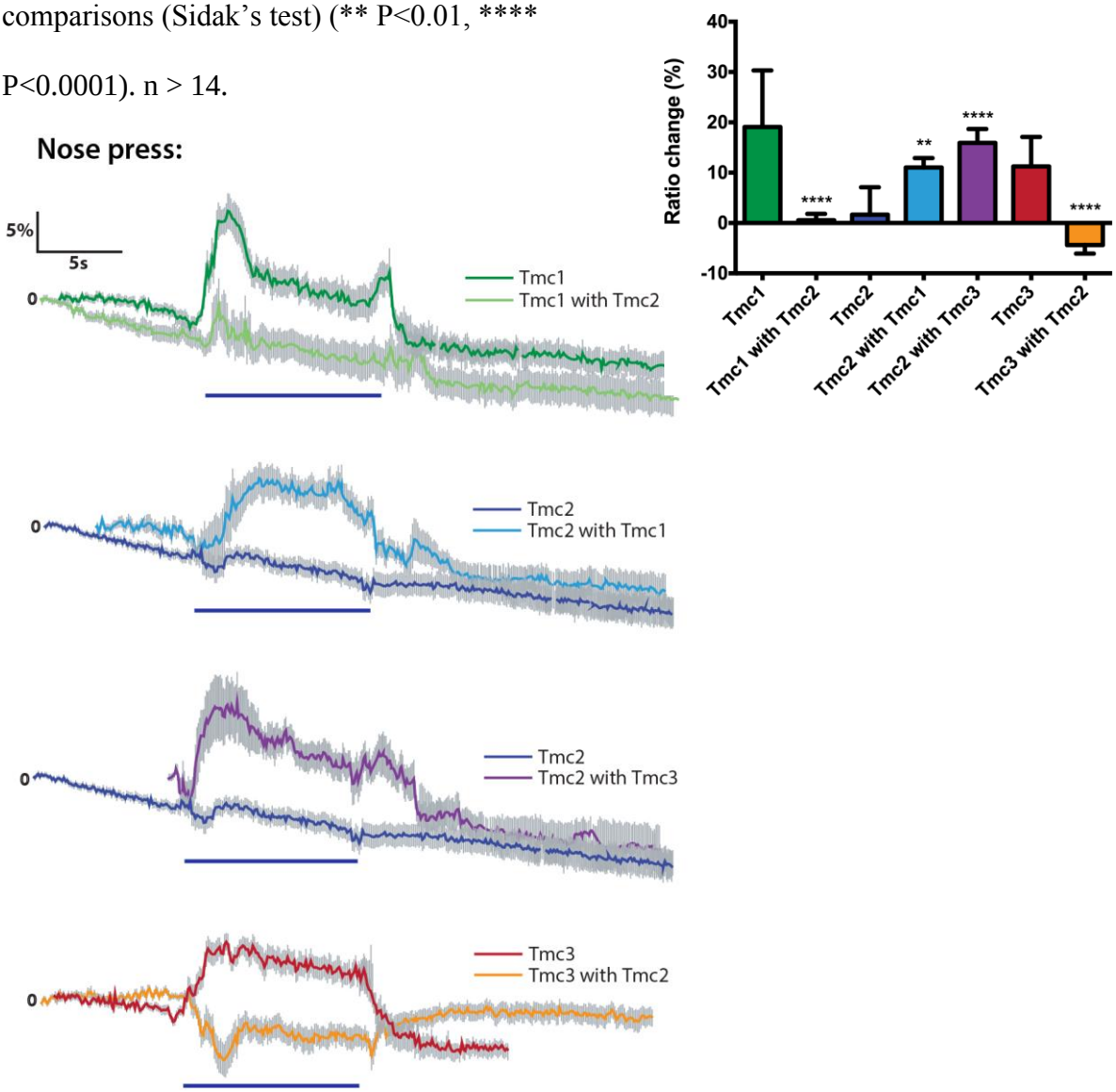

In comparison to these findings, when the TM4/5 domain from TMC2 was swapped into TMC1 or TMC3, the native mechanosensory response was retained and there was no activation in response to salt (**Fig 3.11**). Likewise, animals with the TMC2 protein containing TM4/5 from TMC3 still had a salt response and did not receive the mechanosensitivity conferred by Tmc3 (**Fig 3.12**).

Fig 3.11: Calcium imaging of TM4/5 chimeras in response to 500mM NaCl.

Exchanging the TM4/5 loop from TMC2 animals does not confer TMC1 and TMC3 animals with any difference in their salt response, while inserting the loop from TMC3 into TMC2 does not significantly affect its native salt response. Traces show the average change in fluorescence ratio of YFP to CFP (R/R_0), with the blue line indicating stimulus application. Grey shading shows the SEM of the mean response. Columns show peak R/R_0 with SEM error bars. Statistical significance (chimeras compared to unmodified protein) calculated by ordinary one-way ANOVA with multiple comparisons (Sidak's test). n > 11.

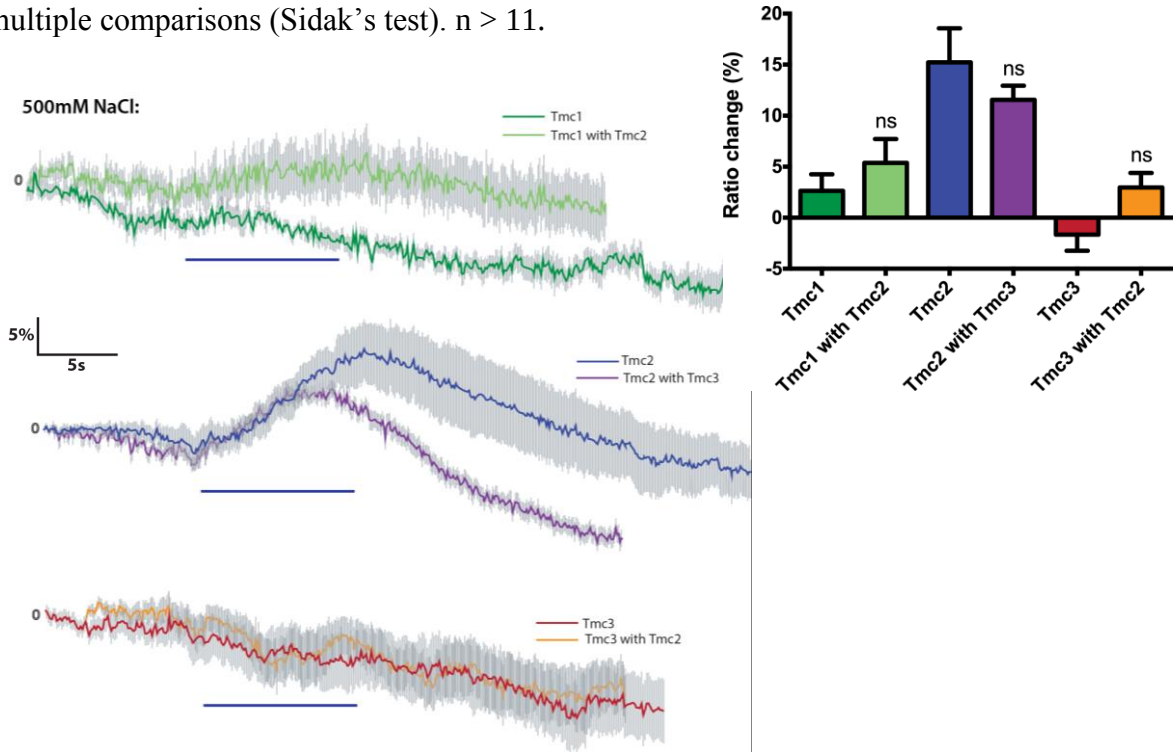

Fig 3.12: Calcium imaging of TM4/5 chimeras in response to mechanical stimuli. Exchanging the TM4/5 loop from TMC3 animals does not confer TMC2 animals with a mechanosensory response, while inserting the loop from TMC2 into TMC1 or TMC3 similarly has no impact on their native mechanosensory responses. Traces show the average change in fluorescence ratio of YFP to CFP (R/R_0), with the blue line indicating stimulus application. Grey shading shows the SEM of the mean response. Columns show peak R/R_0 with SEM error bars. Statistical significance (chimeras compared to unmodified protein) calculated by ordinary one-way ANOVA with multiple comparisons (Sidak's test). n > 13.

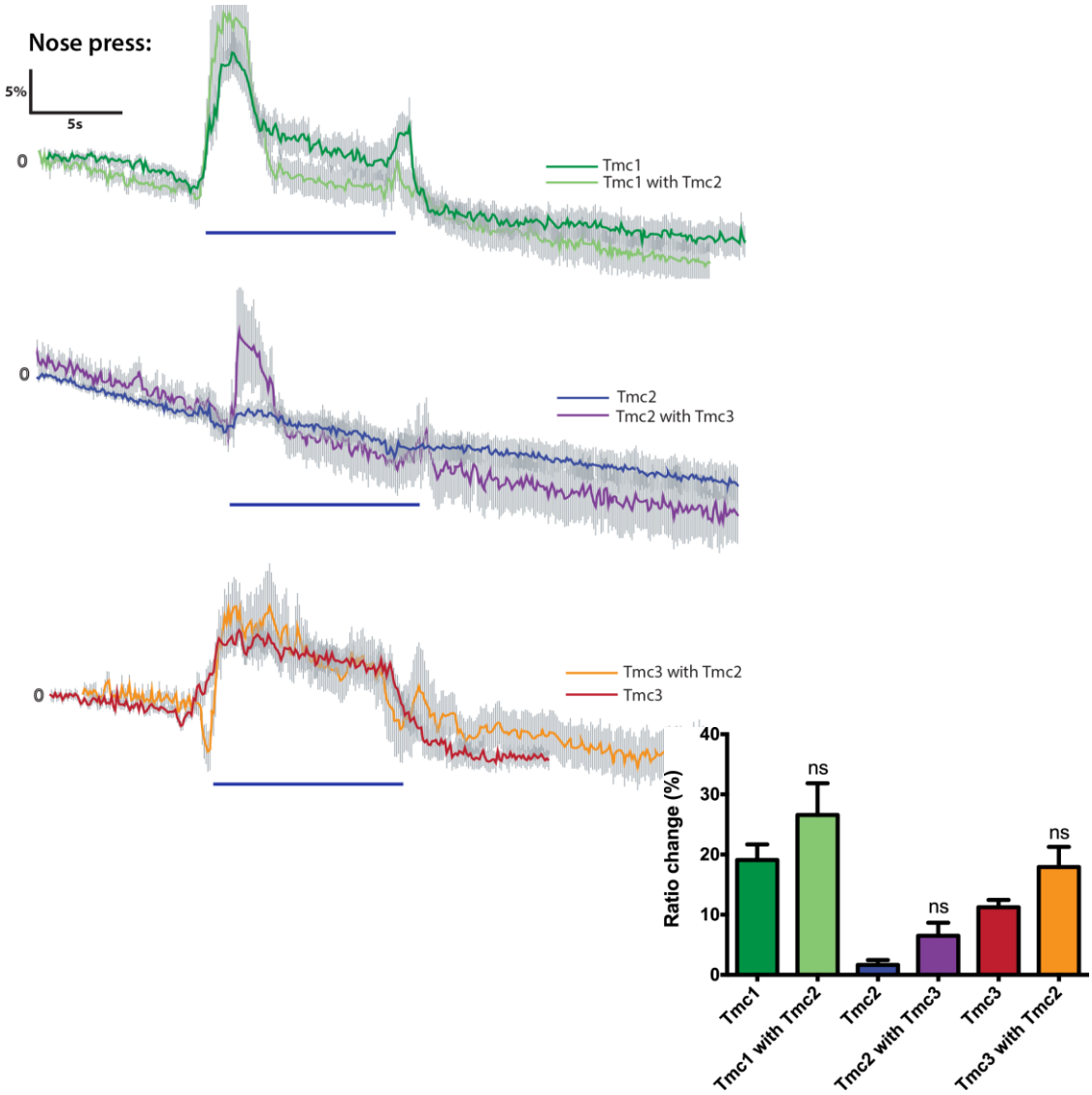

Based on the promising results from the TM3/4 swaps, I went a step further by creating chimeras from smaller areas within this loop – the hydrophobic region that was thought to be transmembrane penetrating/spanning, and the only area of significant sequence variability in this loop (hypothesizing that this variability could define the different salt/touch responses) (**Fig 3.13**).

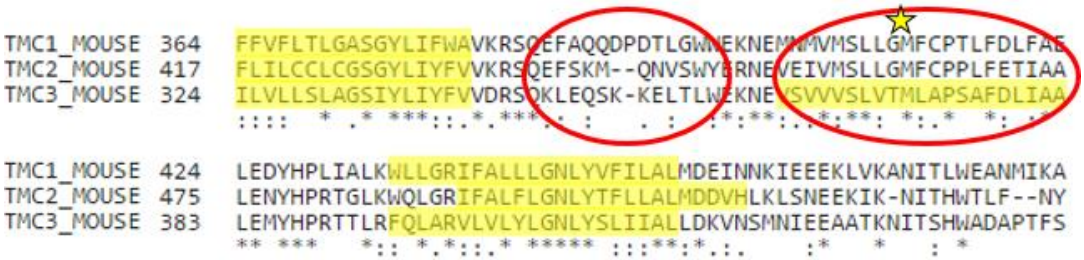

Fig 3.13: Design of chimeras within the TM3/4 loop region. Secondary chimeras were created by swapping the regions circled. The first area contains significant variability among the different TMCs, while the second region is predicted to be hydrophobic and as such may be associated with the membrane. Alignment created with Clustal2.1, the star indicates the location of the *Bth* mutation. Computationally predicted hydrophobic regions are highlighted in yellow.

These results were much less definitive, with neither region producing the obvious inversion of sensory specificity that the broader domain swaps had. Placing the 'unconserved region' from TMC1 or TMC3 into TMC2 attenuated its salt response, but the opposite chimeras did not grant TMC1 or TMC3 ectopic salt sensation (**Fig 3.14**). Similarly, putting this region from TMC2 into TMC1 or TMC3 only mildly attenuated their touch responses, but exchanging the 'unconserved region' from

TMC1 or TMC3 with TMC2 did not result in an ectopic touch response in these animals (**Fig 3.15**).

Swapping the potential TM region between TMCs produced similarly stark results, abolishing their responses in all cases: the domain from TMC1 or TMC3 attenuated TMC2's normal salt response (**Fig 3.16**), while neither the domain from TMC1 or TMC3 was able to produce an ectopic mechanosensory response in TMC2 (**Fig 3.17**). These results suggest that neither area alone (the unconserved region or the potential TM domain) is sufficient to determine TMC sensitivity, but the fact that chimeras were able to disrupt normal responses may indicate they are in a critical area of the protein that helps to regulate its function.

Fig 3.14: Calcium imaging of salt responses in chimeras swapping the 'unconserved region' between TMCs. Exchanging this region from TMC2 animals does not confer TMC1 and TMC3 animals with any difference in their salt response, while the converse experiment significantly attenuates TMC2's native response to 500mM NaCl. Traces show the average change in fluorescence ratio of YFP to CFP (R/R_0), with the blue line indicating stimulus application. Grey shading shows the SEM of the mean response. Columns show peak R/R_0 with SEM error bars. Statistical significance (chimeras compared to unmodified protein) calculated by ordinary one-way ANOVA with multiple comparisons (Sidak's test, ** $P<0.01$, **** $P<0.0001$). $n > 11$.

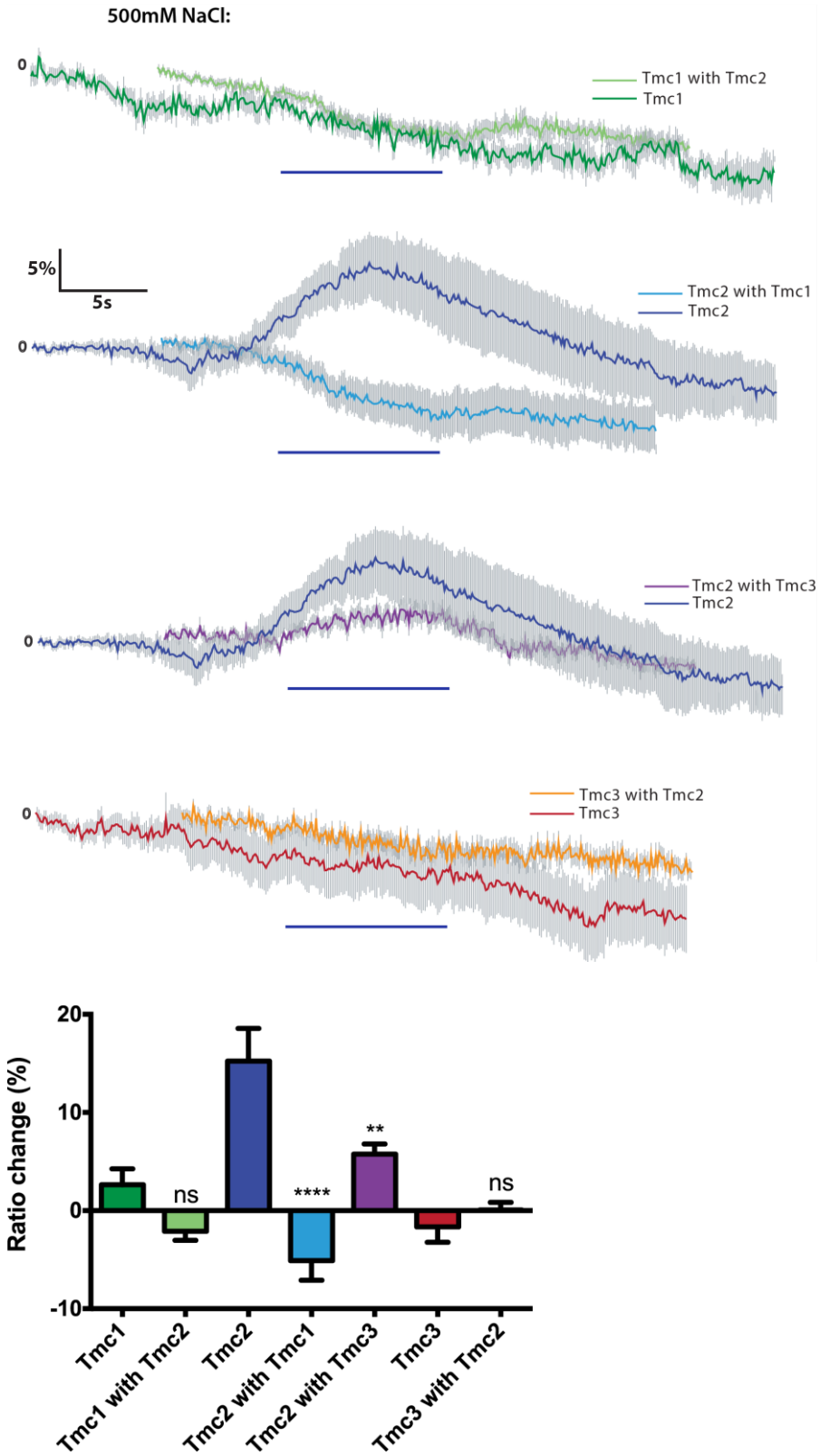
500mM NaCl:
0
Tmc1 with Tmc2
Tmc1
5%
5s
Tmc2 with Tmc1
Tmc2
Tmc2 with Tmc3
Tmc3 with Tmc2
Tmc3
Ratio change (%)
20
10
-10
ns
****
**
ns
Tmc1
Tmc1 with Tmc2
Tmc2
Tmc2 with Tmc1
Tmc2 with Tmc3
Tmc3
Tmc3 with Tmc2

Fig 3.15: Calcium imaging of 'unconserved region' chimeras in response to mechanical stimuli. Exchanging this domain from TMC1 or TMC3 animals does not confer TMC2 animals with a mechanosensory response, while inserting the loop from TMC2 into TMC1 or TMC3 similarly has little impact on their native mechanosensory responses. Traces show the average change in fluorescence ratio of YFP to CFP (R/R_0), with the blue line indicating stimulus application. Grey shading shows the SEM of the mean response. Columns show peak R/R_0 with SEM error bars. Statistical significance (chimeras compared to unmodified protein) calculated by ordinary one-way ANOVA with multiple comparisons (Sidak's test, *** $P<0.001$). n > 11.

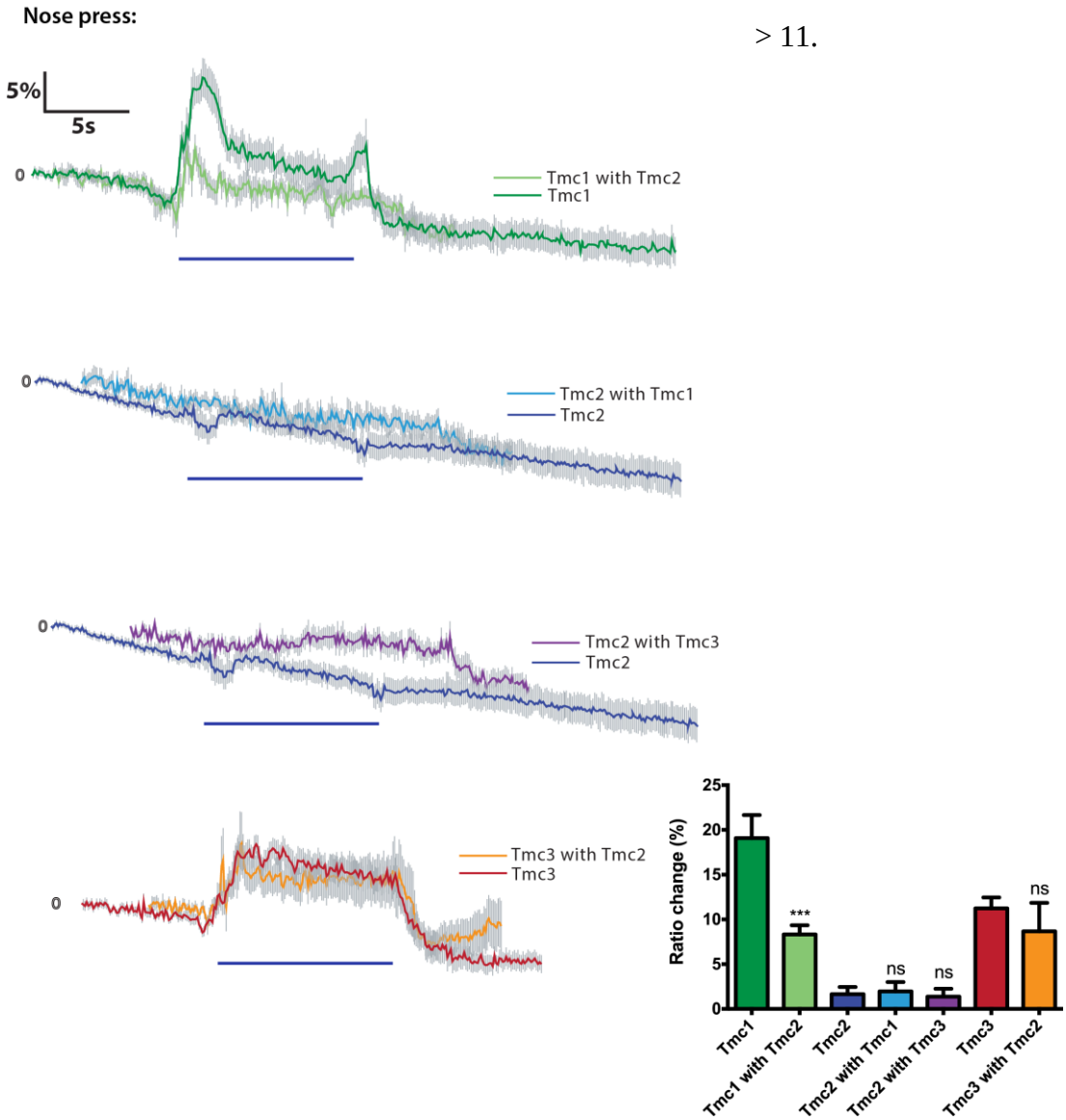

Fig 3.16: Calcium imaging of 'TM domain' chimeras in response to 500mM NaCl. Exchanging the potential TM domain within the TM3/4 loop from TMC2 animals does not confer TMC1 animals with any difference in their salt response, while inserting the loop from TMC1 or TMC3 into TMC2 significantly impacts its native salt response. Traces show the average change in fluorescence ratio of YFP to CFP (R/R_0), with the blue line indicating stimulus application. Grey shading shows the SEM of the mean response. Columns show peak R/R_0 with SEM error bars. Statistical significance (chimeras compared to unmodified protein) calculated by ordinary one-way ANOVA with multiple comparisons (Sidak's test, * $P<0.05$, ** $P<0.01$). $n > 11$.

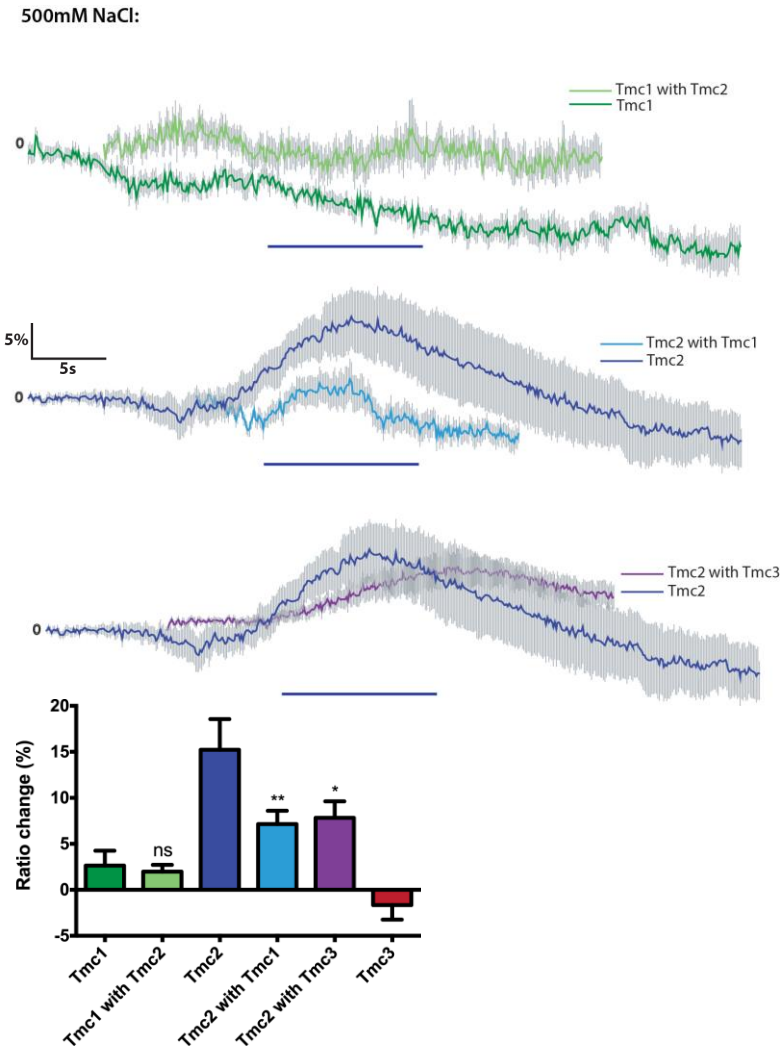

Fig 3.17: Calcium imaging of 'TM domain' chimeras in response to mechanical stimuli. Exchanging the potential TM domain within the TM3/4 loop from TMC1 or TMC3 animals does not confer TMC2 animals with a mechanosensory response, while inserting the loop from TMC2 into TMC1 significantly impacts its native mechanosensory response. Traces show the average change in fluorescence ratio of YFP to CFP (R/R_0), with the blue line indicating stimulus application. Grey shading shows the SEM of the mean response. Columns show peak R/R_0 with SEM error bars. Statistical significance (chimeras compared to unmodified protein) calculated by ordinary one-way ANOVA with multiple comparisons (Sidak's test, **** P<0.0001). n > 16.

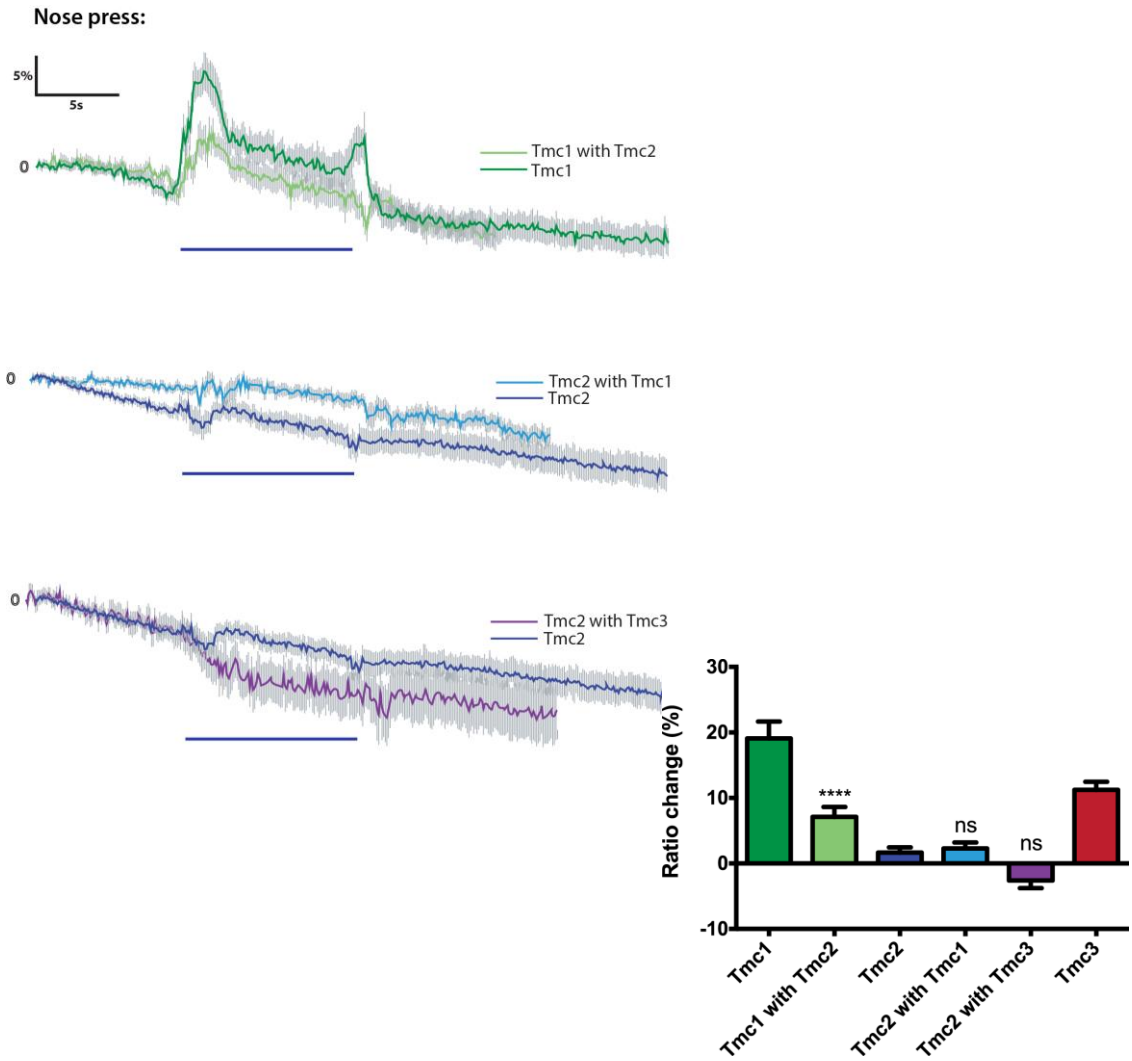

At this point I decided to take a different approach, instead focusing on changing particular residues in the loop that may be functionally important. Charged residues are known to play a number of important functions in regulating channel activity, and the 'unconserved' regions of TMC1, 2 and 3 show a number of differences in the residues expressed (**Fig 3.18**).

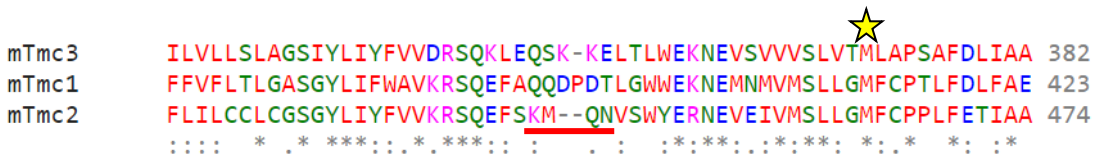

Fig 3.18: Residue alignment of TMC proteins. An area of interest is underlined in red. Negatively charged residues are indicated in blue and positively charged in pink. Location of the *Bth* mutation in *Tmc1* indicated by a yellow star. Alignment created in Clustal Omega.

Cation-specific channels, as the TMC proteins are believed to be, have been shown to have important acidic residues at their pore regions (Hille 2001). Numerous studies have taken advantage of amino acid substitutions from positively or negatively charged residues to the uncharged Alanine in order to demonstrate changes in the channel's core properties, particularly alteration of the ion selectivity of the channel (Kellenberger et al. 2001; Brelidze et al. 2003; Hansen et al. 2008; Kang et al. 2010). It has already been postulated that the TM3/4 loop may form a vestibule at the mouth of any channel the TMC protein forms (Holt et al. 2014), so identifying residues that impact its function would be an important finding. In an effort to determine if this is the case, I began by neutralizing all of the positive and negative residues within this region of variable sequence and again tested animals' responses to both stimuli.

Interestingly, by neutralizing just two residues in TMC1, D391A and D393A, I was able to reverse its normal response to nose press stimuli (**Fig 3.19**). Similarly, neutralization of just a single residue in TMC2, K442A, completely abolishes its native response to 500mM NaCl (**Fig 3.20**).

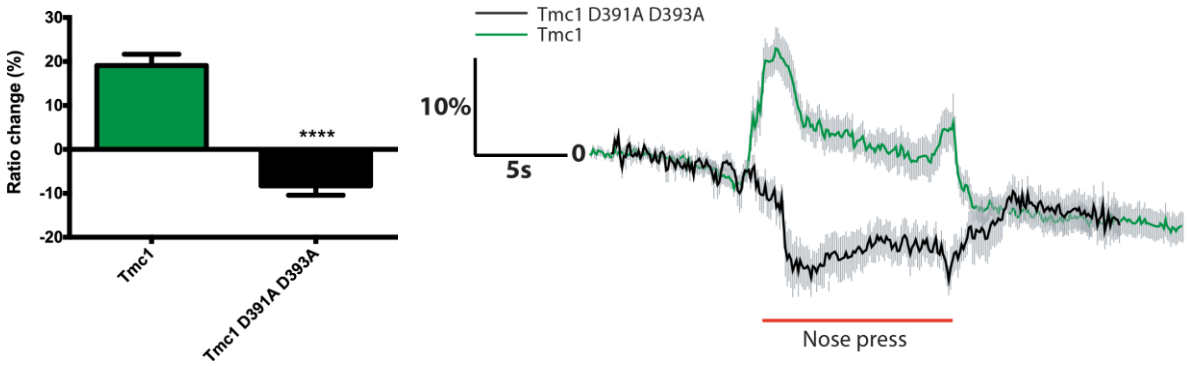

Fig 3.19: Calcium imaging of *Tmc1* D391A D393A mutants. Neutralization of these two negatively charged residues has completely abolished TMC1's native response to a nose press stimuli. Traces show the average change in fluorescence ratio of YFP to CFP (R/R_0), with the red line indicating stimulus application. Grey shading shows the SEM of the mean response. Columns show peak R/R_0 with SEM error bars. Statistical significance calculated by t-test (**** $P<0.0001$). $n > 12$.

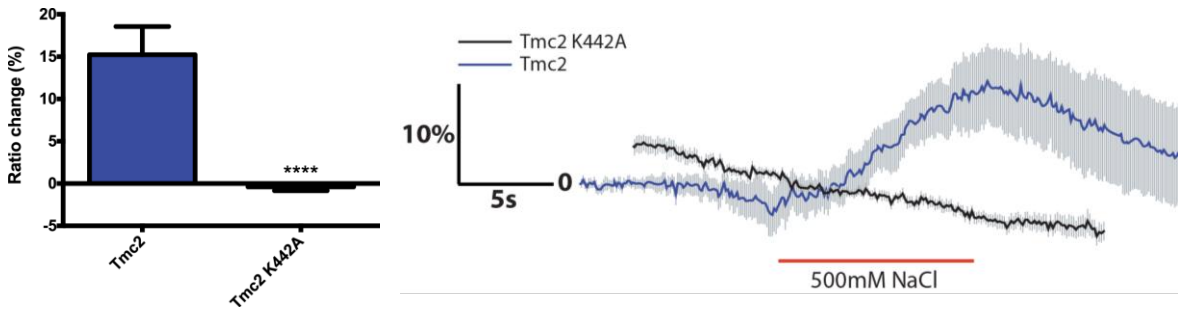

Fig 3.20: Calcium imaging of *Tmc2* K442A mutants. Neutralization of this single positively charged residue appears to be sufficient to abolish TMC2's normal response to 500mM NaCl. Traces show the average change in fluorescence ratio of YFP to CFP (R/R_0), with the red line indicating stimulus application. Grey shading

shows the SEM of the mean response. Columns show peak R/R_0 with SEM error bars. Statistical significance calculated by t-test (**** $P<0.0001$). $n>12$.

Interestingly, neutralization of three residues in TMC3, K351A, K352A and E353A, did not have a significant impact on its response to mechanical touch stimuli - suggesting that a different region of the protein must regulate mechanosensation in TMC3 compared to TMC1 (**Fig 3.21**).

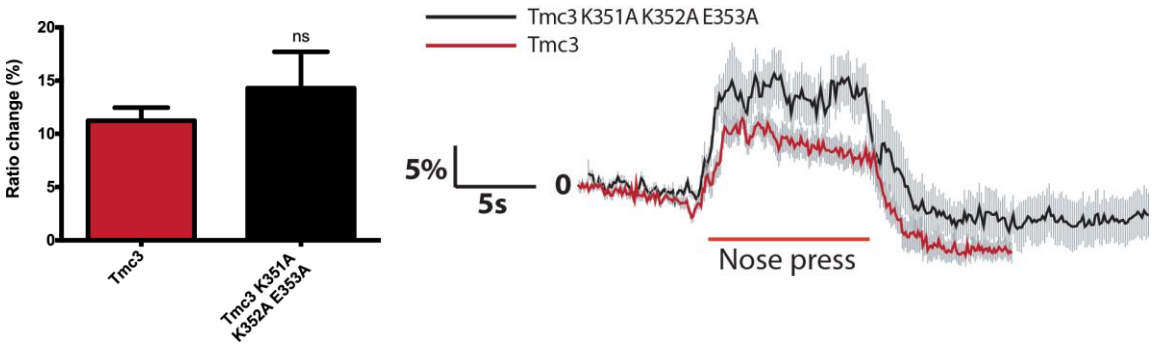

Fig 3.21: Calcium imaging of *Tmc3* K351A K352A E353A mutants. Neutralization of these three resides had no significant effect on TMC3's native response to nose press stimuli. Traces show the average change in fluorescence ratio of YFP to CFP (R/R_0), with the red line indicating stimulus application. Grey shading shows the SEM of the mean response. Columns show peak R/R_0 with SEM error bars. Statistical significance calculated by t-test. $n > 10$.

TO ADD: controls.

3.3 Discussion and conclusions

Despite emerging as promising candidates to form part of the mechanotransduction machinery, details on the structure and function of the TMC proteins were still sorely

lacking. In the HA-tagging experiments, I have suggested that the topology of functional TMC proteins in *C. elegans* neurons is based on six transmembrane-spanning domains. While these experiments initially appeared to be clear-cut, further examination using neuron-specific markers suggests that the cells being detected by the antibodies are not in fact the ASK neurons. Exactly why this is the case is hard to explain. The cells are in the same region as the ASKs, and importantly, nothing is ever seen in N2 controls, suggesting that even though the signal is not coming from the ASKs as expected, it is still reliant on the HA epitope being expressed. Because of this issue and the low success rate of the antibody injection method, we will be repeating this experiment using the recently published 'SpyTag' approach (Bedbrook et al. 2015). Similar to our method, this system is designed to visualize the exposed region of membrane-localized proteins in the neurons of live *C. elegans*. Genetically encoded 'SpyTag' and 'SpyCatcher' pairs are able to covalently bond, but the Catcher-GFP labeling protein is too large to passively cross the cell membrane. As a result, when the Catcher-GFP is secreted into the worm's body cavity, it can only bind to the 13 amino acid Tag if it is expressed on a protein accessible on the cell surface (Bedbrook et al. 2015). It is hoped that using a completely genetically-encoded system such as this will eliminate some of the issues we encountered with antibody labelling, such as maintaining consistency between animals and the low visualization success rate.

Confirming these topology findings will be an important task, as there is still plenty of controversy in the field as to the structure of TMC proteins. Although the results from Labay et al. (2010) and myself both point towards a six transmembrane-spanning protein, the Holt laboratory has recently been proposing a ten transmembrane-

spanning model with some *in vitro* supporting evidence (unpublished). Briefly, they use a cysteine modification approach to examine *Tmc1* point mutations in a *Tmc1/2* double knockout cell line. By perfusing 2-Trimethylammonium ethyl methanethiosulfonate bromide (MTSET) locally they have characterized the effect of these point mutations on the electrophysiology of the channel, as the addition of a charged group like this should alter ion conduction (Akabas et al. 1992). Because MTSET is too large to be membrane permeable (~5.8Å), it should only have an effect on mutations that are extracellularly exposed (T. Li et al. 2011). While the complete results of this work are still unpublished and ongoing, personal communications suggest that the group propose a ten transmembrane-spanning domain topology based on their current results.

Regardless of this confusion, I have used our own topological model to construct chimeric proteins to help unravel further details about the TMCs' function. Surprisingly, I show that the extracellular loop between transmembrane spanning domains three and four is critical for the function of all three TMC proteins, and that swapping this single region can alternate the sensory specificity of the TMCs. It is still not clear how this particular region of the protein is able to code for either mechanical or sodium sensitivity, but it is not without precedent for channels to be modular in this fashion. Recently, Zhao et al. (2016) used a similar approach to identify separate pore module and mechanotransduction components of the PIEZO1 channel. As such, perhaps this region of the TMC proteins comprises a mechanotransduction module – or determines their interaction with a separate force sensor.

A second approach of neutralizing certain charged residues in this region of interest also provided promising results. By changing the charge on just a few resides in TMC1 or TMC2, I was able to abolish their responses to sensory stimuli – both mechanical and salt-based. This suggests that this region of the protein either acts as a sensor domain or is a key region of the pore domain of the channel. Unfortunately, a conclusion cannot be reached based on calcium imaging alone, and electrophysiology of these constructs will be needed to probe the underlying channel dynamics in these mutants. At present, these experiments are too difficult to conduct in live worms, but the protocol is being refined and may be workable in future to provide a definitive answer as to how these residues are affecting the channel. In particular, we are moving towards being able to record currents from *C. elegans* neurons harvested through embryonic cell culture (Christensen et al. 2002; Strange et al. 2007). If this protocol is perfected, strains expressing the neutralized residues can be revisited so that the mutations can be characterized in more detail.

Surprisingly, while neutralization of charged residues in the TM3/4 region abolished responses in TMC1 and TMC2, a similar effect was not observed in TMC3, and its mechanosensory response was unaltered. The residues targeted were one of the most obvious divergences between the *Tmc3* sequence and *Tmc1* and *Tmc2*, but do not appear to have a significant impact on TMC3 protein function. Furthermore, equivalent mutations in *Tmc1*, D391A and D393A, were able to abolish TMC1's mechanosensory response. While it is not immediately clear which residues are the most important for TMC3 function, it is obvious that this region is central to the function of the other two TMCs.

Nevertheless, analogous results have been found for other channels. Zhao et al. (2016) were able to identify the pore module of the PIEZO1 channel, including the pore-lining residues and a vestibule over its entrance. They find a stretch of negatively charged residues at a vestibule over the pore of the channel that helps to enrich cations, allowing efficient ion conduction and cation selectivity. Neutralization of these residues resulted in reduced mechanically activated currents, which they attributed to a change towards a significantly higher permeability to chloride (Zhao et al. 2016). Thus, although this portion of the protein did not form the actual pore, mutation of particular residues still resulted in changes in core channel properties that are usually considered to be determined by the pore region.

Promisingly, it has already been hypothesized that the TM3/4 loop of the TMC proteins may form a vestibule on the exterior of the mechanotransducer channel (Holt et al. 2014). In fitting with the vestibule theory, this loop does have a number of hydrophobic and negatively charged residues, which we would expect from a cation channel like the mechanotransducer (Farris et al. 2004). Comparable to what is seen in PIEZO1 (Zhao et al. 2016), perhaps these charged residues help to enrich for cations around the pore of the channel. Taking this view may explain why neutralization of the residues resulted in loss of channel activity in my hands - if this ionic selectivity is altered, the normally cation-selective channel could instead admit anions, preventing the cell from depolarizing and reaching the threshold potential. Consequently, we would not see excitation of the neuron and Ca^{2+} influx in response to stimuli, resulting in the negative calcium imaging results (Mank & Griesbeck 2008). One simple method to probe this hypothesis is to take advantage of genetically encoded voltage sensors, which use a similar method to the cameleon proteins. In

place of a calcium binding domain, they use a voltage-sensing domain which is fused between two fluorescent proteins (a FRET donor and acceptor) (Akemann et al. 2012). FRET activation occurs in response to membrane depolarization, which would give us a clearer view as to how these mutations are affecting membrane potential – but electrophysiology will remain the gold standard.

There have been conflicting studies in the past that suggest mutation of TMC proteins affect the core properties of the mechanotransduction channel - Pan et al. (2013) show that the conductance and selectivity of the channel depends on which TMC protein is expressed, and that the *Bth* mutation in *Tmc1* reduces the single channel conductance and calcium permeability of the hair cell channel (Beurg et al. 2015; Corns et al. 2016). While these results may suggest that the TMC proteins are part of the pore of the hair cell mechanotransduction channel, opponents argue that they may simply be an accessory unit that is able to modulate the actual channel's permeation properties (Corey & Holt 2016). If the TMC proteins do form a vestibule which is responsible for ferrying ions towards the actual channel's pore, then these mutations which affect its charge could result in changes in channel conductance and ion flux towards the pore (Beurg, Kim, et al. 2014; Marcotti et al. 2014), without actually implicating TMC as a pore forming subunit. It is not unheard of for accessory subunits to alter the selectivity of a channel, such as MinK and the potassium channel Kv7.1 in *Xenopus* oocytes (Barhanin et al. 1996; Sanguinetti et al. 1996), or STIM1 and the CRAC1 channel (McNally & Prakriya 2012). These complications illustrate how even relying on properties that are traditionally believed to be strongly linked to the pore forming subunit of a channel may not be a foolproof method to determine channel composition. Clearly, there are cases where accessory subunits are tightly linked to

function, and given the complexity of mechanotransduction channels and the breadth of components expect to be involved in force transduction; this is likely to also be the case for the hair cell channel. While our experiments have helped to unravel some clues about the structure and function of the TMC proteins, it is still a mystery as to whether they are a pore forming subunit of the mechanotransduction channel.

3.4 Materials and methods

3.4.1 Hemagglutinin tagging

Previously published work has used hemagglutinin (HA) tags to try and determine the topology of TMC1 in mammalian cell culture lines, identifying six transmembrane domains (Labay et al. 2010). However, a disadvantage of this study is that TMC1 was retained in the endoplasmic reticulum, making it uncertain if the topology determined is the protein's native structure. Additionally, HA tags were not included around a number of regions that are identified by hydropathy plots as possible transmembrane spanning domains. To address these issues, I have added HA epitopes to both the TMC1 protein and TMC3. Using the Q5 Site-Directed Mutagenesis kit (NEB) on plasmids for ASK expression (P*sra-9::Tmc1::unc-54* and P*sra-9::Tmc3::unc-54*), the HA epitope tag (YPYDVPDYA) was added in TMC1 between amino acids 237 and 238 (HA1), 327 and 328 (HA2), 402 and 403 (HA3), and 510 and 511 (HA4), as published by Labay et al. (2010). Additionally, I tagged at two additional sites, denoted HA1.1 (between 260 and 261), and HA3.1 (between 428 and 429). The equivalent residues were also tagged in TMC3: between residues 196 and 197 (HA1), 219 and 220 (HA1.1), 287 and 288 (HA2), 361 and 362 (HA3), 387 and 388 (HA3.1),

498 and 499 (HA4). These constructs were then injected into wild type (N2) worms, as previously described (Mello et al. 1991).

3.4.2 Visualising HA tags in live worms

Worms expressing the HA tagged proteins were visualized as described by Gottschalk & Schafer (2006). The mouse monoclonal antibody α-HA (16B12) coupled to Alexa488 (ThermoFisher) was diluted 50-fold in injection buffer (20mM K_3PO_4, 3mM K-citrate, 2%PEG 6000, pH7.5) and injected into the pseudocoelom of animals expressing the HA epitopes. The solution was injected until a few eggs were pushed out, in order to maintain equal concentrations between animals. N2 worms were also injected in order to visualize the amount of background fluorescence in animals.

Animals were inspected by mounting them on 4% agar pads after anesthesia with 0.03% tetramisole. Fluorescence microscopy was performed using an upright Zeiss AxioImager Z1 equipped with a Photometrics Cool Snap HQ^2 camera. Images acquired in InfinityAnalyse software were further processed in Adobe Photoshop CS6. For confocal imaging, a Zeiss LSM710 microscope with 40x objective was used, with further processing in Zen2012 Software.

3.4.3 Chimeric proteins and calcium imaging

Chimeric proteins were constructed by swapping two regions that were hypothesized to be of interest – referenced to the topology predicted by Kawashima et al. (2014). These regions are the loop between the transmembrane-spanning (TM) domains three and four (defined as between amino acids 375 and 449 (TMC1), 428 and 500 (TMC2), 335 and 408 (TMC3)), and the loop between TM four and five (defined as

between amino acids 445 and 633 (TMC1), 496 and 677 (TMC2), 404 and 621 (TMC3)) (**Fig 3.22**). Chimeras were constructed between TMC1 and TMC2, and between TMC2 and TMC3. Constructs were created using the Gibson cloning strategy (Gibson et al. 2009), whereby the region to be swapped was PCR amplified with overhangs that overlap with the region of the protein to be inserted into. These constructs were cloned after the P*sra-9* promoter with Gateway cloning and then injected into worms carrying the P*sra-9::YC3.60* imaging line.

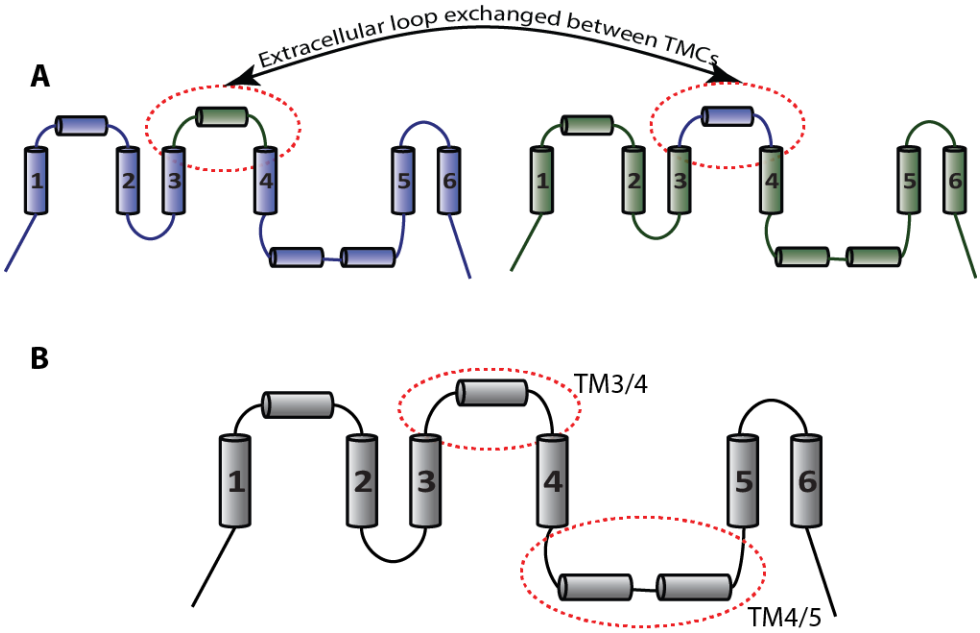

Fig 3.22: Illustration of protein chimera strategy. A) Diagram showing the resulting chimeric protein. **B)** Illustration of the two regions of interest (denoted TM3/4 and TM4/5) which were swapped between TMC proteins that exhibit different sensory specificities.

For the 'TM domain' chimeras, the regions of the proteins that were swapped are as follows: between amino acids 404 and 424 in TMC1, 455 and 475 in TMC2, 363 and

383 in TMC3. For the ‘unconserved region’, between amino acids 385 and 397 in TMC1, 438 and 452 in TMC2, 345 and 357 in TMC3. To construct more specific chimeras and single-residue changes, the Q5 Site-Directed Mutagenesis kit (NEB) was used on ASK expression plasmids for TMC1, TMC2 and TMC3. Charged residues around the transmembrane area of interest were neutralized by substitution with Alanine: D391A and D393A in TMC1, K442A in TMC2 and K351, K352A and E353A in TMC3.

Calcium imaging was carried out as described previously, using a Zeiss Axioskop 2 upright compound microscope with a 63x Zeiss Achroplan water-immersion objective, equipped with a Dual View beam splitter and a Uniblitz Shutter. Adult worms are immobilized on 2% agar pads with Dermabond 2-Octyl Cyanoacrylate glue before a perfusion pencil delivers a 10s flow of osmotically balanced CTX buffer, followed by a 10s flow of the chemical of interest, and then continues imaging for another 10s. Mechanical stimuli of 8µm displacement is delivered to the nose with a blunted glass needle from a motorized stage (Polytec/PI M-111.1DG microtranslation stage with C-862 Mercury II controller). Images are recorded at 100ms exposure using an iXon EM camera (Andor Technology) and captured with IQ1.9 software (Andor Technology). Analysis of both recordings was conducted in a custom written MatLab program (Mathlabs) that focuses on a region of interest around the cell body and compares fluorescence intensity from each channel to deliver a ratio change of fluorescence.

Chapter 4: Examining the *in vivo* function of TMC proteins in mice

4.1 Introduction

Although we talk about mechanosensation in a general sense, eukaryotes have a number of specialized systems in place for different modalities of touch – bodily contact, acceleration, gravity, sound waves, muscle fibre stretch, flow and pressure within organs. Each of these roles uses a catalogue of specialized mechanosensory proteins and accessory units within sensory cells to convert physical stimuli into electrical signals. Because of the scarcity and difficulty in reconstituting these channels (Gillespie & Walker 2001), simplified approaches like those we have used in *C. elegans* can help break down the individual components involved.

In humans and mice, there are two main structures that are of interest to us – hair cells (the site of auditory sensory transduction), and the various mechanosensory cells found in the skin which detect body touch. In both cases, it is believed that these specialized cells transmit deflections onto the mechanotransduction channel via connections with the intracellular and extracellular matrices. Thus, although these organs vary structurally, the underlying mechanistic and molecular mechanisms of touch sensation are shared (Gillespie & Walker 2001).

Numerous studies have tried to confirm the identity of the vertebrate hair cell mechanotransducer (Fuchs 2015), but as yet it is still unknown. There are believed to only be two channels per hair cell stereocilia (Ricci et al. 2003), meaning it is very

difficult to isolate and investigate proteins in hair cells (Arnadóttir & Chalfie 2010). As such, we have decided to focus instead on the sensory neurons of the dorsal root ganglion (DRG). The DRG is a processing hub which contains the cell bodies of primary afferent neurons which project from the skin and other bodily organs (Delmas et al. 2011). Each of these cells are functionally distinct, detecting a specific range and type of mechanosensory stimuli. The afferents can therefore be grouped into broad categories based on their morphology and conduction properties - either Aβ, Aδ or C-fibres. Thickly myelinated Aβ fibres are mostly light touch receptors due to their low thresholds, whereas thinly myelinated Aδ fibres and unmyelinated C-fibres are more likely to be nociceptive because of their high activation thresholds (Lumpkin et al. 2010). There is also a subset of C-fibres with low mechanosensory thresholds, which are hypothesized to be involved in affective (personal) touch.

While these classifications are based on structural and electrophysiological properties of the fibres, a more recent approach has been to look at the transcriptional profile of neurons in order to create more accurate functional classifications of sensory afferents (Friedel et al. 1997; Gabashvili et al. 2007; Usoskin et al. 2015). To this end, Usoskin et al. (2015) have used an unbiased RNA sequencing approach to divide DRG neurons into eleven types: three low-threshold mechanosensors, two proprioceptive, and six types of thermosensitive, low threshold mechanoceptive and nociceptive neurons. For each of these populations they have identified an antibody marker that may be used to delineate cell-types (**Fig 4.1**). We can therefore use immunohistochemistry to examine TMC proteins *in vivo*, taking advantage of these cell-type markers to make inferences about potential functions and then make a more informed selection of behavioural experiments to conduct in live mice. One of the

main aims of this chapter is to characterize the expression profile of the subfamily A TMC proteins, in order to determine if more targeted behavioural experiments (such as examination of proprioception, nociception or thermosensation) would be warranted.

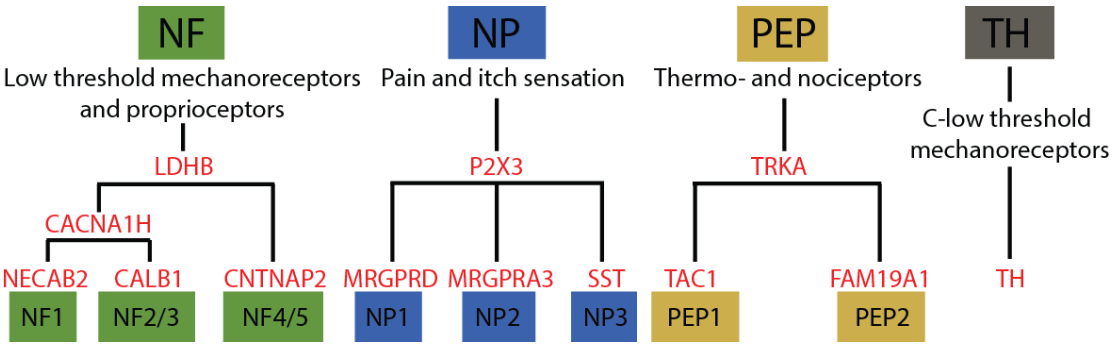

Fig 4.1: Cell-type specific markers used for immunofluorescence of DRG samples. Usoskin et al. (2015) divide the neuron population into eleven different subtypes, which are outlined with cell-type specific markers here.

While our studies in *C. elegans* have been very informative, to get a true idea of TMC function, particularly TMC3, it would be best to return to experimental paradigms in mice. TMC3 has never been fully investigated in mice, although a knockout line does exist. These mice were generated by the Wellcome Trust Sanger Institute (WTSI), but were only passed through a very basic phenotyping pipeline. The only phenotype tested that may be relevant to mechanosensory function is a brain stem auditory response, which showed no defect in *Tmc3* mutants (Brown & Moore 2012) (**Fig 4.2**).

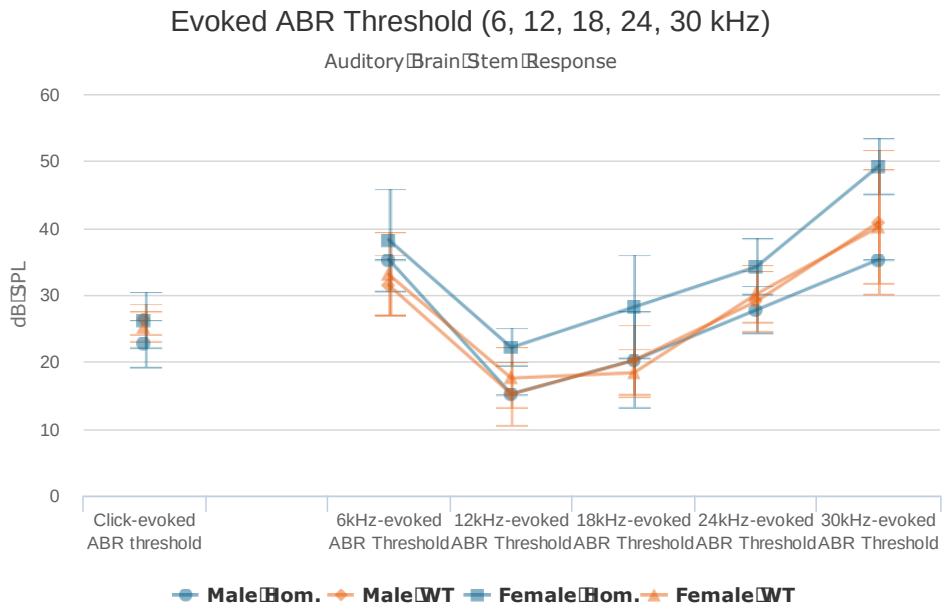

Fig 4.2: Auditory brainstem response in *Tmc3* knockout animals measured by the WTSI. Mutant animals do not show a significantly different response to wild type animals at any of the threshold tested.

Consequently, we have decided to examine phenotypes in *Tmc3* mutants more closely, in particular with mechanosensory tests such as the Von Frey fibres. Von Frey fibres allow for the examination of mechanical sensitivity in the hind paw of a rat or mouse, using a nylon filament of defined stiffness to deliver a reproducible force to the animal (Bradman et al. 2015). By cycling between filaments and calculating the response threshold of the animal, we are therefore able to determine a '50% response threshold' which corresponds to the stimulus range which an animal responds to in 50% of presentations. Perturbations from this threshold thus reflect a defect in cutaneous mechanosensation (Norrsell et al. 1999). These experiments, together with the immunohistochemistry of sensory neurons, should help provide

clues as to whether TMC proteins play a role in sensory transduction outside of the ear.

4.2 Results

4.2.1 TMC proteins are predominately found in mechanosensitive cells

The DRG neuronal population can be subdivided into eleven discrete groups based on RNA-seq analysis of gene expression (Usoskin et al. 2015). Broadly, there are four main classes of neurons:

1. NF, expressing NEFH and PVALB
2. PEP, expressing TAC1, NTRK1 and CALCA
3. NP, expressing MRGPRD and P2RX3
4. TH, expressing TH

Within these groups are further subpopulations, resulting in the final eleven categories: NF1-5, PEP1-2, NP1-3 and TH. By examining the complement of genes expressed in each subtype of cells, Usoskin et al. (2015) are also able to make predictions about the characteristics of the neurons within each class. NF1-3, which express NTRK2, NTRK3 and CALB1, are likely low-threshold mechanoreceptors (L. Li et al. 2011). NF4-5 are expected to be proprioceptive, due to their expression of TRKC and PV (Ernfors et al. 1994). All of the neurons within the NF population are expected to be myelinated and of large diameter (Usoskin et al. 2015).

Members of the NP class are predicted to transduce pain and itch (Liu et al. 2009; Han et al. 2013), while TH neurons, expressing PIEZO2 and VGLUT3, are likely to

be low-threshold mechanoreceptors for pain and pleasant touch (Seal et al. 2009; Coste et al. 2010). Finally, PEP neurons that express either TAC1 (PEP1) or NTRK1 (PEP2), are anticipated to be thermosensitive and Aδ nociceptors respectively (Tominaga et al. 1998; Caterina et al. 1999; McKemy et al. 2002; Usoskin et al. 2015).

Promisingly, RNA-seq from this study identified possible expression of each of the subfamily A TMCs in a small subset of cells: TMC1 in NF1-3 and NF5, TMC2 in NF2, and TMC3 in PEP1 neurons (**Fig 4.3**). Putatively, this suggests that TMC1 and TMC2 may function as low-threshold mechanoreceptors, and TMC3 could be involved in thermosensation.

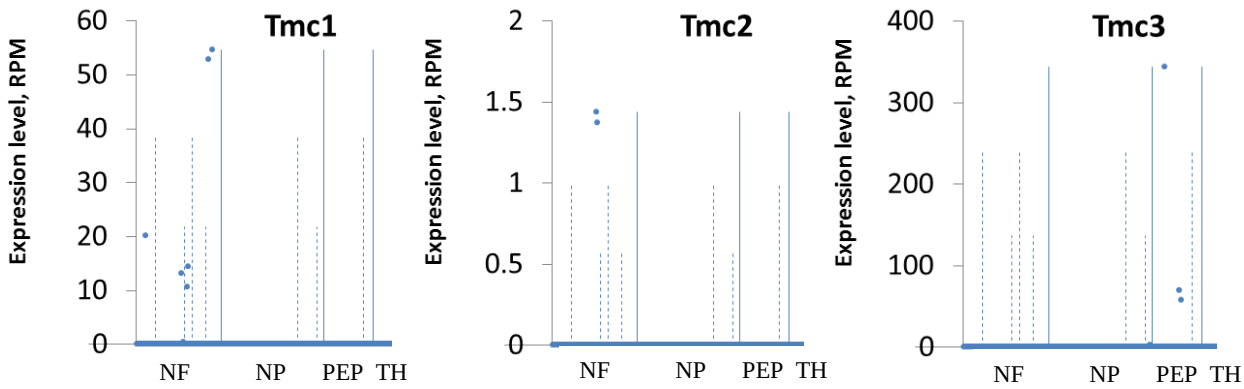

Fig 4.3: RNA-seq readouts for the TMC genes from Usoskin et al. (2015). The expression patterns suggest that TMC1 will be found in relatively high levels in NF1-3 and NF5 populations, TMC3 may be found in high levels in PEP1 cells, and TMC2 could be found in low levels in NF2 cells.

To confirm the DRG expression of the TMC proteins in our own hands, I extracted RNA from wild type DRGs and whole brain samples, using these transcripts to transcribe cDNA. TMC-specific primers were then used to amplify portions of the

genes, which were confirmed by DNA sequencing. Together, these results confirm that we can find all three members of TMC subfamily A in both whole brain and DRG tissue samples (**Fig 4.4**).

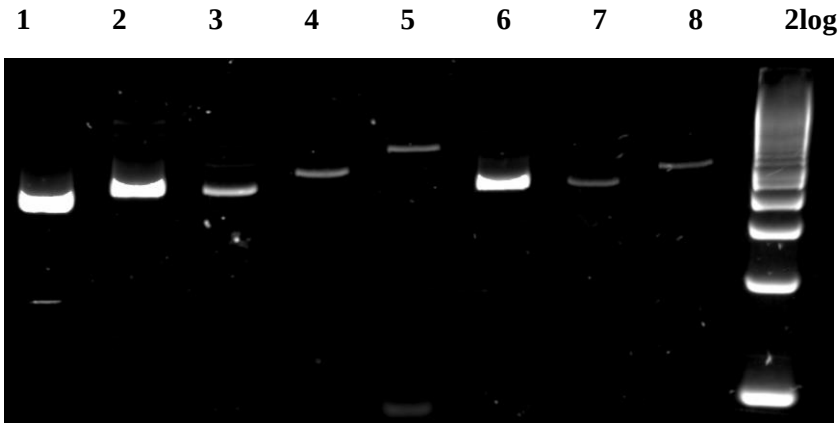

Fig 4.4: RNA amplification of TMC genes from whole brain and DRG samples. Confirmation that the TMC genes are expressed in DRG (lanes 1-4) and whole brain (lanes 5-8). Positive control *Cacan1b* is in lane 1 and 5, *Tmc3* in lane 2 and 6, *Tmc2* in lane 3 and 7, *Tmc1* in lane 4 and 8. Transcripts were confirmed by DNA sequencing.

To try to confirm these expression results, I began by using a range of broad antibody markers for these subpopulations on DRG slices from wild type animals: LDHB to stain all NF class neurons, P2X3 for the NP class, TH for the TH class and TAC1 to visualize a subset of the PEP family. Satisfied that these populations could be visualized, I also confirmed staining with more specific markers: CACNA1H for the NF1-3 classes, NECAB2 for NF1, and CNTNAP2 for the NF4-5 classes (**Fig 4.5**). All the antibodies appeared to stain single, discrete cells within the DRG slices.

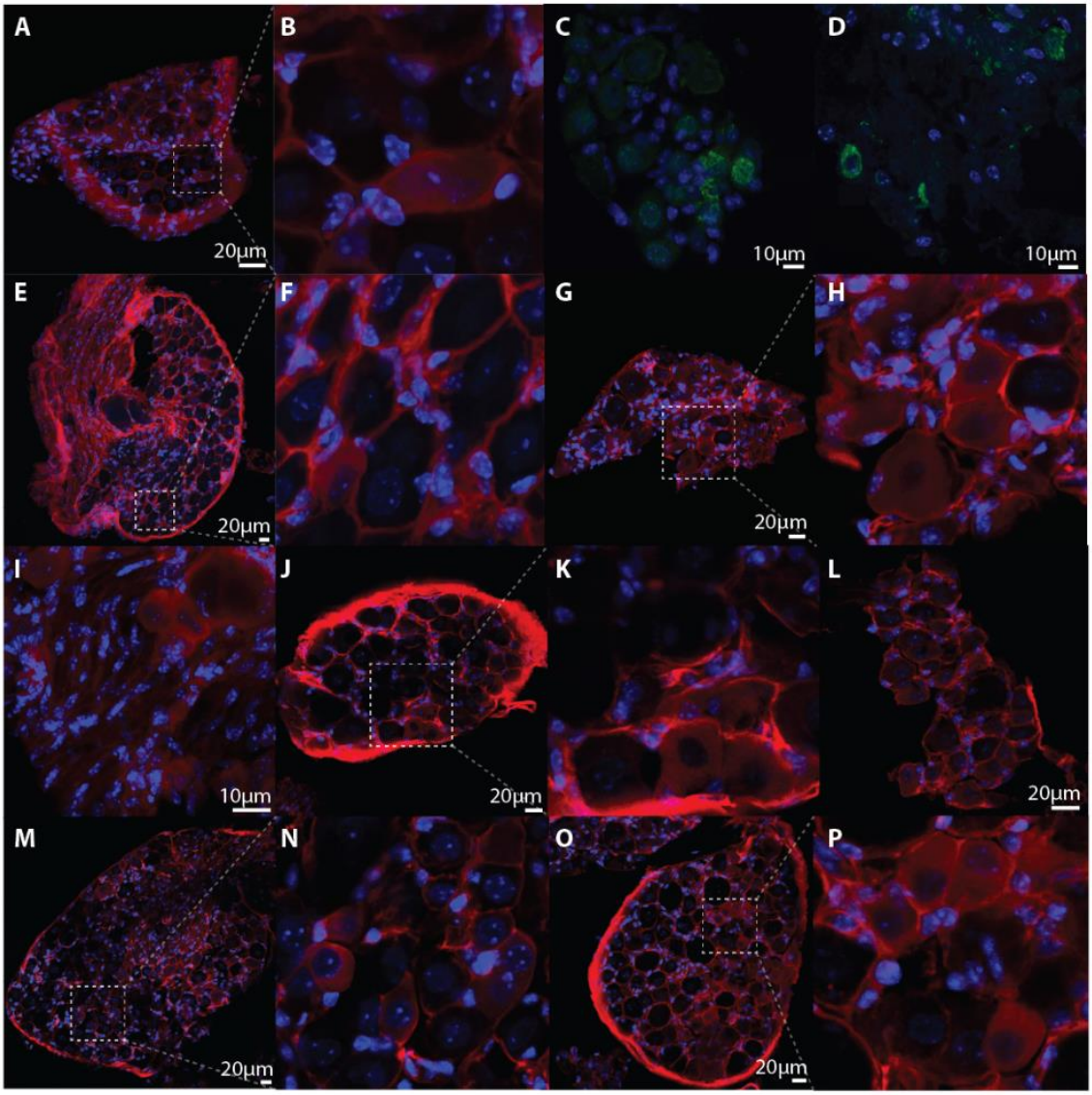

Fig 4.5: Immunofluorescence images looking at antibody markers for specific subtypes of cells within the DRG. A) and insert **B)** LDHB. **C)** and **D)** TAC1. **E)** and insert **F)** TH. **G)** and insert **H)** P2X3. **I)** NECAB2. **J)** and insert **K)** and CACNA1H. **L)** CACNA1H. **M)** and insert **N)** CNTNAP2. **O)** and insert **P)** CNTNAP2. All images show DAPI in blue, scale bar as indicated.

Having confirmed that individual cell markers appeared to work correctly, I next conducted double staining of DRG slices using antibodies that are predicted to be non-overlapping, as a further control for their accuracy. Double staining for LDHB

(NF class) and TAC1 (PEP1 class), showed that the two populations do not overlap. Further combinations of staining established that a number of the antibodies are exclusive as expected, and that we can distinguish the NF, NP, TH and PEP classes of neurons (**Fig 4.6**).

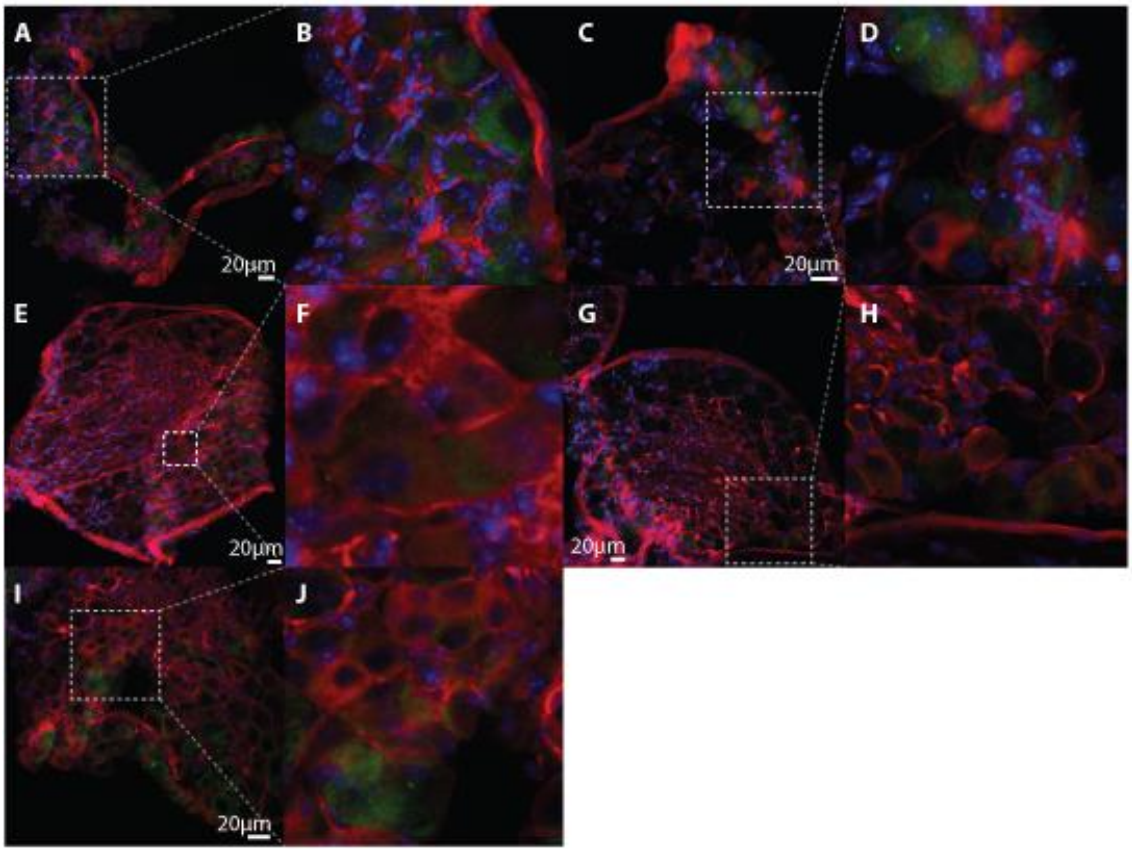

Fig 4.6: Immunofluorescence images using double-stains for non-overlapping DRG cell types. A) and insert **B)** LDHB in red and TAC1 in green establish independent NF and PEP1 populations. **C)** and insert **D)** TH in red and TAC1 in green establish TH and PEP1 populations. **E)** and insert **F)** CNTNAP2 in red and TAC1 in green delineate the NF4/5 and PEP1 groups. **G)** and insert **H)** CACNA1H in red and TAC1 in green separate the NF1-3 and PEP1 cells. **I)** and insert **J)** P2X3 in red and TAC1 in green establish the NP and PEP1 populations. All slices use DAPI staining in blue, scale as indicated.

Having confirmed the cell-specific antibodies, I finally tested antibodies for the three TMC proteins in combination with these markers to try to determine the subset of cells they are expressed in. All TMC antibodies were also used in DRG slices from knockout mice to confirm there was no background fluorescence. Immunofluorescence against TMC1 showed a small subset of neurons in wild type DRGs are TMC1 positive (**Fig 4.7**). These cells were also positive for LDHB, suggesting expression in the NF class of low threshold mechanoreceptors. Immunofluorescence of P2X3 (NP class), TH (TH class) and TAC1 (PEP1 class) was negative for TMC1, suggesting it is exclusively found in the NF neurons.

To narrow down which subset of NF neurons express TMC1, co-staining was also conducted with CACNA1H (NF1-3), NECAB2 (NF1), and CNTNAP2 (NF4-5). NECAB2 and CNTNAP2 appear to be negative for TMC1, but there is an overlap in the expression profile for CACNA1H and TMC1. Based on the negative profile for TMC1 in NECAB2 cells, this infers it is found in the NF2/3 population (see **Fig. 4.1**) Based on the other genes expressed in this subset of neurons, TMC1 is therefore predicted to function as a low threshold mechanoreceptor (L. Li et al. 2011; Usoskin et al. 2015).

Fig 4.7: Co-staining with TMC1 and cell-type markers in DRG slices. A) and **B)** TMC1 in wild type animals. **C)** and **D)** TMC1 in knockout mutants. **E)** and insert **F)** LDHB (NF class) in red and TMC1 in green. **G)** and insert **H)** LDHB in red and TMC1 in green. **I)** and **J)** NECAB2 (NF1 class) in red and TMC1 in green. **K)** and insert **L)** TH (TH class) in red and TMC1 in green. **M)** and insert **N)** Positive staining

for CACNA1H (NF1-3 class) in red and TMC1 in green. **O)** and insert **P)** Positive staining for CACNA1H (NF1-3) in red and TMC1 in green. **Q)** and insert **R)** CNTNAP2 (NF4-5 class) in red and TMC1 in green. **S)** and insert **T)** P2X3 (NP class) in red and TMC1 in green. All slices use DAPI staining in blue, scale as indicated.

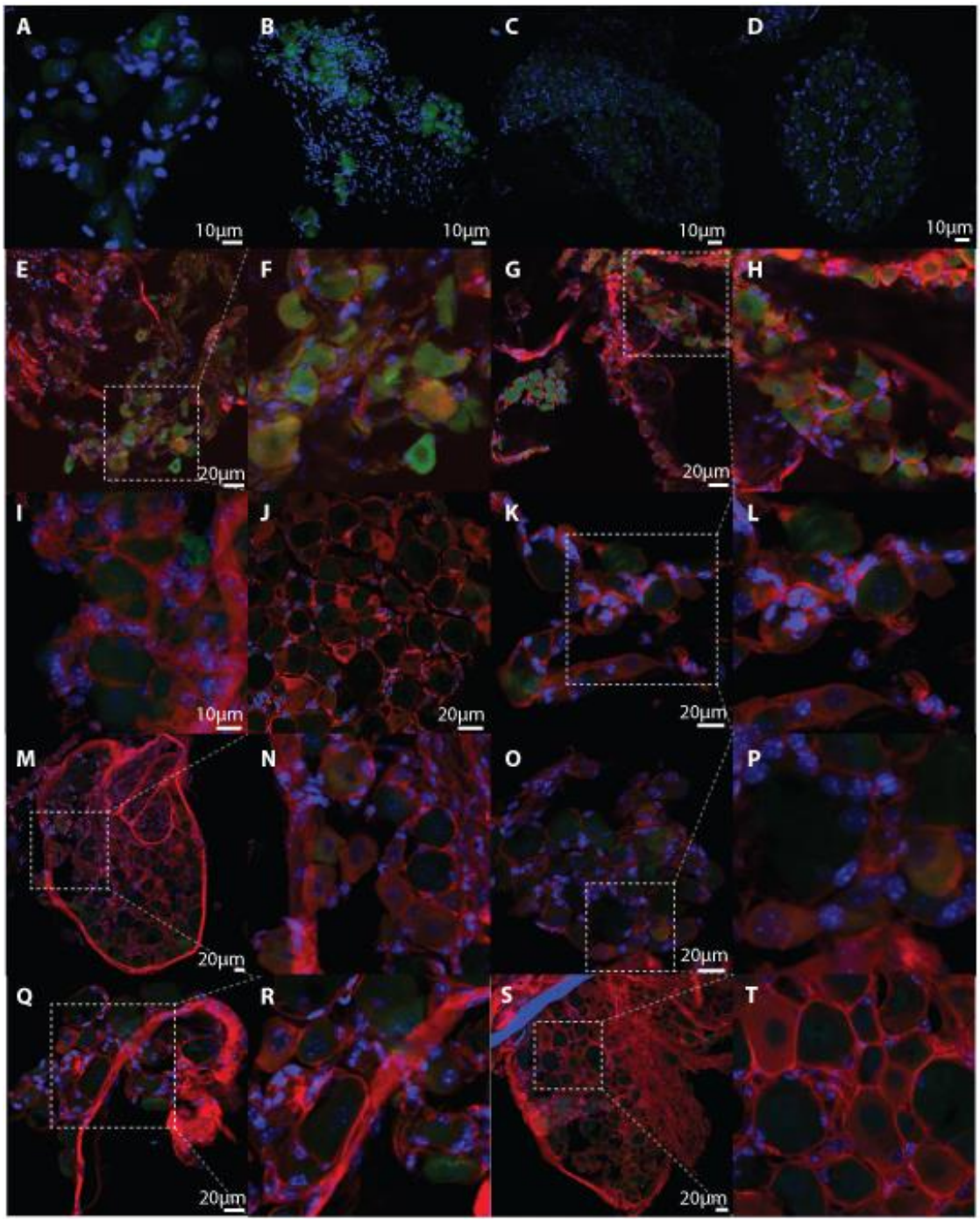

Although we found a subset of cells in wild type DRGs expressing TMC2 (**Fig 4.8**), it was much harder to visualise than TMC1. Co-immunofluroescence for LDHB (NF class), P2X3 (NP class), TH (TH class) and TAC1 (PEP1) were all negative, though it is impossible to determine whether this is due to absense of the protein or simply because the expression level is too low to be detected. It is worth noting that in the RNA-seq results of Usoskin et al. (2015), expression levels of TMC2 were found to be several orders of magnitude lower than either TMC1 or TMC3. Furthermore, in the auditory system it is known that expression of TMC2 decreases after the second postnatal week (Kawashima et al. 2011) – if a similar pattern occurs in the rest of the body then this could also account for lower levels of antibody detection.

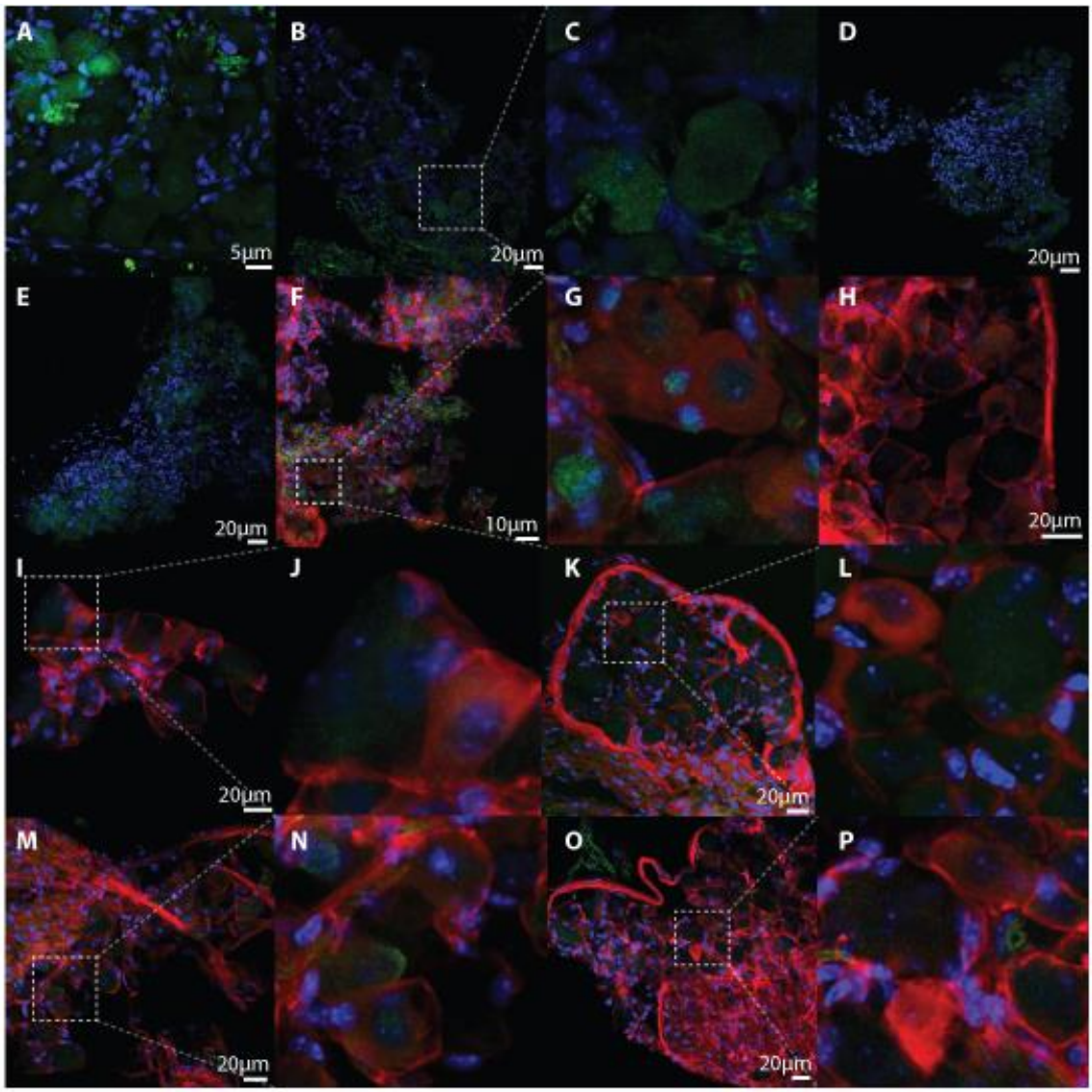

Fig 4.8: Immunofluorescence of TMC2 and DRG cell-type markers. A), **B)** and insert **C)** TMC2 in wild type animals. **D)** and **E)** TMC2 in knockout mutants. **F)** and insert **G)**, **H)** LDHB in red and TMC2 in green. **I)** and insert **J)** P2X3 in red and TMC2 in green. **K)** and insert **L)** TH in red and TMC2 in green. **M)** and insert **N)** CACNA1H in red and TMC2 in green. **O)** and insert **P)** CACNA1H in red and TMC2 in green. All slices use DAPI staining in blue, scale as indicated.

TMC3 positive cells were seen at a reasonable level in DRG slices from wild type animals, and control immunofluroescence in knock out mutants suggests low levels of background staining (**Fig 4.9**). TMC3 positive cells were not present in slices with P2X3 positive cells, indicating it is not present in the NP class of neurons. Similarly, LDHB (NF class) and CACNA1H (NF1-3 class) positive cells were distinct from TMC3 positive cells, suggesting it is not expressed in the NF class of mechanoreceptors. However, in TMC3 positive cells there is a distinct overlap in expression with TAC1 (PEP1 class) and TH (TH class). Intriguinely, this suggests TMC3 is found in Aδ cells responsible for thermosensation (Tominaga et al. 1998; Caterina et al. 1999), and in the distinct set of C-fibres responsible for low-threshold mechanosensation (Seal et al. 2009). Both these classes of neurons are recognized as small-to-medium sized, with little-to-no myelination around the nerve fibres (Lumpkin & Bautista 2005).

Fig 4.9: Immunofluorescence of TMC3 and DRG cell-type markers. A) and **B)** TMC3 in wild type animals. **C)** and **D)** TMC3 in knockout mutants. **E)** and **F)** Positive staining for TAC1 (PEP1 class) in green and TMC3 in red. **G)** and insert **H)** P2X3 (NP class) in red and TMC3 in green. **I)** and insert **J)** Positive staining for TH (TH class) in red and TMC3 in green. **K)** and insert **L)** Positive staining for TH in red and TMC3 in green. **M)** and insert **N)** LDHB (NF class) in red and TMC3 in green. **O)** and insert **P)** LDHB in red and TMC3 in green. **Q)** and insert **R)** CACNA1H (NF1-3 class) in red and TMC3 in green. All slices use DAPI staining in blue, scale as indicated.

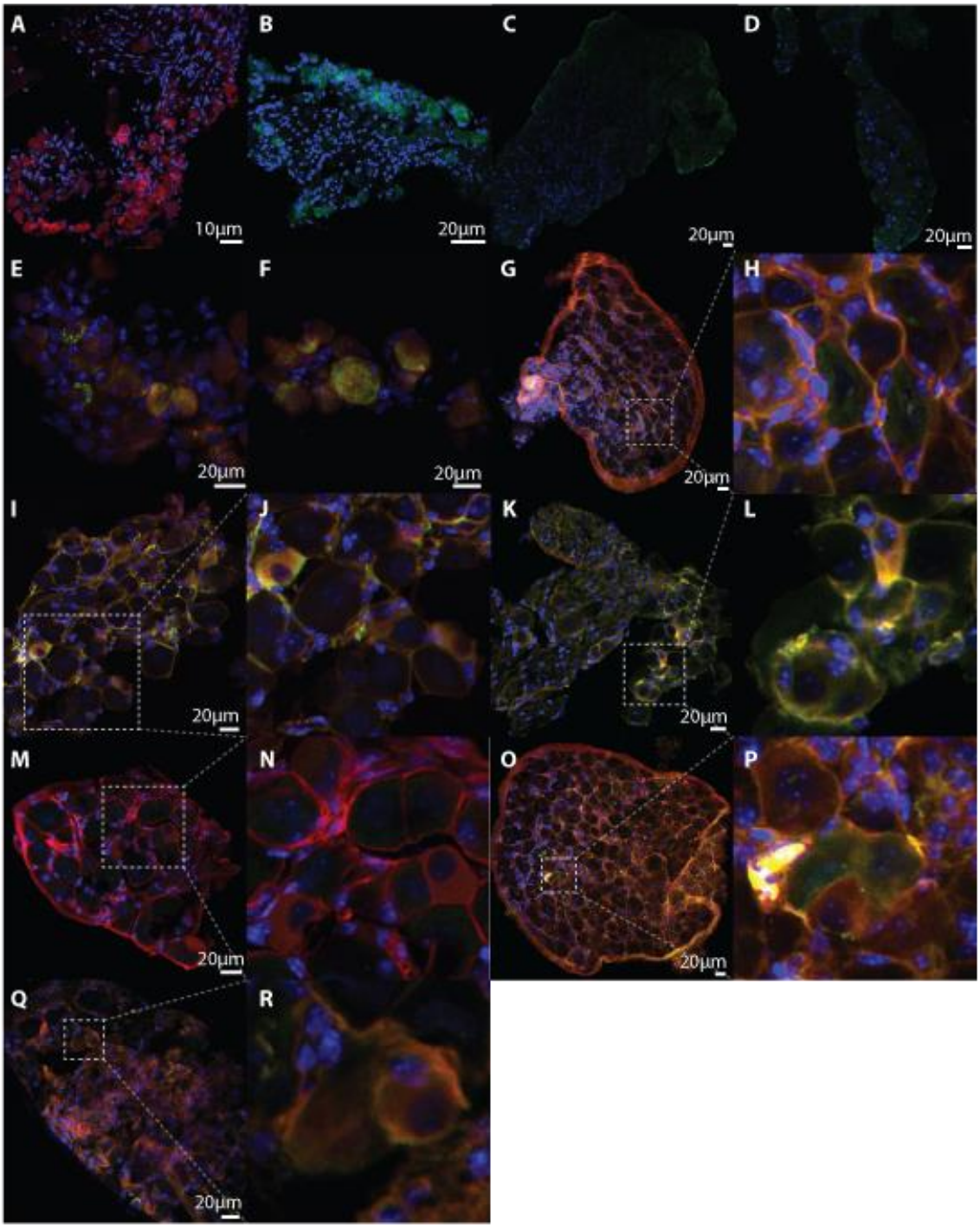
A
10µm
B
20µm
C
20µm
D
20µm
E
20µm
F
20µm
G
20µm
H
I
20µm
J
K
20µm
L
M
20µm
N
O
20µm
P
Q
20µm
R

As a final control, we stained DRG slices from heterozygous animals with antibodies for both β-galactosidase and the TMC genes. Because the TMC mutations in these mice have been constructed with a lacZ knock-in, heterozygous animals should display co-staining for both markers within the DRG (**Fig 4.10**). This staining appeared to show the accuracy of the antibodies, with clear overlap in most samples of both the TMC and βgal signal.

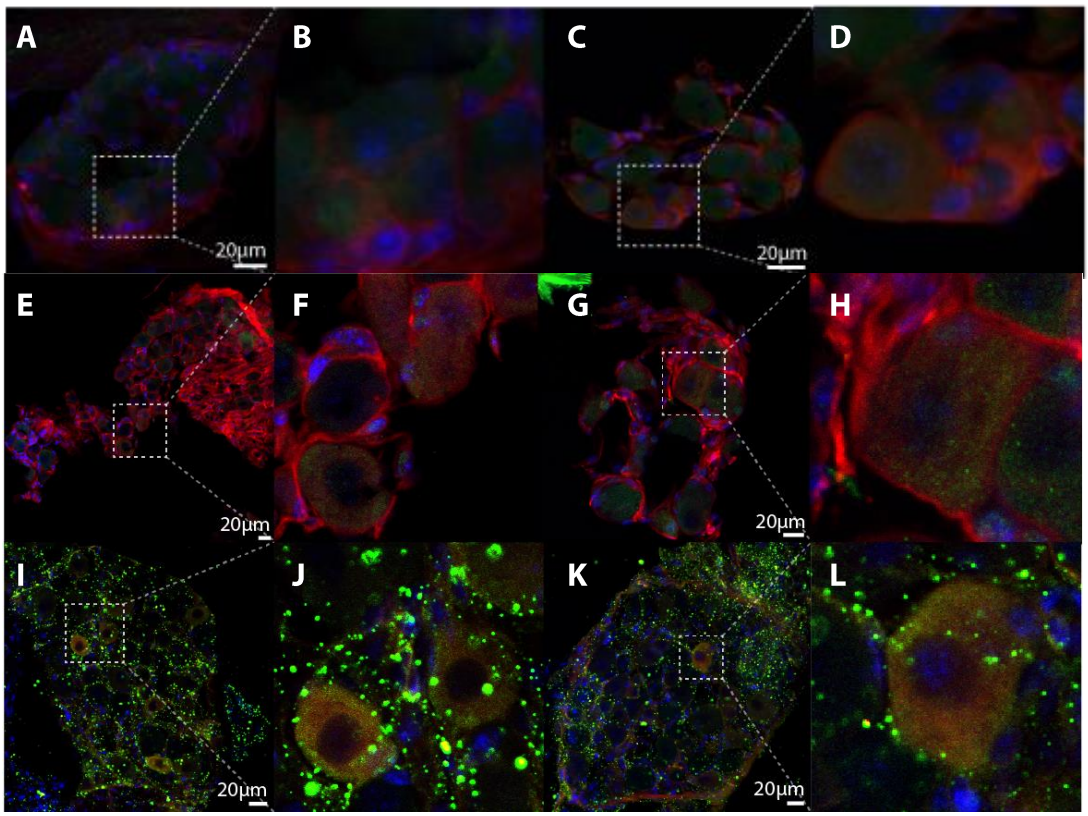

Fig 4.10: Immunofluorescence for βgal and TMC genes in heterozygous animals. Co-staining appears to confirm the accuracy of TMC antibodies. **A)** and insert **B)** TMC1 in green and βgal in red. **C)** and insert **D)** TMC1 in green and βgal in red. **E)** and insert **F)** TMC2 in green and βgal in red. **G)** and insert **H)** TMC2 in green and βgal in red. **I)** and insert **J)** TMC3 in green and βgal in red. **K)** and insert **L)** TMC3 in green and βgal in red. All slices use DAPI staining in blue, scale as indicated.

4.2.2 Mice lacking TMC proteins do not show a cutaneous touch defect

TMC proteins are already of interest to scientists based on their role in hearing, suggesting an important function in the hair cell mechanotransduction channel. Combined with the promising results from our expression analysis, which suggest that several of the TMC proteins are expressed in mechanosensory cells, we decided to begin *in vivo* experiments with the Von Frey test. Named after the inventor of this technique, the test involves using calibrated fibres to deliver a known force to the hindpaw of a mouse, with the expectation that animals exhibiting a cutaneous touch defect will display a higher response threshold before they withdraw from the fibre. This threshold is defined as the stimuli level at which the animal withdraws 50% of the time (Chaplan et al. 1994). Von Frey experiments were carried out on mutant mice for *Tmc1*, *Tmc2* and *Tmc3*, alongside age-matched wild type animals. In every case, there was no significant difference in the touch threshold between wild type and TMC mutant animals (**Fig. 4.11**).

Fig 4.11: 50% response thresholds from Von Frey fibres tested on *Tmc1, Tmc2* and *Tmc3* knockout mice. None of the mutants displayed a significant change in response threshold compared to age-matched wild type animals (Mann-Whitney U-test, n > 50 presentations per genotype).

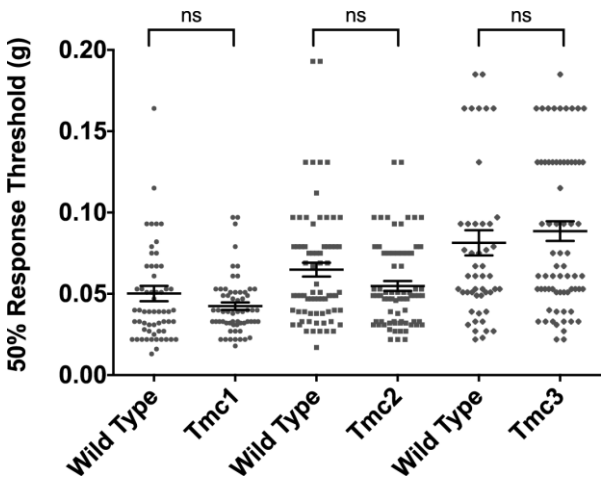

4.2.3 Assaying temperature responsiveness of TMC3

Based on the expression profile of TMC3, which indicates that it is found in thermosensory neurons, we next decided to examine these mutants for any temperature sensation defects. In mice, there are two main protocols used for assaying temperature sensitivity: the hot/cold plate test or the Hargreaves test (Allen & Yaksh 2004). These paradigms use transient stimuli that do not result in tissue damage. For the hot plate test, investigators measure the time before an animal responds to noxious temperatures when placed onto a hot plate, whereas the Hargreaves test utilizes a focused light beam on the animal's paw and similarly measures the response latency.

Due to complications in carrying out experiments in mice, we determined that the most appropriate action would be to carry out pilot tests in our heterologous expression system, *C. elegans*, before returning to mammalian experiments. As a result, we returned to calcium imaging of our ectopically expressing TMC3 line. Using a pressurized perfusion setup, we can gradually increase the buffer temperature and monitor calcium responses in immobilized worms. A TMC3 control with the perfusion system delivering room temperature buffer established that any responses are due to temperature and not mechanical stimulation from buffer flow. In wild type animals, increased temperature results in a gradual increase in calcium responses, reaching around 20% after a minute (**Fig 4.12**). TMC3-expressing animals show an increased temperature response, reaching up to 40%. While not quite significantly different, this does appear to be a clear trend that needs to be explored further – both in another *C. elegans* neuron, and in mice.

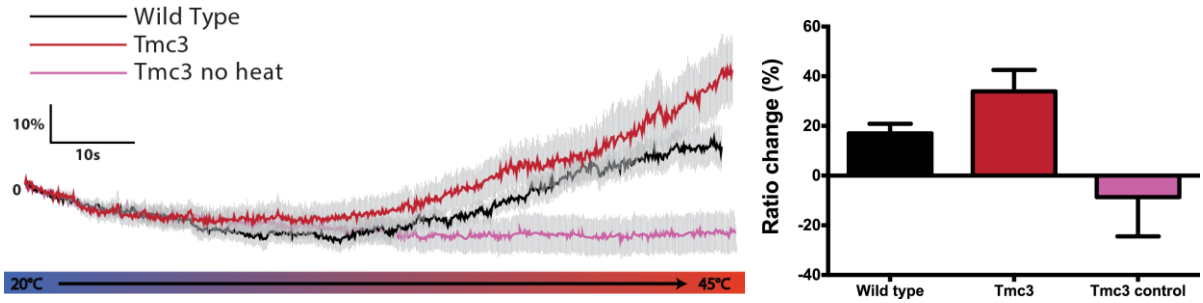

Fig 4.12: Temperature responses in TMC3 expressing *C. elegans*. TMC3-expressing animals show an increased response to temperatures up to 45°C, though not significantly different from wild type (t-test, P<0.08). Control TMC3-expressing animals using the same perfusion setup but with continuous room temperature buffer show no responses. n > 9 traces.

4.3 Discussion and conclusions

Mechanosensation is a key property of many systems throughout our bodies, and the receptor complexes involved are likely to be highly specialized based on their cellular context. For example, even within the cochlear there is a huge variation in the sensitivity of hair cell mechanotransduction channels (Ricci et al. 2003). More broadly, mechanotransduction channels must be able to respond to osmotic stresses, muscle stretching or tensing, fluid shear, and physical distortion (Sukharev & Sachs 2012). With such a broad range of mechanosensory functions, it can be difficult to determine where one should begin looking when investigating a possible mechanosensitive protein. Consequently, we decided to begin our study of murine TMCs with an expression analysis, hoping that the types of cells they are found in would narrow down the possible *in vivo* function of the proteins.

While analysis of TMC2 was largely unsuccessful due to low levels of expression, we did observe TMC1 and TMC3 in a subset of low-threshold mechanosensory cells in the DRG. Another unexpected outcome from the expression analysis was the finding that TMC3 appears to be expressed in cells involved in thermosensation. However, it is well known that many nociceptors are polymodal and capable of responding to an array of aversive stimuli. It is now generally accepted that a single protein may be involved in the transmission of multiple senses, such as touch and heat, and that individual cells may be capable of responding to both (Lumpkin & Caterina 2007).

Initially, we used the Von Frey paradigm to examine whether TMC mutant mice exhibited cutaneous touch defects, but found no effect in any of the subfamily A TMCs. However, there are a number of caveats to this experiment. Firstly, the Von Frey fibres are a very 'coarse' testing method – due to the range of fibres available, they are unlikely to detect small changes in touch sensation and instead are more effective where a drastic defect is expected. Consequently, if loss of the TMC proteins only produces a small change in touch sensitivity, this would most likely go undetected. Because we already know that TMCs can function redundantly in other forms of mechanosensation (Kawashima et al. 2011), it is also possible that looking at single mutants will not reveal significant differences. Thus, a key aim going forward is to breed double- and triple-mutant mice for the TMCs, so that touch sensation can be re-examined in a stronger genetic background.

Another area for future investigation is the possible role of TMC3 in thermosensation, which was hinted at with the finding that the protein is expressed in a subset of thermosensory cells in the DRG. Although none of the other TMC proteins have been

implicated in thermosensation, further review suggests there could an evolutionary basis for this role. *Anonctamin1*, a distant relation to the TMC gene family (Hahn et al. 2009), has been shown to act as a heat sensor in nociceptive neurons of the DRG (Cho et al. 2012). When we did examine the temperature responses of *C. elegans* ectopically expressing TMC3, there was an increased calcium response compared to wild type, though this was not statistically significant. A confounding factor in these experiments was the fact that the ASK neurons, which had been an inert background in our other sensory experiments, appear to have an inherent response to temperature increases. It is therefore more difficult to distinguish any TMC3-specific increase. To return more definitive results, further experiments will need to focus on a more appropriate neuron for temperature experiments, and TMC3-expressing constructs will need to be re-made.

The possibility of TMC3 functioning in temperature sensation raises further questions as to its mechanism of function – how could this protein regulate both temperature and touch sensation? It has been postulated that in some cases temperature-responsive channels could in fact be relying on a mechanosensitive process. For example, temperature changes may alter the plasma membrane's structure, affecting its tension or thickness and in turn gating a mechanosensitive ion channel (Vriens et al. 2014). These authors highlight that channels such as TREK1, TREK2 and TRAAK are all both mechano- and thermosensitive and may rely on such a mechanism, so it is not beyond comprehension that TMC3 could operate in a similar way.

4.4 Materials and Methods

4.4.1 Mouse derivation and breeding

All animal studies were carried out in accordance with local ethics committee and Home Office regulations. Sperm from *Tmc3* mutant mice ($Tmc3^{tm2b(KOMP)Wtsi}$) was sourced from MRC Harwell and used for IVF with C57BL/6 JAX donors in the MRC ARES facility. Genotyping was carried out at LMB facilities using the primers detailed in the WTSI's supporting document for the strain (Tmc3_112637_F: AAGACTGGATTGGGCTCACG, Tmc3_112637_R: CTAGGCTGGGGAATC ACAGG, CAS_R1_Term: TCGTGGTATCGTTATGCGCC). Homozygous animals were bred and used for all further experiments.

Tmc1 and *Tmc2* knockout mice were obtained from the Holt Lab in the Department of Otolaryngology, F.M. Kirby Neurobiology Center, Children's Hospital Boston/Harvard Medical School (Kawashima et al. 2011).

4.4.2 DRG dissection

Adult mice (6-8 weeks old) were anaesthetized by intraperitoneal injection with 0.1ml Eutethal and then killed by transcardial perfusion fixation with 25ml PBS followed by 25ml 4% paraformaldehyde (PFA) in PBS (ChemCruz). DRGs were dissected according to Sleigh et al. (2016) and post-fixed in 4% PFA for one hour. DRGs were then allowed to settle in 30% sucrose overnight as a cryoprotectant before being embedded and frozen in OCT (VWR International) and stored at -80C. Tissue was sectioned on a cryostat at 14µm and then collected in PBS in 24-well plates for processing.

4.4.3 Reverse transcription of RNA from DRG samples

To confirm the presence of TMC protein transcripts in wild type DRGs, RNA was extracted using a conventional chloroform/phenol method (Chomczynski & Sacchi 1987). This sample was used to create first strand cDNA with the ProtoScript II Reverse Transcriptase (NEB), which was subsequently amplified with TMC-specific primers and confirmed by DNA sequencing (Source Bioscience).

4.4.4 Immunohistochemistry

Samples were blocked for one hour with 5% normal goat serum (Invitrogen), before primary antibodies were applied for two hours at room temperature, or overnight at 4°C. After three washes in PBS, secondary antibodies were likewise applied for two hours at room temperature or overnight at 4°C. Following three more washes in PBS, samples were mounted with slow-fade gold antifade mountant with DAPI (ThermoFisher). All antibodies were diluted in antibody buffer (0.5% Triton X-100, 1mM EDTA pH8, 1% BSA in PBS pH 7.2).

The primary antibodies I have used are mouse anti-NECAB2 (Atlas Antibodies, 1:1000, AMAb90808), goat anti-SPP1 (R&D Systems, 1:500, AF808), mouse anti-LDHB (Abcam, 1:500, ab85319), goat anti-FAM19A1 (R&D Systems, 1:100, af5154), goat anti-CALB1 (R&D Systems, 1:1000, AF3320), goat anti-TRKA (R&D Systems, 1:200, AF1056), rabbit anti-TRKA (Santa Cruz Biotechnology, 1:200, a763) rabbit anti-TAC1 (CusaBio, 1:100, CSB-PA559959), goat anti-TMC3 (Santa Cruz Biotechnology, 1:250, sc-248835), rabbit anti-TMC2 (Santa Cruz Biotechnology, 1:250, sc-85965), rabbit anti-TMC1 (Abcam, 1:250, ab72434), mouse anti-P2X3 (Santa Cruz Biotechnology, 1:250, sc-390572), mouse anti-TH (Santa Cruz

Biotechnology, 1:250, sc-25269), mouse anti-beta galactosidase (Promega, 1:1000, Z378), mouse anti-Cacna1h (CamBioscience, 1:1000, SMC-303), mouse anti-Cntnap2 (Antibodies online, 1:500, MABN465).

For detection, donkey 488- and 568-conjugated Alexa secondary antibodies against goat (ThermoFisher A11055 and A11057, respectively), and goat 488- and 568-conjugated Alexa secondary antibodies against mouse (ThermoFisher A11001 and A11004, respectively), and rabbit (ThermoFisher A11008) were used at a concentration of 1:1000.

4.4.5 Confocal imaging

Slides were imaged on a Zeiss LSM 710 confocal microscope with a 20x objective. Images were further processed in Zen2012 software and Adobe Illustrator CS6.

4.4.6 Calcium imaging for temperature responses

Calcium imaging for temperature responsiveness was conducted in a similar manner as previously described, with a few key differences. Rather than gravity powered perfusion, a pressurized system (Digitimer) was used to deliver neuronal buffer at approximately 3psi. Immobilized worms were bathed in room temperature (20°C) buffer for 10s, before the perfusion system delivered heated buffer for the next minute, gradually increasing the temperature to approximately 45°C (monitered with a temperature probe). To ensure that any responses were due to the heat and not because of increased force from the pressurized perfusion system, controls were also carried out using pressurized perfusion of room temperature buffer. All other calcium imaging equipment and analysis is carried out as described in previous chapters.

4.4.7 Behavioural tests

Adult mice (6-8 weeks old) were selected for all tests. In each experiment, six knockouts and six age-matched wild type animals were tested over two days, with at least two experimental series on each paw (resulting in at least 48 threshold calculations). Animals were unrestrained in a plexiglass enclosure on a raised, mesh-bottomed platform (BioSeb Instruments), where they were allowed to acclimatize for at least an hour. Von Frey fibres were then applied to the plantar surface of each hindpaw until the fibre buckled. Fibres were held for approximately two seconds, with withdrawal responses being noted to determine the fibre weight that results in a 50% response threshold.

The threshold was determined using the 'Up-Down method' (Dixon 1980), which works as follows: rather than testing animals a set number of times with each fibre, the fibre used is decided sequentially, based on the animal's response to the previous stimuli. For example, stimuli are usually presented starting with the 0.4g fibre, which is in the middle of the series. If the animal does not show a paw withdrawal response, then a stronger stimulus is presented; if it does respond then a weaker stimuli is presented (Chaplan et al. 1994). This method usually arrives at the response threshold faster, leaving less chance for animals to acclimatize to stimuli.

Responses are recorded using an O for no-withdrawal and an X for a withdrawal, with stimuli presented until six responses in the immediate vicinity of the 50% threshold are reached, as seen by sequential up-down variations in stimuli (Chaplan et al. 1994). The response threshold is then calculated using 50% g threshold = $(10^{[\,Xf + k\,\delta\,]})/10000$,

where X_f = value (in log units) of the final Von Frey hair used; k = tabular value (see **Fig 4.13** below) for the pattern of positive/negative responses; and δ = mean difference (in log units) between stimuli levels (here, 0.278 – see **Table 4.1**). Because these thresholds do not adhere to a mathematical continuum, they are considered to be non-parametrically distributed and so the Mann-Whitney U-test is used to statistically compare thresholds.

Size (log units)	2.36	2.44	2.83	3.22	3.61	3.84	4.08	4.31
Force (g)	.02	.04	.07	.16	.4	.7	1.2	2

Table 4.1: Von Frey fibres used in the experimental paradigm. The animal's paw is touched with a series of eight Von Frey hairs with logarithmically incremental stiffness (BioSeb), such that $\delta = 0.278$

Values for k, based on response pattern (modified from Dixon, 1980)

Pattern	Value for k	Pattern	Value for k	Pattern	Value for k	Pattern	Value for k
OX	−0.5	OOOXOOOO	−0.547	XO	0.5	XXXOXXXX	0.547
OOX	−0.388	OOOOXOOOO	−0.547	XXO	0.388	XXXXOXXXX	0.547
OOOX	−0.378	OXOOOX	−1.25	XXXO	0.378	XOXXXO	1.25
OOOOX	−0.377	OOXOOOX	−1.247	XXXXO	0.377	XXOXXXO	1.247
OXO	0.842	OOOXOOOX	−1.246	XOX	−0.842	XXXOXXXO	1.246
OOXO	0.89	OOOOXOOOX	−1.246	XXOX	−0.89	XXXXOXXXO	1.246
OOOXO	0.894	OXOOXO	0.372	XXXOX	−0.894	XOXXOX	−0.372
OOOOXO	0.894	OOXOOXO	0.38	XXXXOX	−0.894	XXOXXOX	−0.38
OXX	−0.178	OOOXOOXO	0.381	XOO	0.178	XXXOXXOX	−0.381
OOXX	0	OOOOXOOXO	0.381	XXOO	0	XXXXOXXOX	−0.381
OOOXX	0.026	OXOOXX	−0.169	XXXOO	−0.026	XOXXOO	0.169
OOOOXX	0.028	OOXOOXX	−0.144	XXXXOO	−0.028	XXOXXOO	0.144
OXOO	0.299	OOOXOOXX	−0.142	XOXX	−0.299	XXXOXXOO	0.142
OOXOO	0.314	OOOOXOOXX	−0.142	XXOXX	−0.314	XXXXOXXOO	0.142
OOOXOO	0.315	OXOXOO	0.022	XXXOXX	−0.315	XOXOXX	−0.022
OOOOXOO	0.315	OOXOXOO	0.039	XXXXOXX	−0.315	XXOXOXX	−0.039
OXOX	−0.5	OOOXOXOO	0.04	XOXO	0.5	XXXOXOXX	−0.04
OOXOX	−0.439	OOOOXOXOO	0.04	XXOXO	0.439	XXXXOXOXX	−0.04
OOOXOX	−0.432	OXOXOX	−0.5	XXXOXO	0.432	XOXOXO	0.5
OOOOXOX	−0.432	OOXOXOX	−0.458	XXXXOXO	0.432	XXOXOXO	0.458
OXXO	1	OOOXOXOX	−0.453	XOOX	−1	XXXOXOXO	0.453
OOXXO	1.122	OOOOXOXOX	−0.453	XXOOX	−1.122	XXXXOXOXO	0.453
OOOXXO	1.139	OXOXXO	1.169	XXXOOX	−1.139	XOXOOX	−1.169
OOOOXXO	1.14	OOXOXXO	1.237	XXXXOOX	−1.14	XXOXOOX	−1.237
OXXX	0.194	OOOXOXXO	1.247	XOOO	−0.194	XXXOXOOX	−1.247
OOXXX	0.449	OOOOXOXXO	1.248	XXOOO	−0.449	XXXXOXOOX	−1.248
OOOXXX	0.5	OXOXXX	0.611	XXXOOO	−0.5	XOXOOO	−0.611
OOOOXXX	0.506	OOXOXXX	0.732	XXXXOOO	−0.506	XXOXOOO	−0.732
OXOOO	−0.157	OOOXOXXX	0.756	XOXXX	0.157	XXXOXOOO	−0.756
OOXOOO	−0.154	OOOOXOXXX	0.758	XXOXXX	0.154	XXXXOXOOO	−0.758
OOOXOOO	−0.154	OXXOOO	−0.296	XXXOXXX	0.154	XOOXXX	0.296
OOOOXOOO	−0.154	OOXXOOO	−0.266	XXXXOXXX	0.154	XXOOXXX	0.266
OXOOX	−0.878	OOOXXOOO	−0.263	XOXXO	0.878	XXXOOXXX	0.263
OOXOOX	−0.861	OOOOXXOOO	−0.263	XXOXXO	0.861	XXXXOOXXX	0.263
OOOXOOX	−0.86	OXXOOX	−0.831	XXXOXXO	0.86	XOOXXO	0.831
OOOOXOOX	−0.86	OOXXOOX	−0.763	XXXXOXXO	0.86	XXOOXXO	0.763
OXOXO	0.701	OOOXXOOX	−0.753	XOXOX	−0.701	XXXOOXXO	0.753
OOXOXO	0.737	OOOOXXOOX	−0.752	XXOXOX	−0.737	XXXXOOXXO	0.752
OOOXOXO	0.741	OXXOXO	0.831	XXXOXOX	−0.741	XOOXOX	−0.831
OOOOXOXO	0.741	OOXXOXO	0.935	XXXXOXOX	−0.741	XXOOXOX	−0.935
OXOXX	0.084	OOOXXOXO	0.952	XOXOO	−0.084	XXXOOXOX	−0.952
OOXOXX	0.169	OOOOXXOXO	0.954	XXOXOO	−0.169	XXXXOOXOX	−0.954
OOOXOXX	0.181	OXXOXX	0.296	XXXOXOO	−0.181	XOOXOO	−0.296
OOOOXOXX	0.182	OOXXOXX	0.463	XXXXOXOO	−0.182	XXOOXOO	−0.463
OXXOO	0.305	OOOXXOXX	0.5	XOOXX	−0.305	XXXOOXOO	−0.5
OOXXOO	0.372	OOOOXXOXX	0.504	XXOOXX	−0.372	XXXXOOXOO	−0.504
OOOXXOO	0.38	OXXXOO	0.5	XXXOOXX	−0.38	XOOOXX	−0.5
OOOOXXOO	0.381	OOXXXOO	0.648	XXXXOOXX	−0.381	XXOOOXX	−0.648
OXXOX	−0.305	OOOXXXOO	0.678	XOOXO	0.305	XXXOOOXX	−0.678
OOXXOX	−0.169	OOOOXXXOO	0.681	XXOOXO	0.169	XXXXOOOXX	−0.681
OOOXXOX	−0.144	OXXXOX	−0.043	XXXOOXO	0.144	XOOOXO	0.043
OOOOXXOX	−0.142	OOXXXOX	0.187	XXXXOOXO	0.142	XXOOOXO	−0.187
OXXXO	1.288	OOOXXXOX	0.244	XOOOX	−1.288	XXXOOOXO	−0.244
OOXXXO	1.5	OOOOXXXOX	0.252	XXOOOX	−1.5	XXXXOOOXO	−0.252
OOOXXXO	1.544	OXXXXO	1.603	XXXOOOX	−1.544	XOOOOX	−1.603
OOOOXXXO	1.549	OOXXXXO	1.917	XXXXOOOX	−1.549	XXOOOOX	−1.917
OXXXX	0.555	OOOXXXXO	2	XOOOO	−0.555	XXXOOOOX	−2
OOXXXX	0.897	OOOOXXXXO	2.014	XXOOOO	−0.897	XXXXOOOOX	−2.014
OOOXXXX	0.985	OXXXXX	0.893	XXXOOOO	−0.985	XOOOOO	−0.983
OOOOXXXX	1	OOXXXXX	1.329	XXXXOOOO	−1	XXOOOOO	−1.329
OXOOOO	−0.547	OOOXXXXX	1.465	XOXXXX	0.547	XXXOOOOO	−1.465
OOXOOOO	−0.547	OOOOXXXXX	1.496	XXOXXXX	0.547	XXXXOOOOO	−1.496

Fig. 4.13: Tabular values used to calculate the 50% response threshold to Von Frey fibres. From Chaplan et al. (1994), maximum likelihood estimation based on the Gaussian cumulative distribution.

Chapter 5: General discussion and Conclusions

5.1 *C. elegans* as a model in which to examine channel function

This work began as an effort to further characterize the TMC protein family, particularly the smaller Subfamily A (TMCs 1-3). TMC1 and TMC2 had received significant attention in humans and mice for their role in hearing, but TMC3 was uninvestigated. Their *C. elegans* homologues, *tmc-1* and *tmc-2*, had also been implicated in sensory transduction as possible channels. Based on our ability to functionally express the mammalian TMCs in *C. elegans*, it was decided to use this more tractable organism to uncover the function of TMC3, before studies would return to mice. Although I was primarily focused on examining TMC3, I have also used this as an opportunity to reveal more about the function of other TMC proteins and of mechanosensory molecules in general.

5.1.1 Human and murine TMC3 encode mechanosensors when expressed in *C. elegans*

By ectopically expressing human and mouse TMC3 in the ASK neurons, I demonstrated that they were able to confer mechanosensory responses to *C. elegans*. Further collaboration with Yiquan Tang showed that the ability to function in *C. elegans* is reliant on expression of CALM-1, the *C. elegans* homologue of the CIB2 protein. Although the mechanism of function is not clear, Dr Tang has shown that CIB proteins physically interact with TMC proteins *in vitro*, suggesting they are critical accessory proteins for TMC function. The ability of TMC3 to generate mechanosensory responses upon heterologous expression strongly suggests it could

be acting as the mechanosensory channel, and perhaps is intrinsically mechanically sensitive.

5.2 Critical domains for TMC protein function

One question that remained about the TMC family of proteins was how they are able to respond to different sensory modalities – with some subfamily members being mechanosensitive and others responding to salt. By using chimeric proteins and examining calcium responses in *C. elegans*, I was able to identify an extracellular loop that appears to confer sensory specificity to the different TMC proteins. Closer examination within this loop also identified some charged residues in TMC1 and TMC2 that appear to be critical for their function. These results were limited by the conclusions we can draw from calcium imaging, and so a key future experiment is electrophysiology on the heterologously expressed proteins to determine if they show channel-like properties. Another question that remains is the exact membrane topology adopted by the TMCs, which was hinted at but not decisively determined in our hands.

5.2.1 Membrane topology of the TMC proteins

I utilized a HA-tagging approach to try and identify membrane-exposed regions of the TMC proteins in *C. elegans* neurons. Antibody staining appeared to confirm a six transmembrane-spanning domain model for TMC1 and TMC3, although further examination suggested that the HA tags were not staining the specific neuron as expected. However, the fact that the chimeric proteins were also based on this six transmembrane-spanning model adds some support, as do previous studies on ER-

retained TMC1 that was determined to have six TM domains (Labay et al. 2010). Further experiments will utilize another *in vivo* tagging technique to finally clarify the membrane topology of TMCs in functional neurons.

5.3 DRG expression of TMC proteins

Based on the information I uncovered about TMC protein function from the *C. elegans* experiments, I then returned to mice to determine if the proteins functioned *in vivo* as we expected. Initially, I used an immunohistochemistry approach to narrow down the functional properties we should examine, looking at all three subfamily A TMCs. While TMC2 could not be detected, I found TMC1 expression in mechanosensory cells, along with TMC3, which corroborates our heterologous expression experiments that showed these proteins were able to generate mechanosensory responses in *C. elegans*.

5.3.1 *In vivo* role of the TMC proteins in mice

With all the supporting experiments suggesting that TMC1 and TMC3 function in mechanosensation, I used the Von Frey test to examine TMC mutant mice for any cutaneous touch defects. Surprisingly, all mutants were indistinguishable from wild type animals. One avenue we will be examining going forward is whether these proteins may function redundantly, by generating double mutant lines and examining if this touch sensitivity is still retained.

5.4 Temperature sensitivity of TMC3

An unexpected result from the immunohistochemistry in DRG neurons was the fact that TMC3 was strongly expressed in a subset of thermosensitive nociceptive neurons. While TMC proteins have not been implicated in thermosensation before, some thermosensitive proteins are also mechanosensitive (Vriens et al. 2014), and so this did not seem beyond the realm of possibility. Before conducting experiments in mice, we wanted to gather some preliminary evidence for this role in *C. elegans*. Although ectopic expression of TMC3 in ASK did confer an increase in temperature sensitivity to worms, the results were obscured by an intrinsic response from the neurons, meaning an alternative expression system will need to be developed. Going forward, our main priority will be to identify an appropriate *C. elegans* neuron for temperature experiments, but also to begin preparing for these assays in mice.

5.5 General Conclusions

Taken together, these three projects have helped to further unravel the roles of TMC proteins in sensory transduction, particularly the previously unstudied TMC3. I have shown for the first time that mouse and human TMC3 are able to form a mechanosensor when heterologously expressed in *C. elegans*, and have identified a key domain of the protein that is critically required for this functionality. I have gathered further support for a six transmembrane-spanning model of the TMC proteins, and for the first time characterized their expression pattern in the DRG, a node for peripheral sensory neurons. I have conducted behavioural experiments looking at the function of TMC proteins in cutaneous touch in mice, and uniquely, in temperature sensation using heterologous expression in *C. elegans*.

My findings lend further credence to the idea that TMC proteins may function more generally in sensory transduction, outside of their already accepted role in hearing. It also highlights the polymodal nature of this protein family, which is now implicated in mechanosensation, salt sensation and putatively in temperature sensation.

References

Ahmad, J. et al., 2005. DFNB48, a new nonsyndromic recessive deafness locus, maps to chromosome 15q23-q25.1. *Human Genetics*, 116(5), pp.407–412.

Akabas, M.H. et al., 1992. Acetylcholine receptor channel structure probed in cysteine-substitution mutants. *Science (New York, N.Y.)*, 258(5080), pp.307–310.

Akemann, W. et al., 2012. Imaging neural circuit dynamics with a voltage-sensitive fluorescent protein. *J Neurophysiol*, 108(8), pp.2323–2337.

Allen, J.W. & Yaksh, T.L., 2004. Assessment of acute thermal nociception in laboratory animals. *Methods in molecular medicine*, 99(1), pp.11–23.

Altun, L.A. et al., 2014. WormAtlas. Available at: http://www.wormatlas.org.

Arnadóttir, J. & Chalfie, M., 2010. Eukaryotic mechanosensitive channels. *Annual review of biophysics*, 39, pp.111–137.

Bae, Y.-K. & Barr, M.M., 2008. Sensory roles of neuronal cilia: cilia development, morphogenesis, and function in C. elegans. *Front Biosci*, 13, pp.5959–74.

Bargmann, C.I. & Horvitz, H.R., 1991. Chemosensory neurons with overlapping functions direct chemotaxis to multiple chemicals in C. elegans. *Neuron*, 7(5), pp.729–742.

Barhanin, J. et al., 1996. K(V)LQT1 and lsK (minK) proteins associate to form the I(Ks) cardiac potassium current. *Nature*, 384(6604), pp.78–80.

Basbaum, A.I. et al., 2009. Cellular and Molecular Mechanisms of Pain. *Cell*, 139(2), pp.267–284.

Baumann, M. & Roth, A., 1986. The Ca++ permeability of the apical membrane in neuromast hair cells. *Journal of Comparative Physiology A*, 158(5), pp.681–688.

Bazopoulou, D. & Tavernarakis, N., 2007. Mechanosensitive Ion Channels in Caenorhabditis elegans. *Current Topics in Membranes*, 59(6), pp.49–79.

Bedbrook, C.N. et al., 2015. Genetically Encoded Spy Peptide Fusion System to Detect Plasma Membrane-Localized Proteins In Vivo. *Chemistry and Biology*, 22(8), pp.1108–1121.

Bessou, P. & Perl, E.R., 1969. Response of cutaneous sensory units with unmyelinated fibers to noxious stimuli. *Journal of neurophysiology*, 32(6), pp.1025–1043.

Beurg, M. et al., 2016. Development and localization of reverse-polarity mechanotransducer channels in cochlear hair cells. *Proceedings of the National Academy of Sciences*, (7), p.201601067.

Beurg, M., Xiong, W., et al., 2014. Subunit determination of the conductance of hair-cell mechanotransducer channels. *Proceedings of the National Academy of Sciences*, 112(5), pp.1589–94.

Beurg, M., Goldring, a. C. & Fettiplace, R., 2015. The effects of Tmc1 Beethoven mutation on mechanotransducer channel function in cochlear hair cells. *The Journal of General Physiology*, 146(3), pp.233–243.

Beurg, M., Kim, K.X. & Fettiplace, R., 2014. Conductance and block of hair-cell mechanotransducer channels in transmembrane channel-like protein mutants. *The Journal of general physiology*, 144(1), pp.55–69.

Bradman, M.J.G. et al., 2015. Practical mechanical threshold estimation in rodents using von Frey hairs/Semmes–Weinstein monofilaments: Towards a rational method. *Journal of Neuroscience Methods*, 255, pp.92–103.

Brelidze, T.I., Niu, X. & Magleby, K.L., 2003. A ring of eight conserved negatively

charged amino acids doubles the conductance of BK channels and prevents inward rectification. *Proceedings of the National Academy of Sciences of the United States of America*, 100(15), pp.9017–9022.
Brenner, S., 1974. The Genetics of Caenorhabditis Elegans. *Genetics*, 77, pp.71–94.
Brohawn, S.G., Campbell, E.B. & MacKinnon, R., 2014. Physical mechanism for gating and mechanosensitivity of the human TRAAK K+ channel. *Nature*, 516(7529), pp.126–130.
Brohawn, S.G., Su, Z. & MacKinnon, R., 2014. Mechanosensitivity is mediated directly by the lipid membrane in TRAAK and TREK1 K+ channels. *Proceedings of the National Academy of Sciences of the United States of America*, 111(9), pp.3614–9.
Brown, S.D.M., Hardisty-Hughes, R.E. & Mburu, P., 2008. Quiet as a mouse: dissecting the molecular and genetic basis of hearing. *Nature reviews. Genetics*, 9(april), pp.277–290.
Brown, S.D.M. & Moore, M.W., 2012. The International Mouse Phenotyping Consortium: Past and future perspectives on mouse phenotyping. *Mammalian Genome*, 23(9–10), pp.632–640.
Buck, L. & Axel, R., 1991. A novel multigene family may encode odorant receptors: A molecular basis for odor recognition. *Cell*, 65(1), pp.175–187.
Burger, E.H. & Klein-Nulend, J., 1999. Mechanotransduction in bone - role of the lacuno-canalicular network. *The FASEB Journal*, 13, pp.S101–S112.
Caterina, M.J. et al., 1999. A capsaicin-receptor homologue with a high threshold for noxious heat. *Nature*, 398(6726), pp.436–441.
Caterina, M.J. et al., 1997. The capsaicin receptor: a heat-activated ion channel in the pain pathway. *Nature*, 389(6653), pp.816–824.
Chalfie, M., 2009. Neurosensory mechanotransduction. *Nature reviews. Molecular cell biology*, 10(1), pp.44–52.
Chalfie, M. & Sulston, J., 1981. Developmental genetics of the mechanosensory neurons of Caenorhabditis elegans. *Developmental biology*, 82(2), pp.358–370.
Chaplan, S.R. et al., 1994. Quantitative assessment of tactile allodynia in the rat paw. *Journal of Neuroscience Methods*, 53(1), pp.55–63.
Chatzigeorgiou, M. et al., 2010. Specific roles for DEG/ENaC and TRP channels in touch and thermosensation in C. elegans nociceptors. *Nature neuroscience*, 13(7), pp.861–868.
Chatzigeorgiou, M. et al., 2013. tmc-1 encodes a sodium-sensitive channel required for salt chemosensation in C. elegans. *Nature*, 494(7435), pp.95–9.
Chelur, D.S. et al., 2002. The mechanosensory protein MEC-6 is a subunit of the C. elegans touch-cell degenerin channel. *Nature*, 420, pp.669–673.
Chen, Y. et al., 2015. Subunit composition of a DEG/ENaC mechanosensory channel of Caenorhabditis elegans. *Proceedings of the National Academy of Sciences*, 4, p.201515968.
Cho, H. et al., 2012. The calcium-activated chloride channel anoctamin 1 acts as a heat sensor in nociceptive neurons. *Nat Neurosci*, 15(7), pp.1015–1021.
Chomczynski, P. & Sacchi, N., 1987. Single-step method of RNA isolation by acid guanidinium thiocyanate-phenol-chloroform extraction. *Analytical Biochemistry*, 162(1), pp.156–159.
Christensen, A.P. & Corey, D.P., 2007. TRP channels in mechanosensation: direct or indirect activation? *Nat Rev Neurosci*, 8(7), pp.510–521.
Christensen, M. et al., 2002. A primary culture system for functional analysis of C.

elegans neurons and muscle cells. *Neuron*, 33(4), pp.503–514.
Colbert, H.A., Smith, T.L. & Bargmann, C.I., 1997. OSM-9, a novel protein with structural similarity to channels, is required for olfaction, mechanosensation, and olfactory adaptation in Caenorhabditis elegans. *The Journal of neuroscience : the official journal of the Society for Neuroscience*, 17(21), pp.8259–69.
Corey, D.P. & Holt, J.R., 2016. Are TMCs the Mechanotransduction Channels of Vertebrate Hair Cells? *Journal of Neuroscience*, 36(43), pp.10921–10926.
Corey, D.P. & Hudspeth, A.J., 1979a. Ionic basis of the receptor potential in a vertebrate hair cell. *Nature*, 281, pp.675–677.
Corey, D.P. & Hudspeth, A.J., 1983. Kinetics of the receptor current in bullfrog saccular hair cells. *J. Neurosci*, 3(5), pp.962–976.
Corey, D.P. & Hudspeth, A.J., 1979b. Response latency of vertebrate hair cells. *Biophysical journal*, 26(3), pp.499–506.
Corns, L.F. et al., 2016. Tmc1 Point Mutation Affects Ca2+ Sensitivity and Block by Dihydrostreptomycin of the Mechanoelectrical Transducer Current of Mouse Outer Hair Cells. *Journal of Neuroscience*, 36(2), pp.336–349.
Corns, L.F. & Marcotti, W., 2016. Piezo1 haploinsufficiency does not alter mechanotransduction in mouse cochlear outer hair cells. *Physiological reports*, 4(3), p.e12701.
Cosgriff, A.J. et al., 2000. A study of AroP-PheP chimeric proteins and identification of a residue involved in tryptophan transport. *Journal of Bacteriology*, 182(8), pp.2207–2217.
Coste, B. et al., 2010. Piezo1 and Piezo2 are essential components of distinct mechanically-activated cation channels. *Science*, 330(6000), pp.55–60.
Coste, B. et al., 2015. Piezo1 ion channel pore properties are dictated by C-terminal region. *Nature Communications*, 6(May), p.7223.
Crawford, A.C., Evans, M.G. & Fettiplace, R., 1991. THE ACTIONS OF CALCIUM ON THE MECHANO-ELECTRICAL TRANSDUCER CURRENT OF TURTLE HAIR CELLS. *Journal of Physiology*, 434, pp.369–398.
Delmas, P. & Coste, B., 2013. Mechano-gated ion channels in sensory systems. *Cell*, 155(2), pp.278–84.
Delmas, P., Hao, J. & Rodat-Despoix, L., 2011. Molecular mechanisms of mechanotransduction in mammalian sensory neurons. *Nature reviews. Neuroscience*, 12(3), pp.139–153.
Dixon, W.J., 1980. EFFICIENT ANALYSIS OF EXPERIMENTAL OBSERVATIONS. *Ann. Rev. Pharcol. Toxicol*, 20, pp.441–62.
Ebrey, T. & Koutalos, Y., 2001. Vertebrate Photoreceptors. *Progress in Retinal and Eye Research*, 20(1), pp.49–94.
Effertz, T., Scharr, A.L. & Ricci, A.J., 2015. The how and why of identifying the hair cell mechano-electrical transduction channel. *Pflugers Arch - Eur J Physiol*, 467, pp.73–84.
Emtage, L. et al., 2004. Extracellular Proteins Organize the Mechanosensory Channel Complex in Touch Receptor Neurons. *Neuron*, 44(5), pp.795–807.
Ernfors, P. et al., 1994. Lack of neurotrophin-3 leads to deficiencies in the peripheral nervous system and loss of limb proprioceptive afferents. *Cell*, 77(4), pp.503–512.
Everaerts, W. et al., 2011. The capsaicin receptor TRPV1 is a crucial mediator of the noxious effects of mustard oil. *Current Biology*, 21(4), pp.316–321.
Farris, H.E. et al., 2004. Probing the pore of the auditory hair cell mechanotransducer

channel in turtle. *Journal of Physiology-London*, 558(3), pp.769–792.
Fettiplace, R., 2016. Is TMC1 the Hair Cell Mechanotransducer Channel? *Biophysical Journal*, 111(1), pp.3–9.
Firestein, S., 2000. The good taste of genomics. *Nature*, 404, pp.552–3.
Florez-Paz, D. et al., 2016. A critical role for Piezo2 channels in the mechanotransduction of mouse proprioceptive neurons. *Scientific Reports*, 6, p.25923.
Friedel, R.H. et al., 1997. Identification of genes differentially expressed by nerve growth factor- and neurotrophin-3-dependent sensory neurons. *Proceedings of the National Academy of Sciences of the United States of America*, 94(23), pp.12670–12675.
Fuchs, P.A., 2015. How many proteins does it take to gate hair cell mechanotransduction? *Proceedings of the National Academy of Sciences*, 112(5), pp.1254–1255.
Gabashvili, I.S. et al., 2007. Ion channel gene expression in the inner ear. *Journal of the Association for Research in Otolaryngology : JARO*, 8(3), pp.305–328.
Gibson, D.G. et al., 2009. Enzymatic assembly of DNA molecules up to several hundred kilobases. *Nature methods*, 6(5), pp.343–345.
Gillespie, P.G. & Walker, R.G., 2001. Molecular basis of mechanosensory transduction. *Nature*, 413(6852), pp.194–202.
Gilron, I. et al., 2006. Neuropathic pain: A practical guide for the clinician. *Cmaj*, 175(3), pp.265–275.
Goodman, M.B. et al., 2012. Electrophysiological Methods for C. elegans Neurobiology. *Methods Cell Biol.*, 107, pp.407–436.
Goodman, M.B. et al., 2002. MEC-2 regulates C. elegans DEG/ENaC channels needed for mechanosensation. *Nature*, 415(6875), pp.1039–1042.
Gottschalk, A. & Schafer, W.R., 2006. Visualization of integral and peripheral cell surface proteins in live Caenorhabditis elegans. *Journal of Neuroscience Methods*, 154(1–2), pp.68–79.
Gu, G., Caldwell, G. a & Chalfie, M., 1996. Genetic interactions affecting touch sensitivity in Caenorhabditis elegans. *Proceedings of the National Academy of Sciences of the United States of America*, 93(13), pp.6577–6582.
Haga, J.H., Li, Y.-S.J. & Chien, S., 2007. Molecular basis of the effects of mechanical stretch on vascular smooth muscle cells. *Journal of biomechanics*, 40(5), pp.947–960.
Hahn, Y. et al., 2009. Anoctamin and transmembrane channel-like proteins are evolutionarily related. *Int J Mol Med*, 24(1), pp.51–55.
Han, L. et al., 2013. A subpopulation of nociceptors specifically linked to itch. *Nature neuroscience*, 16(2), pp.174–82.
Hansen, S.B. et al., 2008. An Ion Selectivity Filter in the Extracellular Domain of Cys-loop Receptors Reveals Determinants for Ion Conductance. *The Journal of Biological Chemistry*, 283(52), pp.36066–36070.
Hao, J. et al., 2014. Transduction and encoding sensory information by skin mechanoreceptors. *Pflugers Archiv European Journal of Physiology*, 467(1), pp.109–119.
Hilgert, N., Smith, R.J.H. & Camp, G. Van, 2009. Forty-six genes causing nonsyndromic hearing impairment: which ones should be analyzed in DNA diagnostics? *Mutat Res.*, 681(2–3), pp.189–196.
Hille, B., 2001. *Ion Channels of Excitable Membranes*,

Hilliard, M. a et al., 2004. Worms taste bitter: ASH neurons, QUI-1, GPA-3 and ODR-3 mediate quinine avoidance in Caenorhabditis elegans. *The EMBO journal*, 23(5), pp.1101–1111.
Holt, J.R. et al., 2002. A chemical-genetic strategy implicates myosin-1c in adaptation by hair cells. *Cell*, 108(3), pp.371–381.
Holt, J.R. et al., 2014. TMC function in hair cell transduction. *Hearing Research*.
Huang, M. et al., 1995. A stomatin-like protein necessary for mechanosensation in C. elegans. *Nature*, 378(6554), pp.292–295.
Huang, M. & Chalfie, M., 1994. Gene interactions affecting mechanosensory transduction in Caenorhabditis elegans. *Nature*, 367(6462), pp.467–470.
Hudspeth, A.J., 1989. How the ear's works work. *Nature*, 341(6241), pp.397–404.
Hudspeth, a J. & Jacobs, R., 1979. Stereocilia mediate transduction in vertebrate hair cells (auditory system/cilium/vestibular system). *Proceedings of the National Academy of Sciences of the United States of America*, 76(3), pp.1506–1509.
Ikeda, R. et al., 2014. Merkel cells transduce and encode tactile stimuli to drive aβ-Afferent impulses. *Cell*, 157(3), pp.664–675.
Jaalouk, D.E. & Lammerding, J., 2009. Mechanotransduction gone awry. *Nature reviews. Molecular cell biology*, 10(1), pp.63–73.
Jørgensen, F. & Kroese, a B., 1995. Ca selectivity of the transduction channels in the hair cells of the frog sacculus. *Acta physiologica Scandinavica*, 155(4), pp.363–76.
Kang, L. et al., 2010. C. elegans TRP Family Protein TRP-4 Is a Pore-Forming Subunit of a Native Mechanotransduction Channel. *Neuron*, 67(3), pp.381–391.
Kawashima, Y. et al., 2011. Mechanotransduction in mouse inner ear hair cells requires transmembrane channel – like genes. *Journal of Clinical Investigation*, 121(25), pp.4796–4809.
Kawashima, Y. et al., 2014. Transmembrane channel-like (TMC) genes are required for auditory and vestibular mechanosensation. *Pflügers Archiv - European Journal of Physiology*, 467(1), pp.85–94.
Kazmierczak, P. et al., 2007. Cadherin 23 and protocadherin 15 interact to form tip-link filaments in sensory hair cells. *Nature*, 449(7158), pp.87–91.
Kellenberger, S. et al., 2001. Permeability properties of ENaC selectivity filter mutants. *The Journal of general physiology*, 118(6), pp.679–92.
Keresztes, G., Mutai, H. & Heller, S., 2003. TMC and EVER genes belong to a larger novel family, the TMC gene family encoding transmembrane proteins. *BMC genomics*, 4(1), p.24.
Kroese, A., Das, A. & Hudspeth, A., 1989. Blockage of the transduction channels of hair cells in the bullfrog's sacculus by aminoglycoside antibiotics. *Hearing Research*, 37, pp.203–17.
Kung, C., 2005. A possible unifying principle for mechanosensation. *Nature*, 436(7051), pp.647–654.
Kurima, K. et al., 2003. Characterization of the transmembrane channel-like (TMC) gene family: Functional clues from hearing loss and epidermodysplasia verruciformis. *Genomics*, 82(3), pp.300–308.
Kurima, K. et al., 2002. Dominant and recessive deafness caused by mutations of a novel gene, TMC1, required for cochlear hair-cell function. *Nature genetics*, 30(3), pp.277–284.
Kurima, K. et al., 2015. TMC1 and TMC2 Localize at the Site of Mechanotransduction in Mammalian Inner Ear Hair Cell Stereocilia. *Cell*

Reports, 12, pp.1–12.
Labay, V. et al., 2010. Topology of transmembrane channel-like gene 1 protein. *Biochemistry*, 49(39), pp.8592–8598.
Lammerding, J., Kamm, R.D. & Lee, R.T., 2004. Mechanostransduction in Cardiac Myocytes. *Annals of the New York Academy of Sciences*, 0(1), pp.53–70.
Li, J. et al., 2014. Piezo1 integration of vascular architecture with physiological force. *Nature*, 515(7526), pp.279–282.
Li, L. et al., 2011. The functional organization of cutaneous low-threshold mechanosensory neurons. *Cell*, 147(7), pp.1615–1627.
Li, T., Yang, Y. & Canessa, C.M., 2011. Outlines of the pore in open and closed conformations describe the gating mechanism of ASIC1. *Nature communications*, 2, p.399.
Liu, C. & Montell, C., 2015. Forcing open TRP channels: Mechanical gating as a unifying activation mechanism. *Biochemical and Biophysical Research Communications*, 460(1), pp.22–25.
Liu, Q. et al., 2009. Sensory Neuron-Specific GPCR Mrgprs Are Itch Receptors Mediating Chloroquine-Induced Pruritus. *Cell*, 139(7), pp.1353–1365.
Lumpkin, E. a. & Bautista, D.M., 2005. Feeling the pressure in mammalian somatosensation. *Current Opinion in Neurobiology*, 15(4), pp.382–388.
Lumpkin, E. a., Marshall, K.L. & Nelson, A.M., 2010. The cell biology of touch. *Journal of Cell Biology*, 191(2), pp.237–248.
Lumpkin, E. a & Caterina, M.J., 2007. Mechanisms of sensory transduction in the skin. *Nature*, 445(7130), pp.858–865.
Macosko, E.Z. et al., 2009. A Hub-and-Spoke Circuit Drives Pheromone Attraction and Social Behavior in C. elegans. *Nature*, 458(7242), pp.1171–1175.
Maeda, R. et al., 2014. Tip-link protein protocadherin 15 interacts with transmembrane channel-like proteins TMC1 and TMC2. *Proceedings of the National Academy of Sciences of the United States of America*, pp.1–6.
Maksimovic, S. et al., 2014. Epidermal Merkel cells are mechanosensory cells that tune mammalian touch receptors. *Nature*, 509(7502), pp.617–621.
Mank, M. & Griesbeck, O., 2008. Genetically encoded calcium indicators. *Chemical Reviews*, 108(5), pp.1550–1564.
Marcotti, W. et al., 2014. Transduction without tip links in cochlear hair cells is mediated by ion channels with permeation properties distinct from those of the mechano-electrical transducer channel. *The Journal of neuroscience : the official journal of the Society for Neuroscience*, 34(16), pp.5505–14.
McKemy, D.D., Neuhausser, W.M. & Julius, D., 2002. Identification of a cold receptor reveals a general role for TRP channels in thermosensation. *Nature*, 416(6876), pp.52–58.
McNally, B.A. & Prakriya, M., 2012. Permeation and gating mechanisms in store-operated CRAC channels. *J Physiol*, 590(17), pp.4179–4191.
Mello, C.C. et al., 1991. Efficient gene transfer in C. elegans: extrachomosomal maintenace and integration of transforming sequences. *EMBO Journal*, 10(12), pp.3959–3970.
Minor, D.L., 2010. Chapter 30 – An Overview of Ion Channel Structure. In *Handbook of Cell Signaling*. pp. 201–207.
Mombaerts, P., 1999. Seven-transmembrane proteins as odorant and chemosensory receptors. *Science (New York, N.Y.)*, 286(5440), pp.707–711.
Mutai, H., Mann, S. & Heller, S., 2005. Identification of chicken transmembrane

channel-like (TMC) genes: Expression analysis in the cochlea. *Neuroscience*, 132(4), pp.1115–1122.
Nagai, T. et al., 2004. Expanded dynamic range of fluorescent indicators for Ca(2+) by circularly permuted yellow fluorescent proteins. *Proc Natl Acad Sci U S A*, 101(29), pp.10554–10559.
Nance, W.E., 2003. The genetics of deafness. *Mental Retardation and Developmental Disabilities Research Reviews*, 9(2), pp.109–119.
Ng, C.P., Helm, C.L.E. & Swartz, M.A., 2004. Interstitial flow differentially stimulates blood and lymphatic endothelial cell morphogenesis in vitro. *Microvascular Research*, 68(3), pp.258–264.
Noel, J. et al., 2009. The mechano-activated K+ channels TRAAK and TREK-1 control both warm and cold perception. *The EMBO journal*, 28(9), pp.1308–1318.
Norrsell, U., Finger, S. & Lajonchere, C., 1999. Cutaneous sensory spots and the "law of specific nerve energies": history and development of ideas. *Brain Research Bulletin*, 48(5), pp.457–465.
O'Hagan, R., Chalfie, M. & Goodman, M.B., 2005. The MEC-4 DEG/ENaC channel of Caenorhabditis elegans touch receptor neurons transduces mechanical signals. *Nature neuroscience*, 8(1), pp.43–50.
Pan, B. et al., 2013. TMC1 and TMC2 are components of the mechanotransduction channel in hair cells of the mammalian inner ear. *Neuron*, 79(3), pp.504–515.
Pan, B. & Holt, J.R., 2015. The molecules that mediate sensory transduction in the mammalian inner ear. *Current Opinion in Neurobiology*, 34, pp.165–171.
Perozo, E. et al., 2002. Open channel structure of MscL and the gating mechanism of mechanosensitive channels. *Nature*, 418(6901), pp.942–948.
Le Pichon, C.E. & Chesler, A.T., 2014. The functional and anatomical dissection of somatosensory subpopulations using mouse genetics. *Frontiers in neuroanatomy*, 8(April), p.21.
Pickles, J.O. & Corey, D.P., 1992. Mechanoelectrical transduction by hair cells. *Trends in neurosciences*, 15(7), pp.254–259.
Pugh, E.N., 1999. Variability in single photon responses: A cut in the Gordian knot of rod phototransduction? *Neuron*, 23(2), pp.205–208.
Purves, D. et al. eds., 2001. The Molecular Structure of Ion Channels. In *Neuroscience*. Sunderland (MA): Sinauer Associates.
Qi, Y. et al., 2015. Membrane stiffening by STOML3 facilitates mechanosensation in sensory neurons. *Nature Communications*, 6, p.8512.
Ramoz, N. et al., 2002. Mutations in two adjacent novel genes are associated with epidermodysplasia verruciformis. *Nature genetics*, 32(december), pp.1–3.
Ranade, S.S. et al., 2014. Piezo1, a mechanically activated ion channel, is required for vascular development in mice. *Proceedings of the National Academy of Sciences of the United States of America*, 111(28), pp.10347–52.
Ranade, S.S. et al., 2014. Piezo2 is the major transducer of mechanical forces for touch sensation in mice. *Nature*, 516(7529), pp.121–125.
Redemann, S. et al., 2011. Codon adaptation-based control of protein expression in C. elegans. *Nature methods*, 8(3), pp.250–252.
Riazuddin, S. et al., 2012. Alterations of the CIB2 calcium- and integrin-binding protein cause Usher syndrome type 1J and nonsyndromic deafness DFNB48. *Nature Genetics*, 44(11), pp.1265–1271.
Ricci, A.J., Crawford, A.C. & Fettiplace, R., 2003. Tonotopic Variation in the

Conductance of the Hair Cell Mechanotransducer Channel. *Neuron*, 40(5), pp.983–990.
Ricci, A.J. & Fettiplace, R., 1998. Calcium permeation of the turtle hair cell mechanotransducer channel and its relation to the composition of endolymph. *Journal of Physiology*, 506(1), pp.159–173.
Riddle DL, Blumenthal T, Meyer BJ, et al. ed., 1997. *C. elegans II* 2nd editio., Cold Spring Harbor (NY): Cold Spring Harbor Laboratory Press.
Rüsch, A., Kros, C.J. & Richardson, G.P., 1994. Block by amiloride and its derivatives of mechano-electrical transduction in outer hair cells of mouse cochlear cultures. *The Journal of physiology*, 474(1), pp.75–86.
Sambrook, J., Fritsch, E.F. & Maniatis, T., 1989. *Molecular cloning: a laboratory manual*, Cold Spring Harbor Laboratory.
Sanguinetti, M.C. et al., 1996. Coassembly of KvLQT1 and minK (IsK) proteins to form cardiac IKs potassium channel. *Nature*, 384(6604), pp.80–83.
Schafer, W.R., 2014. Mechanosensory molecules and circuits in C. elegans. *Pflügers Archiv - European Journal of Physiology*.
Schwander, M., Kachar, B. & Müller, U., 2010. The cell biology of hearing. *Journal of Cell Biology*, 190(1), pp.9–20.
Seal, R.P. et al., 2009. Injury-induced mechanical hypersensitivity requires C-low threshold mechanoreceptors. *Nature*, 462(7273), pp.651–5.
Serluca, F.C., Drummond, I.A. & Fishman, M.C., 2002. Endothelial signaling in kidney morphogenesis: A role for hemodynamic forces. *Current Biology*, 12(6), pp.492–497.
Sleigh, J.N., Weir, G.A. & Schiavo, G., 2016. A simple, step-by-step dissection protocol for the rapid isolation of mouse dorsal root ganglia. *BMC Research Notes*, 9(1), p.82.
Smith, C.J. et al., 2010. Time-lapse imaging and cell-specific expression profiling reveal dynamic branching and molecular determinants of a multi- dendritic nociceptor in C. elegans. *Dev Biol*, 345(1), pp.18–33.
Smith, E.S.J. & Lewin, G.R., 2009. Nociceptors: a phylogenetic view. *J Comp Physiol A*, 195(12), pp.1089–1106.
Smith, R.J. et al., 1999. *Deafness and Hereditary Hearing Loss Overview* P. RA, A. MP, & A. HH, eds., Seattle (WA): GeneReviews.
Stauffer, E.A. et al., 2005. Fast Adaptation in Vestibular Hair Cells Requires Myosin-1c Activity. *Neuron*, 47(4), pp.541–553.
Strange, K., Christensen, M. & Morrison, R., 2007. Primary culture of Caenorhabditis elegans developing embryo cells for electrophysiological, cell biological and molecular studies. *Nature protocols*, 2(4), pp.1003–1012.
Sukharev, S. & Sachs, F., 2012. Molecular force transduction by ion channels - diversity and unifying principles. *Journal of Cell Science*, 125(13), pp.3075–3083.
Sulston, J.E. et al., 1983. The embryonic cell lineage of the nematode Caenorhabditis elegans. *Developmental biology*, 100(1), pp.64–119.
Sulston, J.E. & Horvitz, H.R., 1977. Post-embryonic cell lineages of the nematode, Caenorhabditis elegans. *Developmental Biology*, 56(1), pp.110–156.
Tobin, D.M. et al., 2002. Combinatorial expression of TRPV channel proteins defines their sensory functions and subcellular localization in C. elegans neurons. *Neuron*, 35(2), pp.307–318.
Tominaga, M. et al., 1998. The cloned capsaicin receptor integrates multiple pain-

producing stimuli. *Neuron*, 21(3), pp.531–543.
Usoskin, D. et al., 2015. Unbiased classification of sensory neuron types by large-scale single-cell RNA sequencing. *Nature Neuroscience*, 18(1), pp.145–153.
Vollrath, M. a, Kwan, K.Y. & Corey, D.P., 2007. The micromachinery of mechanotransduction in hair cells. *Annual review of neuroscience*, 30, pp.339–365.
Vreugde, S. et al., 2002. Beethoven, a mouse model for dominant, progressive hearing loss DFNA36. *Nature genetics*, 30(3), pp.257–258.
Vriens, J., Nilius, B. & Voets, T., 2014. Peripheral thermosensation in mammals. *Nature Reviews Neuroscience*, 15(9), pp.573–589.
Wang, F. et al., 2016. Mechanosensitive ion channel Piezo2 is important for enterochromaffin cell response to mechanical forces. *The Journal of Physiology*, 0, pp.1–13.
Way, J.C. & Chalfie, M., 1989. The mec-3 gene of Caenorhabditis elegans requires its own product for maintained expression and is expressed in three neuronal cell types. *Genes and Development*, 3(12 A), pp.1823–1833.
Wicks, S.R. et al., 2001. Rapid gene mapping in Caenorhabditis elegans using a high density polymorphism map. *Nat Genet*, 28(2), pp.160–164.
Woo, S. et al., 2015. Piezo2 is the principal mechanotransduction channel for proprioception. *Nature Neuroscience*, 18(12), pp.1756–1763.
Woo, S.-H. et al., 2014. Piezo2 is required for Merkel-cell mechanotransduction. *Nature*, 509(7502), pp.622–626.
Wu, Z. et al., 2016. Mechanosensory hair cells express two molecularly distinct mechanotransduction channels. *Nature Neuroscience*, (November).
Xiong, W. et al., 2012. TMHS is an integral component of the mechanotransduction machinery of cochlear hair cells. *Cell*, 151(6), pp.1283–1295.
Zhang, L. et al., 2015. TMC-1 attenuates C. elegans development and sexual behaviour in a chemically defined food environment. *Nature Communications*, 6, p.6345.
Zhang, S. et al., 2004. MEC-2 Is Recruited to the Putative Mechanosensory Complex in C. elegans Touch Receptor Neurons through Its Stomatin-like Domain. *Curr Biol.*, 14, pp.1888–1896.
Zhang, W. et al., 2015. Ankyrin Repeats Convey Force to Gate the NOMPC Mechanotransduction Channel. *Cell*, 162(6), pp.1391–1403.
Zhao, B. et al., 2014. TMIE Is an Essential Component of the Mechanotransduction Machinery of Cochlear Hair Cells. *Neuron*, 84(5), pp.954–967.
Zhao, B. & Muller, U., 2015. The elusive mechanotransduction machinery of hair cells. *Current Opinion in Neurobiology*, 34(Figure 2), pp.172–179.
Zhao, Q. et al., 2016. Ion Permeation and Mechanotransduction Mechanisms of Mechanosensitive Piezo Channels. *Neuron*, 89(6), pp.1248–1263.
Zygmunt, P.M. et al., 1999. Vanilloid receptors on sensory nerves mediate the vasodilator action of anandamide. *Nature*, 400(6743), pp.452–457.

Appendices

Appendix 1: Strains used

NAME	GENOTYPE
AQ3093	ljEx543[sra-9::YC3.60;unc-122::rfp]
AQ3222	dbEx651;ljEx605[sra-9::mTMC2::SL2RFP;elt-2::rfp]
AQ3286	dbEx651[sra-9::YC3.60;unc-122::rfp]; ljEx651[sra-9::mTMC1;elt-2::rfp]
AQ3353	ljEx700[Prsa-9::mtmc3; unc-122:gfp]; AQ3093 [ljEx543[sra-9::YC3.60; unc-122:rfp]]
AQ3484	ljEx543[sra-9::YC3.60;unc-122::rfp]; ljEx795[(042) sra-9::mTMC1 with TM4-5 from mTMC2::unc-54]; unc-122::gfp]
AQ3485	ljEx543[sra-9::YC3.60;unc-122::rfp]; ljEx796[(038) sra-9::mTMC1 with TM3-4 from mTMC2::unc-54]; unc-122::gfp]
AQ3486	ljEx543[sra-9::YC3.60;unc-122::rfp]; ljEx797[(039) sra-9::mTMC2 with TM3-4 from mTMC1::unc-54]; unc-122::gfp]
AQ3492	ljEx543[sra-9::YC3.60;unc-122::rfp]; ljEx801[(041) sra-9::mTMC3 with TM3-4 from mTMC2::unc-54]; unc-122::gfp]
AQ3493	ljEx543[sra-9::YC3.60;unc-122::rfp]; ljEx802[(045) sra-9::mTMC3 with TM4-5 from mTMC2::unc-54]; unc-122::gfp]
AQ3494	ljEx543[sra-9::YC3.60;unc-122::rfp]; ljEx803[(040) sra-9::mTMC2 with TM3-4 from mTMC3::unc-54]; elt-2::rfp]
AQ3495	ljEx543[sra-9::YC3.60;unc-122::rfp]; ljEx804[(063) sra-9::mTMC2 with TM4-5 from mTMC3::unc-54]; unc-122::gfp]
AQ3512	ljEx543[sra-9::YC3.60;unc-122::rfp]; ljEx812[(074) sra-9::mTMC2 with miniloop from mTMC1::unc-54]; elt-2::rfp]
AQ3520	ljEx543[sra-9::YC3.60;unc-122::rfp]; ljEx819[(073) sra-9::mTMC1 with miniloop from mTMC2::unc-54]; elt-2::rfp]
AQ3524	calm-1(tm1353);outcrossed*4
AQ3527	ljEx543[sra-9::YC3.60;unc-122::rfp]; ljEx823[(076) sra-9::mTMC2 with miniloop from mTMC3::unc-54]; elt-2::rfp]
AQ3563	ljEx853[sra-9::mTMC1(HA1.1)::unc-54; unc-122::rfp] LINE 1
AQ3564	ljEx853[sra-9::mTMC1(HA1.1)::unc-54; unc-122::rfp] LINE 2
AQ3583	ljEx859[sra-9::mTMC1(HA1)::unc-54; unc-122::rfp]
AQ3591	ljEx862[sra-9::mTMC1(HA3.1)::unc-54; unc-122::rfp]
AQ3594	ljEx543[sra-9::YC3.60;unc-122::rfp]; ljEx864[(077) sra-9::mTMC1 with unconserv from mTMC2::unc-54]; elt-2::rfp]
AQ3595	ljEx543[sra-9::YC3.60;unc-122::rfp]; ljEx865[(080) sra-9::mTMC2 with unconserv from mTMC3::unc-54]; elt-2::rfp]
AQ3619	ljEx543[sra-9::YC3.60;unc-122::rfp]; ljEx884[(078) sra-9::mTMC2 with unconserv from mTMC1::unc-54]; elt-2::rfp]
AQ3620	ljEx885[sra-9::mTMC1(HA4)::unc-54; elt-2::rfp]
AQ3629	ljEx543[sra-9::YC3.60;unc-122::rfp]; ljEx893[(079) sra-9::mTMC3 with unconserv from mTMC2::unc-54]; elt-2::rfp]
AQ3634	ljEx896[sra-9::mTMC3(HA2)::unc-54; elt-2::rfp]
AQ3663	ljEx912[sra-9::mTMC3(HA1.1)::unc-54; unc-122::rfp]
AQ3664	ljEx913[sra-9::mTMC3(HA4)::unc-54; elt-2::rfp]
AQ3665	ljEx914[sra-9::mTMC3(HA1)::unc-54; elt-2::rfp]
AQ3670	ljEx919[Psra-9::CALM-1::SL2mKate2 (50ng/ul); Pelt-2::mCherry (50ng/ul)]
AQ3686	ljEx922[sra-9::mTMC1(HA3)::unc-54; elt-2::rfp]
AQ3687	ljEx543[sra-9::YC3.60;unc-122::rfp]; ljEx923 [Psra-9::mTmc1 with D391A D393A::unc-54; elt-2::RFP)
AQ3688	ljEx543[sra-9::YC3.60;unc-122::rfp]; ljEx924 [Psra-9::mTmc2 with K442A::unc-54; elt-2::RFP)

AQ3689	ljEx543[sra-9::YC3.60;unc-122::rfp]; ljEx925 [Psra-9::mTmc3 with K351A K352A E353A::unc-54; elt-2::RFP)
AQ3690	ljEx543[sra-9::YC3.60;unc-122::rfp]; ljEx926 [Psra-9::hTMC3::unc-54; elt-2::RFP)
AQ3705	calm-1(tm1353);outcrossed*4; ljEx700[Prsa-9::mtmc3; unc-122:gfp]; AQ3093 [ljEx543[sra-9::YC3.60; unc-122:rfp]]
AQ3730	ljEx700[Prsa-9::mtmc3; unc-122:gfp]; ljEx543[sra-9::YC3.60; unc-122:rfp]; ljEx919[Psra-9::CALM-1::SL2mKate2 (50ng/ul); Pelt-2::mCherry (50ng/ul)]
AQ3747	ljEx942[Psra-9::hCIB2-isoform1::SL2mKate2 (120ng/ul); Punc-122::mCherry (50ng/ul)]
AQ3748	ljEx943[Psra-9::hCIB3-isoform1::SL2mKate2 (120ng/ul); Punc-122::mCherry (50ng/ul)]
AQ3766	ljEx948[sra-9::mTMC3(HA3.1)::unc-54; elt-2::rfp]
AQ3767	ljEx948[sra-9::mTMC3(HA3.1)::unc-54; elt-2::rfp]; ljEx543[sra-9::YC3.60;unc-122::rfp]
AQ3887	ljEx1037[Psra-9::mTmc1(HA2)::unc-54;elt-2::RFP]
AQ3888	ljEx1038[Psra-9::mTmc3(HA3)::unc-54;elt-2::RFP]

Appendix 2: Plasmids used

NAME	VECTOR	SELECTION	PROMOTER	INSERT	3'	PURPOSE
PRK000		Amp		mTMC3		mTMC3 synthesized plasmid
PRK001	pDEST	Amp	sra-9	mTMC3	unc-54	
PRK007	pENTR	Kan		mTMC3		gateway pos 2 mTMC3
PRK009	pENTR	Kan	sra-9			Gateway pos-1 promoter
PRK012	pENTR	Kan			unc-54	Gateway pos-3
PRK014	pENTR	Kan		mTMC2		Gateway pos 2
PRK037	pENTR	Kan		mTMC1		mTMC1 gateway pos 2
PRK038	pENTR	Kan		mTMC1		Domain swap - Tm3/4 from mTMC2
PRK039	pENTR	Kan		mTMC2		Domain swap - Tm3/4 from mTMC1
PRK040	pENTR	Kan		mTMC2		Domain swap - Tm3/4 from mTMC3
PRK041	pENTR	Kan		mTMC3		Domain swap - Tm3/4 from mTMC2
PRK042	pENTR	Kan		mTMC1		Domain swap - Tm4/5 from mTMC2
PRK043	pENTR	Kan		mTMC2		Domain swap - Tm4/5 from mTMC1
PRK044	pENTR	Kan		mTMC2		Domain swap - Tm4/5 from mTMC3
PRK045	pENTR	Kan		mTMC3		Domain swap - Tm4/5 from mTMC2
PRK047	pDEST	Amp	sra-9	(042) mTMC1 with TM4-5 from mTMC2	unc-54	Expressed in ASK, mTMC1 Domain swap - Tm4/5 from mTMC2
PRK048	pDEST	Amp	sra-9	(038) mTMC1 with TM3-4 from mTMC2	unc-54	Expressed in ASK, mTMC1 Domain swap - Tm3/4 from mTMC2
PRK049	pDEST	Amp	sra-9	(039) mTMC2 with TM3-4 from mTMC1	unc-54	Expressed in ASK, mTMC2 Domain swap - Tm3/4 from mTMC1
PRK050	pDEST	Amp	sra-9	(041) mTMC3 with TM3-4 from mTMC2	unc-54	Expressed in ASK, mTMC3 Domain swap - TM3/4 from mTMC2
PRK051	pDEST	Amp	sra-9	(045) mTMC3 with TM4-5 from mTMC2	unc-54	Expressed in ASK, mTMC3 Domain swap - Tm4/5 from mTMC2
PRK059	pDEST	Amp	sra-9	mTMC2 (014)	unc-54	Tmc2 expressed in ASK for chimera study control
PRK062	pDEST	Amp	sra-9	(043) mTmc2 with TM4/5 from mTmc1	unc-54	Expressed in ASK, mTmc2 Domain swap - TM4/5 from mTMC1
PRK063	pDEST	Amp	sra-9	(044) mTmc2 with TM4/5 from mTmc3	unc-54	Expressed in ASK, mTmc2 Domain swap - TM4/5 from mTMC3
PRK064	pDEST	Amp	sra-9	(073) mTMC1	unc-54	expressed in ASK, with the possible TM loop between 3/4 from mTMC2
PRK066	pDEST	Amp	sra-9	(075) mTMC3	unc-54	expressed in ASK, with the possible TM loop between 3/4 from mTMC2
PRK067	pDEST	Amp	sra-9	(076) mTMC2	unc-54	expressed in ASK, with the possible TM loop between 3/4 from mTMC3
PRK069	pDEST	Amp	sra-9	(078) mTMC2	unc-54	expressed in ASK, with the unconserved

						region between 3/4 from mTMC1
PRK070	pDEST	Amp	sra-9	(079) mTMC3	unc-54	expressed in ASK, with the unconserved region between 3/4 from mTMC2
PRK071	pDEST	Amp	sra-9	(080) mTMC2	unc-54	expressed in ASK, with the unconserved region between 3/4 from mTMC3
PRK072	pDEST	Amp	sra-9	(040) mTmc2 with TM3/4 from mTmc3	unc-54	Expressed in ASK, mTMC2 Domain swap - Tm3/4 from mTMC3
PRK073	pENTR	Kan		mTMC1		with the possible TM loop between 3/4 from mTMC2
PRK074	pENTR	kan		mTMC2		with the possible TM loop between 3/4 from mTMC1
PRK075	pENTR	kan		mTMC3		with the possible TM loop between 3/4 from mTMC2
PRK076	pENTR	kan		mTMC2		with the possible TM loop between 3/4 from mTMC3
PRK077	pENTR	kan		mTMC1		with the unconserved region between 3/4 from mTMC2
PRK078	pENTR	kan		mTMC2		with the unconserved region between 3/4 from mTMC1
PRK079	pENTR	kan		mTMC3		with the unconserved region between 3/4 from mTMC2
PRK080	pENTR	kan		mTMC2		with the unconserved region between 3/4 from mTMC3
PRK085	pDEST	Amp	sra-9	(074) mTmc2 with miniloop	unc-54	mTmc2 with the possible TM loop between 3/4 from mTMC1
PRK088	pDEST	Amp	sra-9	(077) mTmc1 w unconserved	unc-54	mtmc1 with the unconserved region from mtmc2
PRK089	pDEST	Amp	sra-9	mTMC1	unc-54	mtmc1 expressed in ASK
PRK090	pDEST	Amp	sra-9	mTMC1	unc-54	HA1
PRK091	pDEST	Amp	sra-9	mTMC1	unc-54	HA1.1
PRK092	pDEST	Amp	sra-9	mTMC1	unc-54	HA2
PRK093	pDEST	Amp	sra-9	mTMC1	unc-54	HA3
PRK094	pDEST	Amp	sra-9	mTMC1	unc-54	HA3.1
PRK095	pDEST	Amp	sra-9	mTMC1	unc-54	HA4
PRK096	pDEST	Amp	sra-9	mTMC3	unc-54	HA1
PRK097	pDEST	Amp	sra-9	mTMC3	unc-54	HA1.1
PRK098	pDEST	Amp	sra-9	mTMC3	unc-54	HA2
PRK099	pDEST	Amp	sra-9	mTMC3	unc-54	HA3
PRK100	pDEST	Amp	sra-9	mTMC3	unc-54	HA3.1
PRK101	pDEST	Amp	sra-9	mTMC3	unc-54	HA4
PRK114	pDEST	Amp	sra-9	mTmc1 (089) with D391A D393A	unc-54	
PRK115	pDEST	Amp	sra-9	mTmc2 (059) with K442A	unc-54	
PRK116	pDEST	Amp	sra-9	mTmc3 (001) with K351A	unc-54	

				K352A E353A		
PRK117		Kan		hTmc3		codon optimized hTmc3 for c elegans
PRK118	PENTR	Kan		hTmc3		BP reaction, hTmc3 pos 2
PRK119	pDEST	Amp	sra-9	hTmc3	unc-54	LR rxn, hTmc3 in ASK
PRK125	pDEST	Amp	sra-9	mTmc2 (059) with F440A	unc-54	controls for neutralisation
PRK126	pDEST	Amp	sra-9	mTmc2 (059) with R436A	unc-54	
PRK127	pDEST	Amp	sra-9	mTmc2 (059) with R412A	unc-54	
PRK128	pDEST	Amp	sra-9	mTmc2 (059) with V413A	unc-54	

Appendix 3: Primers used

NAME	SEQUENCE	DESCRIPTION	TARGET
GIBCLO 1 FW	TCACACTTGGTGCAAGTGGATACCTCATCTACTTTGTGGTGAAACGGTC	mTMC2 TM3/4 for mTMC1 backbone	038
GIBCLO 1 RV	ATCAAGGCGAGAATGAATACATACAAGTTGCCTAGGAAGAGGGCAAAGATGCGGC	mTMC2 TM3/4 for mTMC1 backbone	038
GIBCLO 2 FW	GCTGTCTGTGTGGAAGCGGGTACCTCATTTTTTGGGCTGTGAAGCGATC	mTMC1 TM3/4 for mTMC2 backbone	039
GIBCLO 2 RV	ATGAGGGCCAGGAGAAACGTGTAGAGGTTTCCCAGAAGAAGAGCAAAAATGCGCC	mTMC1 TM3/4 for mTMC2 backbone	039
GIBCLO 3 FW	GCTGTCTGTGTGGAAGCGGGTACCTCATTTACTTTGTGGTGGACCGTTCCCAAAAGCTCGA	mTMC3 TM3/4 for mTMC2 backbone	040
GIBCLO 3 RV	ATGAGGGCCAGGAGAAACGTGTAGAGGTTTCCCAGGTAGAGGACGAGGACACGGG	mTMC3 TM3/4 for mTMC2 backbone	040
GIBCLO 4 FW	TCTCCCTCGCCGGATCCATCTACCTCATCTACTTCGTCGTCAAACGGTCCCAGGAGTTCTC	mTMC2 TM3/4 for mTMC3 backbone	041
GIBCLO 4 RV	AGGAGGGCGATGATGAGGGAGTAGAGGTTTCCGAGGAAGAGGGCAAAGATGCGGC	mTMC2 TM3/4 for mTMC3 backbone	041
GIBCLO 5 FW	GGCGCATTTTTGCTCTTCTTCTAGGCAACCTCTACACGTTTCTCCTGGC	mTMC2 TM4/5 for mTMC1 backbone	042
GIBCLO 5 RV	TAGCAGCATGCCGAGGTAGAAGTTGTTGGATCTGGAAGCTTTGAACACACGTTCGTGGGGAACGTTGC	mTMC2 TM4/5 for mTMC1 backbone	042
GIBCLO 6 FW	GCCGCATCTTTGCCCTCTTCCTGGGAAACTTGTATGTATTCATTCTCGC	mTMC1 TM4/5 for mTMC2 backbone	043
GIBCLO 6 RV	CAGCAGCAGGCCCATGTAGAAGTTGTTGGATCTGGAGGCTTTAAACACCCTGGCCTCGGGAACATTGC	mTMC1 TM4/5 for mTMC2 backbone	043
GIBCLO 7 FW	GCCGCATCTTTGCCCTCTTCCTGGGAAACCTCTACTCCCTCATCATCGCCCTCCT	mTMC3 TM4/5 for mTMC2 backbone	044
GIBCLO 7 RV	ACCAACAGCAGCAGGCCCATGTAGAAGTTGTTGGAACGGGAGGCACGGAAGACTT	mTMC3 TM4/5 for mTMC2 backbone	044
GIBCLO 8 FW	CCCGTGTCCTCGTCCTCTACCTCGGAAACCTCTACACGTTTCTCCTGGCCCTCAT	mTMC2 TM4/5 for mTMC3 backbone	045
GIBCLO 8 RV	ATGAAGAGGAGCATGGCGAGGTAGAAGTTGTTGGATCTGGAGGCTTTAAACACAC	mTMC2 TM4/5 for mTMC3 backbone	045
GIBCLO 9 RV	GACCGTTTCACCACAAAGTAGATGAGGTATCCACTTGCACCAAGTGTGA	mTMC1 backbone for mTMC1 TM3/4	038
GIBCLO 9 FW	GCCGCATCTTTGCCCTCTTCCTAGGCAACTTGTATGTATTCATTCTCGCCTTGAT	mTMC1 backbone for mTMC1 TM3/4	038
GIBCLO 10 RV	GATCGCTTCACAGCCCAAAAAATGAGGTACCCGCTTCCACACAGACAGC	mTMC2 backbone for mTMC1 TM3/4	039
GIBCLO 10 FW	GGCGCATTTTTGCTCTTCTTCTGGGAAACCTCTACACGTTTCTCCTGGCCCTCAT	mTMC2 backbone for mTMC1 TM3/4	039
GIBCLO 11 RV	TCGAGCTTTTGGGAACGGTCCACCACAAAGTAAATGAGGTACCCGCTTCCACACAGACAGC	mTMC2 backbone for mTMC3 TM3/4	040
GIBCLO 11 FW	CCCGTGTCCTCGTCCTCTACCTGGGAAACCTCTACACGTTTCTCCTGGCCCTCAT	mTMC2 backbone for mTMC3 TM3/4	040
GIBCLO 12 RV	GAGAACTCCTGGGACCGTTTGACGACGAAGTAGATGAGGTAGATGGATCCGGCGAGGGAGA	mTMC3 backbone for mTMC2 TM3/4	041
GIBCLO 12 FW	GCCGCATCTTTGCCCTCTTCCTCGGAAACCTCTACTCCCTCATCATCGCCCTCCT	mTMC3 backbone for mTMC2 TM3/4	041
GIBCLO 13 RV	GCCAGGAGAAACGTGTAGAGGTTGCCTAGAAGAAGAGCAAAAATGCGCC	mTMC1 backbone for mTMC1 TM4/5	042
GIBCLO 13 FW	GCAACGTTCCCCACGAACGTGTGTTCAAAGCTTCCAGATCCAACAACTTCTACCTCGGCATGCTGCTA	mTMC1 backbone for mTMC1 TM4/5	042
GIBCLO 14 RV	GCGAGAATGAATACATACAAGTTTCCCAGGAAGAGGGCAAAGATGCGGC	mTMC2 backbone for mTMC1 TM4/5	043
GIBCLO 14 FW	GCAATGTTCCCGAGGCCAGGGTGTTTAAAGCCTCCAGATCCAACAACTTCTACATGGGCCTGCTGCTG	mTMC2 backbone for mTMC1 TM4/5	043

GIBCLO 15 RV	AGGAGGGCGATGATGAGGGAGTAGAG GTTTCCCAGGAAGAGGGCAAAGATGCG GC	mTMC2 backbone for mTMC3 TM4/5	044
GIBCLO 15 FW	AAGTCTTCCGTGCCTCCCGTTCCAACAA CTTCTACATGGGCCTGCTGCTGTTGGT	mTMC2 backbone for mTMC3 TM4/5	044
GIBCLO 16 RV	ATGAGGGCCAGGAGAAACGTGTAGAGG TTTCCGAGGTAGAGGACGAGGACACGG G	mTMC3 backbone for mTMC2 TM4/5	045
GIBCLO 16 FW	GTGTGTTTAAAGCCTCCAGATCCAACA ACTTCTACCTCGCCATGCTCCTCTTCAT	mTMC3 backbone for mTMC2 TM4/5	045
RV	GGACAAAACATCCCTAGCAAAGACATC ACGATGTTCATTTCATTTTTTTCCCACC ACC	to use on 037 to generate 064	
FW	GTTTTGTCCCCCTCTGTTTGAAACCATC GCTGCCCTGGAAGATTACCATCCTCTCA TTGC	to use on 037 to generate 064	
RV	GGACAAAACATCCCTAGCAAAGACATC ACGATGTTCATTTCATTTTTTTCCCACC ACC	to use on 014 to generate 065	
FW	GTTTTGTCCCCCTCTGTTTGAAACCATC GCTGCCCTGGAAGATTACCATCCTCTCA TTGC	to use on 014 to generate 065	
RV	CAAAACATCCCTAGCAAAGACATCACG ATGGAGACCTCGTTCTTCTCCCAGAGGG TGAGC	to use on 007 to generate 066	
FW	GTTTTGTCCCCCTCTGTTTGAAACCATC GCTGCCCTCGAGATGTACCACCCACGT ACCACC	to use on 007 to generate 066	
RV	GCGAGCATGGTGACGAGGGAGACGACG ACCTCCACCTCATTCCTTTCATACCAGC TGAC	to use on 014 to generate 067	
FW	GCTCGCCCCATCCGCCTTCGACCTCATC GCCGCCTTGGAGAATTATCACCCACGA ACTGG	to use on 014 to generate 067	
RV	TTGCATTTTGGAGAACTCCTGGGATCGC TTCACAGCCCAAAAGATGAGGTATCCA CTTGC	to use on 037 to generate 068	
FW	TGCAAAATGTCAGCTGGTATGAAAAAA ATGAAATGAACATGGTAATGTCCCTCCT GG	to use on 037 to generate 068	
RV	CAGGATCTTGCTGGGCGAACTCCTGGG ACCGTTTCACCACAAAGTAAATGAGGT ACC	to use on 014 to generate 069	
FW	GATCCTGACACCCTTGGGTGGTGGGAA AGGAATGAGGTGGAGATCGTGATGTCT TTGCTAG	to use on 014 to generate 069	
RV	CATTTTGCATTTTGGAGAACTCTTGGGA ACGGTCGACGACGAAGTAGATGAGGTA GATGG	to use on 007 to generate 070	
FW	CAAAATGTCAGCTGGTATGAGAAGAAC GAGGTCTCCGTCGTCGTCTCCCTCGTCA CCATGC	to use on 007 to generate 070	
RV	CCTTCTTGGATTGCTCGAGCTTCTGGGA CCGTTTCACCACAAAGTAAATGAGGTA CC	to use on 014 to generate 071	
FW	GAAGGAGCTCACCCTCTGGGAAAGGAA TGAGGTGGAGATCGTGATGTCTTTGCTA GGG	to use on 014 to generate 071	
RV	AAACAGAGGGGGACAAAACATCCCTAG CAAAGACATCACGATGTTCATTTCATTT TTTTC	to use on 037 to generate 073	
FW	ATGTTTTGTCCCCCTCTGTTTGAAACCA TCGCTGCCCTGGAAGATTACCATCCTCT CATT	to use on 037 to generate 073	
RV	CAGGGTGGGACAGAACATCCCCAGGAG GGACATTACCATCTCCACCTCATTCCTT TCATA	to use on 014 to generate 074	
FW	GGATGTTCTGTCCCACCCTGTTTGACTT ATTTGCTGAATTGGAGAATTATCACCCA CGAA	to use on 014 to generate 074	
RV	GCGGATGGGGCGAGCATGGTGACGAGG GAGACGACGACCTCCACCTCATTCCTTT CATAC	to use on 014 to generate 076	
FW	CACCATGCTCGCCCCATCCGCCTTCGAC CTCATCGCCGCCTTGGAGAATTATCACC CACG	to use on 014 to generate 076	
RV	ATACCAGCTGACATTTTGCATTTTGGAG AACTCCTGGGATCGCTTCACAGCCCAA	to use on 037 to generate 077	

	AAGAT		
FW	GAGTTCTCCAAAATGCAAAATGTCAGC TGGTATGAAAAAAATGAAATGAACATG GTAATG	to use on 037 to generate 077	
RV	CCACCACCCAAGGGTGTCAGGATCTTG CTGGGCGAACTCCTGGGACCGTTTCACC ACAAA	to use on 014 to generate 078	
FW	GAGTTCGCCCAGCAAGATCCTGACACC CTTGGGTGGTGGGAAAGGAATGAGGTG GAGATC	to use on 014 to generate 078	
RV	CCAGAGGGTGAGCTCCTTCTTGGATTGC TCGAGCTTCTGGGACCGTTTCACCACAA AGTA	to use on 014 to generate 080	
FW	AAGCTCGAGCAATCCAAGAAGGAGCTC ACCCTCTGGGAAAGGAATGAGGTGGAG ATCGTG	to use on 014 to generate 080	
CACNA FW1	ACGGACTATGGCCCTGTAC		
CACNA RV1	CCTAAGCACACGCACAGC		
CACNA FW2	CCGGAGAGTTTGCCAAGG		
CACNA RV2	CCACCACACACAGTACCAC		
MTMC3 FW1	GCGCTACAGAAGCATTCG		
MTMC3 RV1	GCGATCAGCTCGGGAAG		
MTMC3 FW 2	CGACCTGGTTTCACGCTG		
MTMC3 RV2	GGGACCTTGTGATTGCCTC		
MTMC2 FW1	GGACGAGGAAGGTGACAAG		DRG RNA
MTMC2 RV1	GTTCCCTCAGCTTCTTTGC		
MTMC2 FW 2	GCCCTCTTCCTGGGAAAC		
MTMC2 RV2	TTGATGCCCACCAGTCC		
MTMC1 FW1	AGATGTCCCTCGCGGTC		
MTMC1 RV1	CCAGGGTCTCACCGATG		
MTMC1 FW 2	CCCAGAAGAGAGAGCTTGAG		
MTMC1 RV2	ACGAGGCCACTGAGGAAC		
FW	GCCGGATTATGCGTATGACTTCAATGGCCT G	HA1 for 089	
RV	ACATCATACGGATACAACACACCAAAGTTG GC		
FW	GCCGGATTATGCGGGATGGCTGAATTTCCG G	HA1.1 for 089	
RV	ACATCATACGGATAGATCGTGCGTTTATTGT C		
FW	GCCGGATTATGCGAAGTTTAACTCTATCAC GATGAAC	HA2 for 089	
RV	ACATCATACGGATAGTTGTCGGCTGTTTCAG G		
FW	GCCGGATTATGCGATGAACATGGTAATGTC CC	ha3 for 089	
RV	ACATCATACGGATATTCATTTTTTTCCCACC AC		
FW	GCCGGATTATGCGCCTCTCATTGCTCTGAA G	ha3.1 for 089	
RV	ACATCATACGGATAATGGTAATCTTCCAGTT CAG		
FW	GCCGGATTATGCGCCCTGCTGGGAAACAAT GG	ha4 for 089	
RV	ACATCATACGGATAACCGCGAGGGACATCT GC		
FW	GCCGGATTATGCGTGGTCCCTCGGAGGATA CC	HA1 for 001	
RV	ACATCATACGGATAGACGGTGTCGAGGTCT TGG		
FW	GCCGGATTATGCGGGACGTGCCGGATACCG TC	HA1.1 for 001	

RV	ACATCATACGGATAGATACGACGCTCACGTCCG		
FW	GCCGGATTATGCGAAGACCGCCGCCATCCTCAAC	HA2 for 001	
RV	ACATCATACGGATAGGACTCGGCGGCCTCTGGG		
FW	GCCGGATTATGCGGTCTCCGTCGTCGTCTCCC	ha3 for 001	
RV	ACATCATACGGATACTCGTTCTTCTCCCAGAGGG		
FW	GCCGGATTATGCGCCACGTACCACCCTCCGTT	ha3.1 for 001	
RV	ACATCATACGGATAGTGGTACATCTCGAGGGCG		
FW	GCCGGATTATGCGCAATGCTGGGAGACCTACG	ha4 for 001	
RV	ACATCATACGGATATCCTTGTGGTCCTTGCATG		
TMC1 FW	CAAGCTCCTGCCACCCTTGGGTGG	Neutralising residues	089 to make 114
TMC1 RV	GGTGGCAGGAGCTTGCTGGGCGA	Neutralising residues	089 to make 114
TMC2 FW	TCCGCAATGCAAAATGTCAGCTGG	Neutralising residues	059 to make 115
TMC2 RV	CATTGCGGAGAACTCCTGGGACC	Neutralising residues	059 to make 115
TMC3 FW	TCCGCGGCGGCGCTCACCCTCTGG	Neutralising residues	001 to make 116
TMC3 RV	GAGCGCCGCCGCGGATTGCTCGAGC	Neutralising residues	001 to make 116
TM1353-1-F	GAACGAGATTCTTCGTAGCAAGATGACT	Calm-1 genotyping	
TM1353-2-R	AACTTATTCGCTGAATTTTTGAATTTTTGGC	Calm-1 genotyping	
TM1353-3-R	AACTTCCTCGTGATCCTGAAGGCG	Calm-1 genotyping	
116	TCTTCTCCCAGAGGGTGAGCGCCGCCGCGGATTGCTCGAGCTTTTGGG		On 001 Makes 116
116	CCCAAAAGCTCGAGCAATCCGCGGCGGCGCTCACCCTCTGGGAGAAGA		On 001 Makes 116
92	TCGTGATAGAGTTAAACTTCGCATAATCCGGCACATCATACGGATAGTTGTCGGCTGTTTCAGGG		On 089 Makes 092
92	CCCTGAAACAGCCGACAACTATCCGTATGATGTGCCGGATTATGCGAAGTTTAACTCTATCACGA		On 089 Makes 092
99	GACGACGACGGAGACCGCATAATCCGGCACATCATACGGATACTCGTTCTTCTCCCA		On 001 Makes 099
99	TGGGAGAAGAACGAGTATCCGTATGATGTGCCGGATTATGCGGTCTCCGTCGTCGTC		On 001 Makes 099
125F	GTCCCAGGAGGCCTCCAAAATG		059
125R	CGTTTCACCACAAAGTAAATG		059
126F	TGTGGTGAAAGCGTCCCAGGAGTTC		059
126R	AAGTAAATGAGGTACCCG		059
127F	AAGATTCCTCGCCGTCCTGGCC		059
127R	GTCAGGTGGATATTCCCTTC		059
128F	TTCCTCCGCGCCCTGGCCAAC		059
128R	TCTTGTCAGGTGGATATTCCCTTCTTTG		059